PB 298262

REPORT NO.
UCB/EERC-79/03
FEBRUARY 1979

EARTHQUAKE ENGINEERING RESEARCH CENTER

LINEAR AND NONLINEAR EARTHQUAKE RESPONSES OF SIMPLE TORSIONALLY COUPLED SYSTEMS

by
CHRISTOPHER L. KAN
ANIL K. CHOPRA

A report on research conducted under Grant ENV76-04264
from the National Science Foundation.

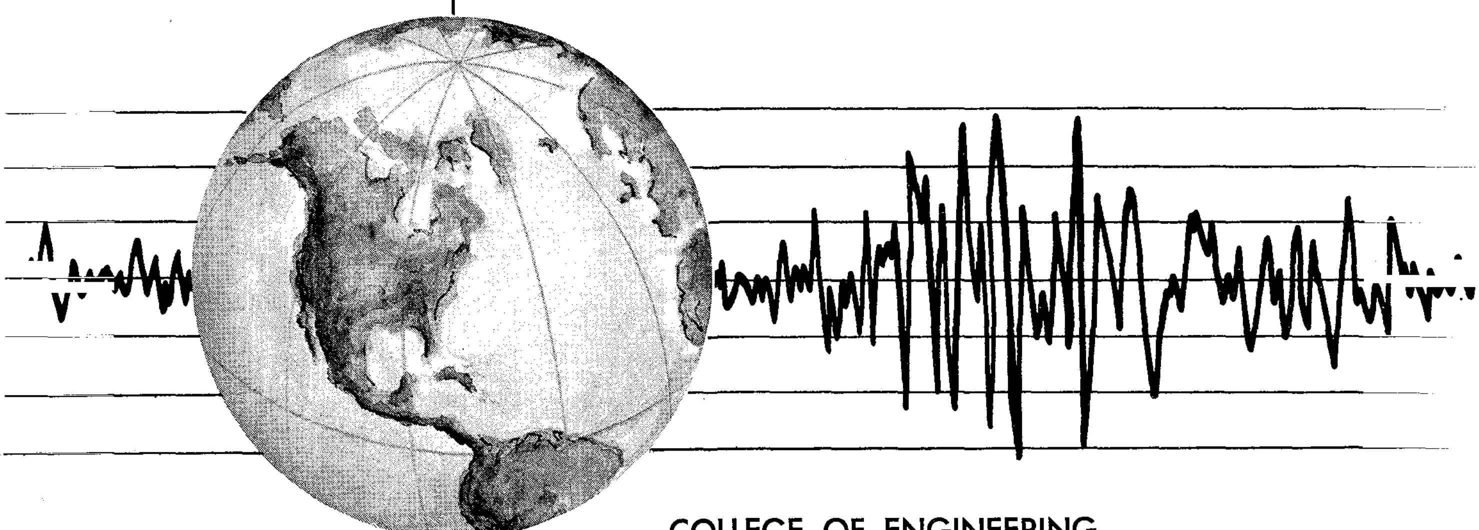

COLLEGE OF ENGINEERING
UNIVERSITY OF CALIFORNIA · Berkeley, California

For sale by the National Technical Information Service, U. S. Dpeartment of Commerce, Springfield, Virginia 22151.

See back of report for up to date listing of EERC reports.

BIBLIOGRAPHIC DATA SHEET	1. Report No. NSF/RA-790122	2.	3. Recipient's Accession No. PB298262

Title and Subtitle

Linear and Nonlinear Earthquake Responses of Simple Torsionally Coupled Systems

5. Report Date: February 1979

6.

Author(s): Christopher L. Kan and Anil K. Chopra

8. Performing Organization Rept. No. UCB/EERC-79/03

Performing Organization Name and Address

Earthquake Engineering Research Center
University of California, Richmond Field Station
47th and Hoffman Blvd.
Richmond, California 94804

10. Project/Task/Work Unit No.

11. Contract/Grant No. ENV76-04264

Sponsoring Organization Name and Address

National Science Foundation
1800 G. Street, N.W.
Washington, D.C. 20550

13. Type of Report & Period Covered

14.

Supplementary Notes

Abstracts

The effects of torsional coupling on the earthquake response of simple one-story structures in both elastic and inelastic ranges of behavior are analyzed. The structures considered are symmetrical about one principal axis of resistance, resulting in coupling between lateral displacement along the perpendicular principal axis and the torsional displacement. Torsional coupling arising only from eccentricity between centers of mass and elastic resistance is considered. Systems with several resisting elements, columns and walls are idealized by a single-element model. Responses of such a model to a selected earthquake ground motion are presented for a wide range of the basic structural parameters. The results presented include maximum lateral and torsional deformations of the system as well as maximum deformations of individual columns. It is shown that the inelastic response is affected by torsional coupling to generally a lesser degree than elastic response. Procedures for estimating, to a useful degree of approximation, the maximum responses of elastic and inelastic systems from the corresponding response spectra and the maximum deformations of individual columns from the displacements at the center of mass are presented.

Identifiers/Open-Ended Terms

COSATI Field/Group

Availability Statement	19. Security Class (This Report)	21. No. of Pages
Release Unlimited	UNCLASSIFIED	120
	20. Security Class (This Page)	22. Price
	UNCLASSIFIED	PC A06 MF A01

LINEAR AND NONLINEAR EARTHQUAKE RESPONSES OF SIMPLE TORSIONALLY COUPLED SYSTEMS

by

Christopher L. Kan

Anil K. Chopra

A Report on Research Conducted Under
Grant ENV76-04264 from the National Science Foundation

Report No. UCB/EERC-79-03
Earthquake Engineering Research Center
University of California
Berkeley, California

February 1979

i (a)

ABSTRACT

The effects of torsional coupling on the earthquake response of simple one-story structures in both elastic and inelastic ranges of behavior are analyzed. The structures considered are symmetrical about one principal axis of resistance, resulting in coupling only between lateral displacement along the perpendicular principal axis and the torsional displacement. Torsional coupling arising only from eccentricity between centers of mass and elastic resistance is considered. Systems with several resisting elements, columns and walls are idealized by a single-element model. Responses of such a model to a selected earthquake ground motion are presented for a wide range of the basic structural parameters. The results presented include maximum lateral and torsional deformations of the system as well as maximum deformations of individual columns. It is shown that the inelastic response is affected by torsional coupling to generally a lesser degree than elastic response. Procedures for estimating, to a useful degree of approximation, the maximum responses of elastic and inelastic systems from the corresponding response spectra and the maximum deformations of individual columns from the displacements at the center of mass are presented.

TABLE OF CONTENTS

1. INTRODUCTION

The lateral and torsional motions are coupled in the response of buildings to earthquake ground motion if the centers of story resistance do not coincide with the centers of floor masses. Assuming linearly elastic force-deformation relations, the earthquake response of buildings with eccentric centers of mass and resistance has been the subject of many studies [1-13,15-22,29-33]. For such systems, the controlling parameters have been identified, the influence of these parameters on response has been studied, the effects of torsional coupling on response have been evaluated, and simple approximate rules have been developed to relate the maximum shears and torques in a torsionally coupled system to the shear forces in the corresponding torsionally uncoupled system -- a system with all properties same except that centers of mass and resistance are coincident [17-20].

Results of these studies of linear response are not applicable directly to calculation of the design forces for buildings because they are usually designed to deform significantly beyond the yield limit during moderate to very intense ground shaking. Thus, there is need to study the response of torsionally coupled buildings beyond the linearly elastic range of behavior. Previous studies [9,31,33] have been concerned with one-story models with each resisting element idealized by two springs acting independently in two perpendicular, lateral directions and each spring having an elastic-perfectly-plastic force-deformation relationship. How well this simple system models the response of complex, real structures is a question that apparently has not been studied. Although these studies have provided valuable information concerning the response of particular systems that were analyzed, because of the many parameters affecting the behavior of such systems, on the whole it has not been possible to generalize the results and to arrive at conclusions that are widely applicable.

The objectives of this study of earthquake response of torsionally coupled systems in both elastic and inelastic ranges of behavior are (1) to identify the basic system parameters that control the response, with the aim of developing a simple model to approximate the response of one-story buildings; (2) to investigate the influence of the basic system parameters on the response; (3) to evaluate the effects of torsional coupling on lateral and torsional deformations of the system and on deformations of individual resisting elements; and (4) to present and evaluate approximate procedures for calculation of yield shear and torque from inelastic response spectra.

This study is concerned with systems in which torsional coupling arises only from eccentricity between center of mass and center of resistance in the linearly elastic range of behavior and input ground motions that are uniform over the base of the structure and contain no rotational components. However, unsymmetric yielding may create eccentricity even in structures with coincident centers of mass and elastic resistance. Torsional coupling may also be induced in such systems with nonlinear force-deformation properties if the uncoupled torsional and translational frequencies of low amplitude vibration are nearly equal; a small perturbation, such as a small accidental torque, to such systems can lead to magnified torque [34,35]. Furthermore, if the horizontal ground motion is not uniform over the base, torsional motions occur, even in buildings with coincident centers of mass and resistance [9,11,21,25,37]. But all these other sources of torsional coupling and response are not considered in this study.

2. SINGLE-ELEMENT MODEL: LINEAR SYSTEM

2.1 One-Story System

Consider the idealized one-story structure in Fig. 2.1, which consists of a rigid deck supported on massless, axially inextensible columns and walls. The three degrees of freedom of the system are lateral displacements u_x and u_y of the center of mass (C.M.) of the deck, relative to the ground, along the principal axes of resistance of the structure, x and y, and the torsional displacement (rotation) u_θ of the deck about the vertical axis.

Let k_{ix} and k_{iy} represent the lateral stiffnesses of the i-th resisting element (column and wall) along the principal axes of resistance x and y, respectively. Then

$$K_x = \sum_i k_{ix} \quad \text{and} \quad K_y = \sum_i k_{iy} \tag{2.1}$$

are the lateral stiffnesses of the structure in the x and y directions, respectively. With the origin at the center of mass, let (x_i, y_i) define the location of the i-th resisting element (Fig. 2.1). Then

$$K_\theta = \sum_i k_{ix} y_i^2 + \sum_i k_{iy} x_i^2 \tag{2.2}$$

is the torsional stiffness of the structure defined at the center of mass. The torsional stiffnesses of the individual resisting elements are not included because they are negligible.

The center of resistance is the point in the plan of the rigid deck through which a horizontal force must be applied in order that it may cause translation without torsion. For a system with discrete resisting elements, the center of resistance is located at distances e_x and e_y, the static eccentricities, where

$$e_x = \frac{1}{K_y} \sum_i x_i k_{iy} \quad \text{and} \quad e_y = \frac{1}{K_x} \sum_i y_i k_{ix} \tag{2.3}$$

measured from the center of mass along the x and y axes.

The structure is assumed to be symmetric with respect to one of the principal axes of resistance, the y-axis (Fig. 2.1); consequently, $e_x = 0$

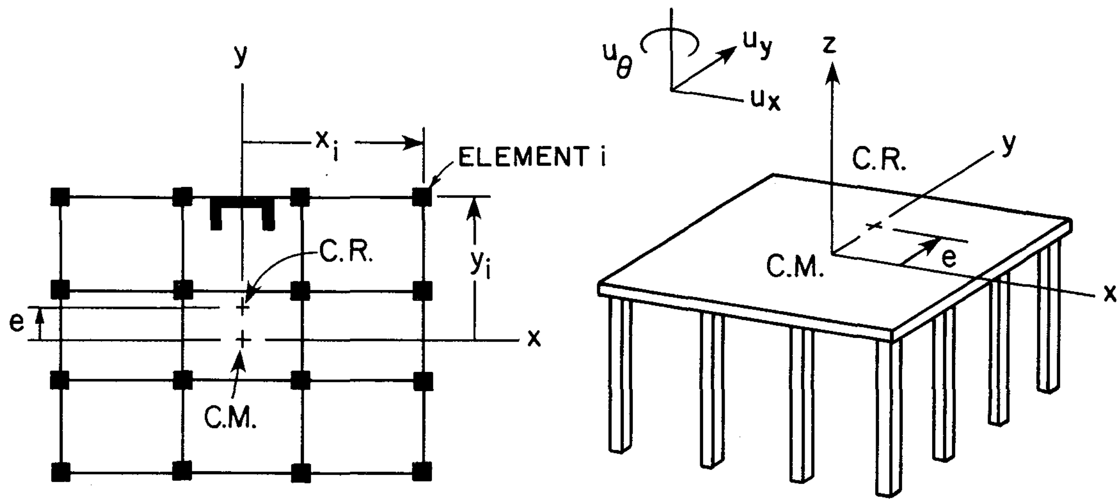

FIG. 2.1 ONE-STORY STRUCTURAL SYSTEM

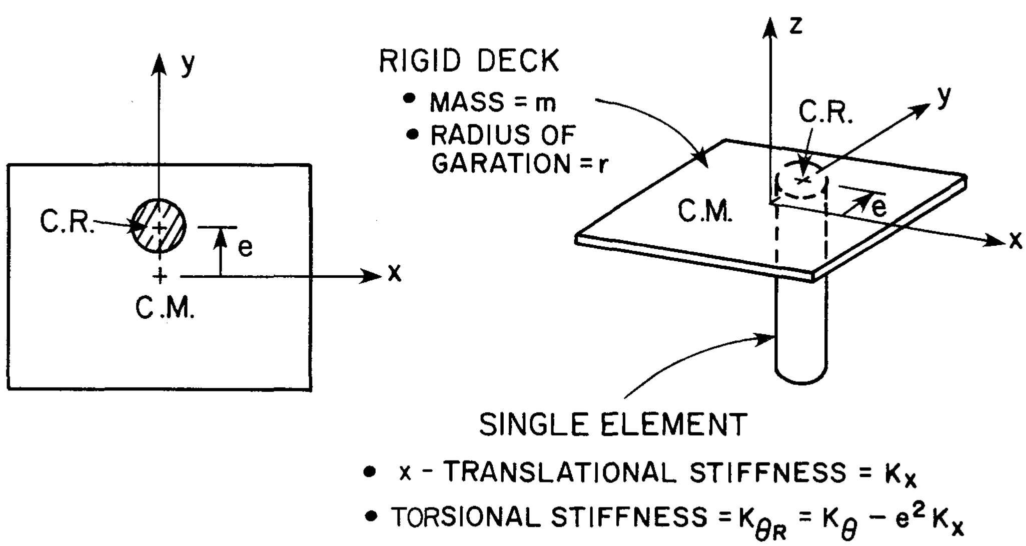

FIG. 2.2 SINGLE-ELEMENT MODEL

and translational motions of the structure in the y direction are not coupled with the torsional motions and may be considered separately. The two degrees of freedom in which coupling occurs are: lateral displacement u_x and torsional displacement u_θ.

2.2 Equations of Motion

Within the range of linear behavior, the equations of motion for coupled lateral-torsional response of the system of Fig. 2.1 to ground acceleration $\ddot{u}_g(t)$ along the x-axis, written in normalized form are

$$\begin{Bmatrix} \ddot{u}_x \\ r\ddot{u}_\theta \end{Bmatrix} + \begin{bmatrix} \omega_x^2 & -\frac{e}{r}\omega_x^2 \\ -\frac{e}{r}\omega_x^2 & \omega_\theta^2 \end{bmatrix} \begin{Bmatrix} u_x \\ ru_\theta \end{Bmatrix} = -\begin{Bmatrix} \ddot{u}_g \\ 0 \end{Bmatrix} \tag{2.4}$$

in which $e = e_y$, r = radius of gyration of the deck about a vertical axis through the center of mass;

$$\omega_x = \sqrt{\frac{K_x}{m}}\,, \quad \text{and} \quad \omega_\theta = \sqrt{\frac{K_\theta}{mr^2}} \tag{2.5}$$

in which m = mass of the deck. The two frequency parameters ω_x and ω_θ may be interpreted as uncoupled frequencies of the system, the natural circular frequencies of the system if it were torsionally uncoupled ($e=0$).

Eq. 2.4 is for an undamped system. Damping is defined directly in each of the two natural modes of vibration of the system. The viscous damping ratio ξ, expressed as a fraction of critical damping, is assumed to be the same in each mode of vibration.

2.3 Vibration Frequencies and Mode Shapes

Consider the eigenvalue problem:

$$\begin{bmatrix} (\omega_x^2 - \omega^2) & -\frac{e}{r}\omega_x^2 \\ -\frac{e}{r}\omega_x^2 & (\omega_\theta - \omega^2) \end{bmatrix} \begin{Bmatrix} \alpha_x \\ \alpha_\theta \end{Bmatrix} = \begin{Bmatrix} 0 \\ 0 \end{Bmatrix} \tag{2.6}$$

The solution of Eq. 2.6 leads to the natural frequencies of vibration of the one-story system, ω_1 and ω_2, given by

$$\omega_{1,2}^2 = \frac{1}{2}\left(\omega_\theta^2 + \omega_x^2\right) \mp \sqrt{\frac{1}{4}\left(\omega_\theta^2 - \omega_x^2\right) + \left(\frac{e}{r}\,\omega_x^2\right)^2} \tag{2.7}$$

and the corresponding mode shapes of vibration $\underline{\alpha}_n$, where $\underline{\alpha}_n^T = \langle \alpha_{xn} \alpha_{\theta n} \rangle$, $n = 1,2$.

2.4 Basic System Parameters

It is apparent from the equations of motion (Eq. 2.4) that the displacement response u_x and u_θ at the C.M. of the idealized one-story system to specified ground acceleration $\ddot{u}_g(t)$ along the x-principal axis of resistance depends on the following system parameters: ω_x, ω_θ, e/r and ξ but not independently on the number, location and stiffness of the individual resisting elements nor on the plan geometry.

2.5 Single-Element Model

In particular, the single-element model of Fig. 2.2 and a multi-element system are equivalent for purposes of calculating the displacement response u_x and u_θ at C.M. and the associated total shear and torque, provided the values for the parameters ω_x, ω_θ, e/r and ξ are the same for the two systems.

3. SINGLE-ELEMENT MODEL: NONLINEAR SYSTEM

3.1 One-Story System

Consider the idealized one-story system of Fig. 2.1, whose properties in the linearly elastic range were described in the preceding section, subjected to the component of ground motion along the x-axis. Because of coupled lateral-torsional motion of the deck, the i-th resisting element will experience not only the shear force V_{ix} in the direction of the excitation but also the shear force in the transverse direction V_{iy}. Generally, the torque acting on the element is relatively small and need not be considered.

The resisting elements in the system are assumed to be elastic-perfectly plastic. When the i-th element is subjected only to a shear force along one of the principal axes of resistance, the relations between shear force and deformation — V_{ix} and u_{ix} in the x direction and V_{iy} and u_{iy} in the *y* direction — are shown in Fig. 3.1a. The yield or plastic shear forces in the x and *y* directions V_{ixp} and V_{iyp} are considered to be equal in the two — positive and negative — directions of deformation. Unloading from regions of inelastic deformations is assumed to take place along lines parallel to the initial elastic portion of the diagram. Under the combined action of V_{ix} and V_{iy}, the criteria of yielding and plasticity is defined by the yield surface (Fig. 3.1b), assumed to be circular in terms of normalized forces. The element i is elastic when the forces are defined by a point within the yield surface and plastic when they represent a point on the yield surface. Whenever yielding is initiated, the locus of the member forces (V_{ix}, V_{iy}) must remain on the yield surface until unloading occurs; it may not go beyond the yield surface.

3.2 Multi-Element System: Equations of Motion

The equations of motion for nonlinear response of the system of Fig. 2.1 to ground acceleration $\ddot{u}_g(t)$ along the x-axis may be written as

$$\begin{Bmatrix} \ddot{u}_x \\ r\ddot{u}_\theta \end{Bmatrix} + \underline{F} = - \begin{Bmatrix} \ddot{u}_g \\ 0 \end{Bmatrix} \qquad (3.1)$$

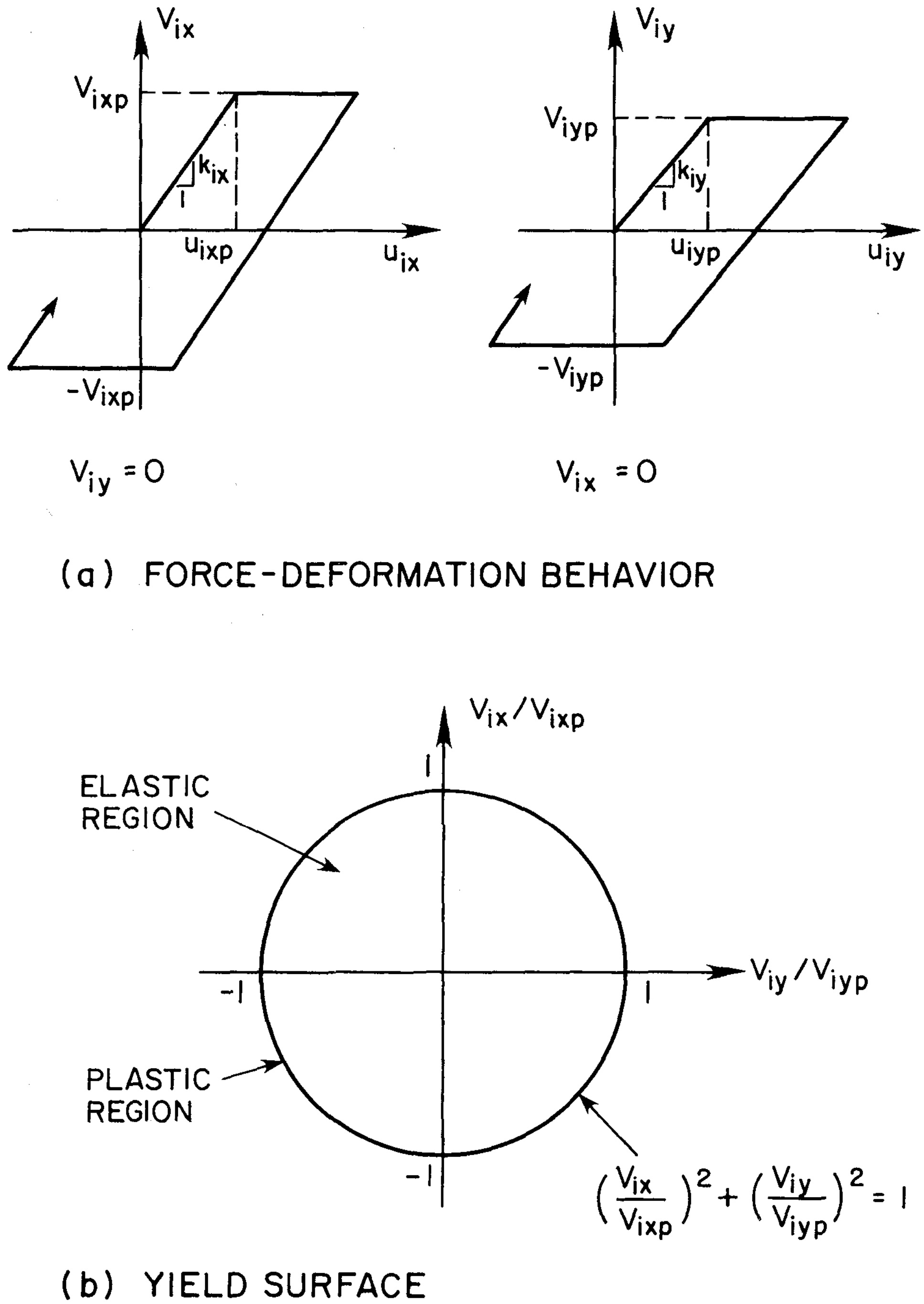

FIG. 3.1 PROPERTIES OF RESISTING ELEMENT

where $\underline{F}$ is the vector of restoring forces associated with stiffness of the structure. The restoring forces and deformations are related by the following incremental equation:

$$\underline{dF} = \frac{1}{m} \underline{K}_t \begin{Bmatrix} du_x \\ r du_\theta \end{Bmatrix} \tag{3.2}$$

where $\underline{K}_t$ = tangent stiffness matrix of the structure.

The tangent stiffness matrix of the structure in any deformation state may be expressed as

$$\underline{K}_t = \underline{K}_e - \underline{K}_c \tag{3.3}$$

where

$$\underline{K}_e = m \begin{bmatrix} \omega_x^2 & -\frac{e}{r} \omega^2 \\ -\frac{e}{r} \omega_x^2 & \omega_\theta^2 \end{bmatrix} \tag{3.4}$$

is the elastic stiffness matrix of the one-story torsionally coupled system (Eq. 2.4) and

$$\underline{K}_c = \sum_i \underline{k}_{ic} \tag{3.5}$$

represents the modification to $\underline{K}_e$ due to elements that are in plastic condition (Appendix III-B). The matrix $\underline{k}_{ic}$, the modification due to element i, is a zero matrix if the element is elastic. If the element is in plastic condition, for the yield surface of Fig. 3.1b, $\underline{k}_{ic}$ is given by

$$\underline{k}_{ic} = \frac{1}{G_i} \begin{bmatrix} B_{ix}^2 & B_{ix} B_{iy} \\ B_{ix} B_{iy} & B_{iy}^2 \end{bmatrix} \tag{3.6a}$$

in which

$$G_i = k_{ix}h_{ix}^2 + k_{iy}h_{iy}^2$$

$$B_{ix} = k_{ix}h_{ix} \tag{3.6b}$$

$$B_{iy} = (x_i/r)\, k_{iy}h_{iy} - (y_i/r)\, k_{ix}h_{ix}$$

and

$$h_{ix} = V_{ix}/V_{ixp}^2$$

$$h_{iy} = V_{iy}/V_{iyp}^2$$

Eq. 3.1 is for an undamped nonlinear system. Damping is defined as described earlier for a linear system by damping ratios for the natural modes of low amplitude linear vibration.

3.3 Single-Element Model: Yield Surface

As shown earlier, in the linear range of behavior, the single-element model of Fig. 2.2 is equivalent to a system with several resisting elements, provided the values of the parameters ω_x, ω_θ, e/r and ξ are the same for the model and system. However, after initiation of yielding, the stiffness properties of the multi-element system depend on the number, location, stiffness and yield strength of all the resisting elements that are in yield condition (Eqs. 3.5-3.6). A single-element model could therefore not be strictly equivalent to a multi-element system. The purpose of this section is to develop the yielding properties of a single-element model so that it is equivalent, in approximate sense, to a multi-element system.

In order to develop an appropriate yield surface for the single-element model, it is instructive to examine first the initial and limit yield surfaces for one of the simpler multi-element systems. Consider the system of Fig. 3.2 consisting of a rigid deck, square in plan, supported on four columns located at the corners. The system is symmetric with respect to the y-axis and eccentricity between centers of mass and resistance is due to difference in stiffnesses of columns on two sides of the x-axis. The columns are assumed to have yield strengths proportional to their stiffnesses and yield surfaces as shown in Fig. 3.1b. The initial yield surface is defined by combinations of total forces for the system, shear V_x in the x-direction and torque T_R defined at the center of resistance (shear V_y in y-direction = 0), at which yielding of the system is initiated, and the limit yield surface by force combinations at which the system becomes a mechanism. Yield surfaces for the system of Fig. 3.2, with the above mentioned properties, were derived (Appendix III-C) and are presented in Fig. 3.3 for two values of e/r. The forces V_{xp} and T_{Rp}, used for normalization of the shear V_x and torque T_R, are the fully plastic shear and torque for the system. The system will become a mechanism under the separate action of V_{xp} at the C.R. and T_{Rp} about the C.R.

The yield surfaces are symmetrical with respect to both the shear and torque axes for systems with e/r = 0, but not when e/r ≠ 0. Because of the eccentricity, the initial yield surface is significantly skewed but the limit yield surface is only slightly affected. For systems with e/r not large, it may be reasonable to ignore the skew and approximate the yield surface by

$$\left(\frac{V_x}{V_{xp}}\right)^2 + c\left(\frac{V_x}{V_{xp}}\right)\left(\frac{T_R}{T_{Rp}}\right) + \left(\frac{T_R}{T_{Rp}}\right)^2 = 1 \qquad (3.7)$$

where the scalar c has the same absolute value for all four quadrants, but positive in the first and third quadrants and negative in the second and fourth. A yield surface described by Eq. 3.7 is symmetrical with respect to both the shear and torque axes and varies from a circle for c = 0 to a set of straight lines for c = 2 (Fig. 3.4).

The initial yield surface for the system of Fig. 3.2 with e/r = 0 is defined exactly by Eq. 3.7 with $c = \sqrt{2}$, and the limit yield surface for the same system is between the curves defined by Eq. 3.7 with c = 0.25 and 0.5 (Fig. 3.4). Thus, Eq. 3.7 with an appropriate value of the parameter c can approximate either yield surface of the system of Fig. 3.2 with e/r = 0. It is also apparent from Fig. 3.5 that yield surfaces of systems with e/r different than zero, but not large, can be approximated by Eq. 3.7 with an appropriate value of c and T_{Rp}.

Consistent with simplicity of the single-element model of Fig. 2.2,

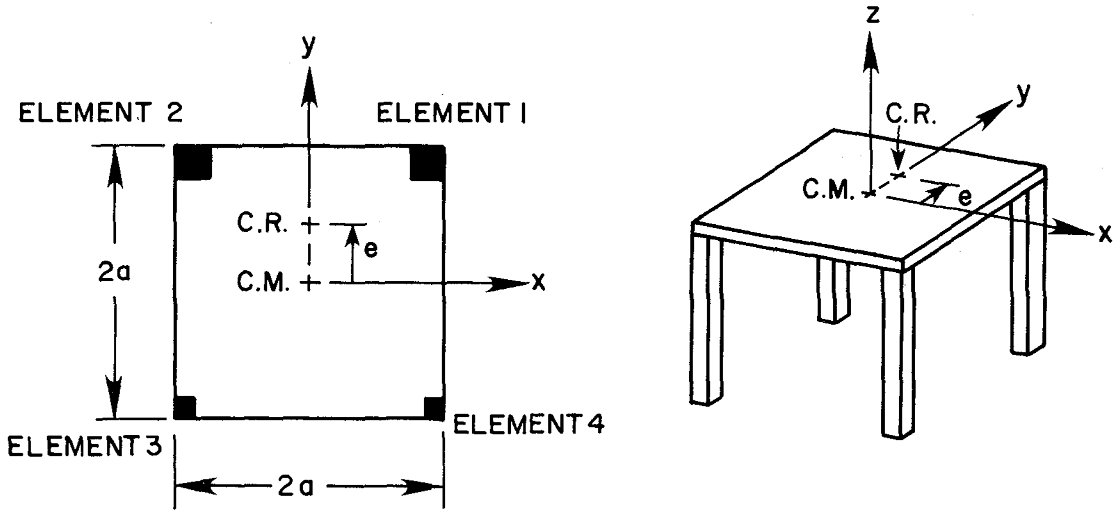

FIG. 3.2 FOUR-ELEMENT SYSTEM

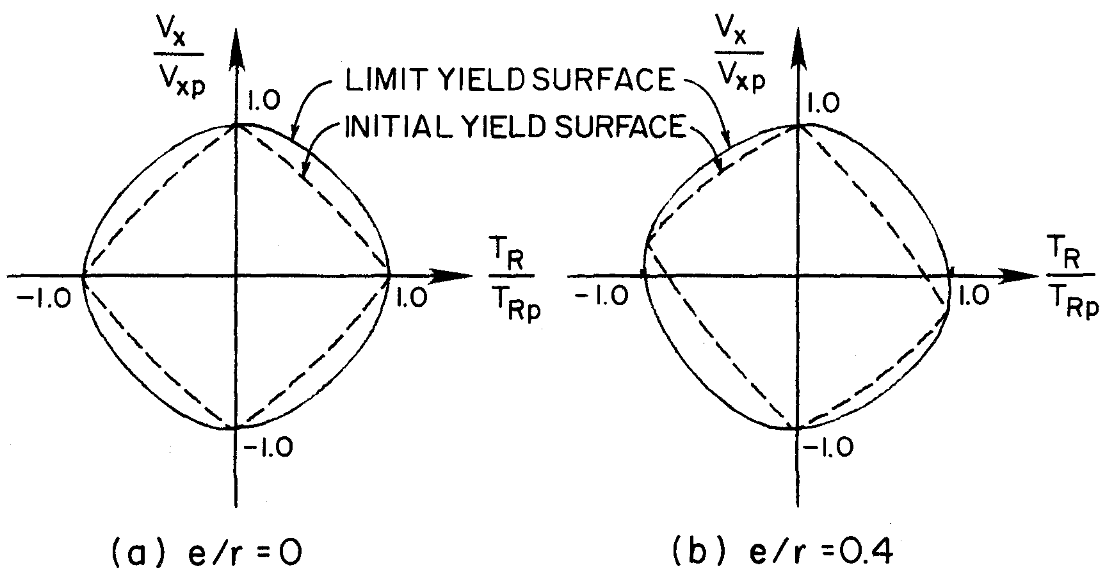

FIG. 3.3 YIELD SURFACES FOR A FOUR-ELEMENT SYSTEM

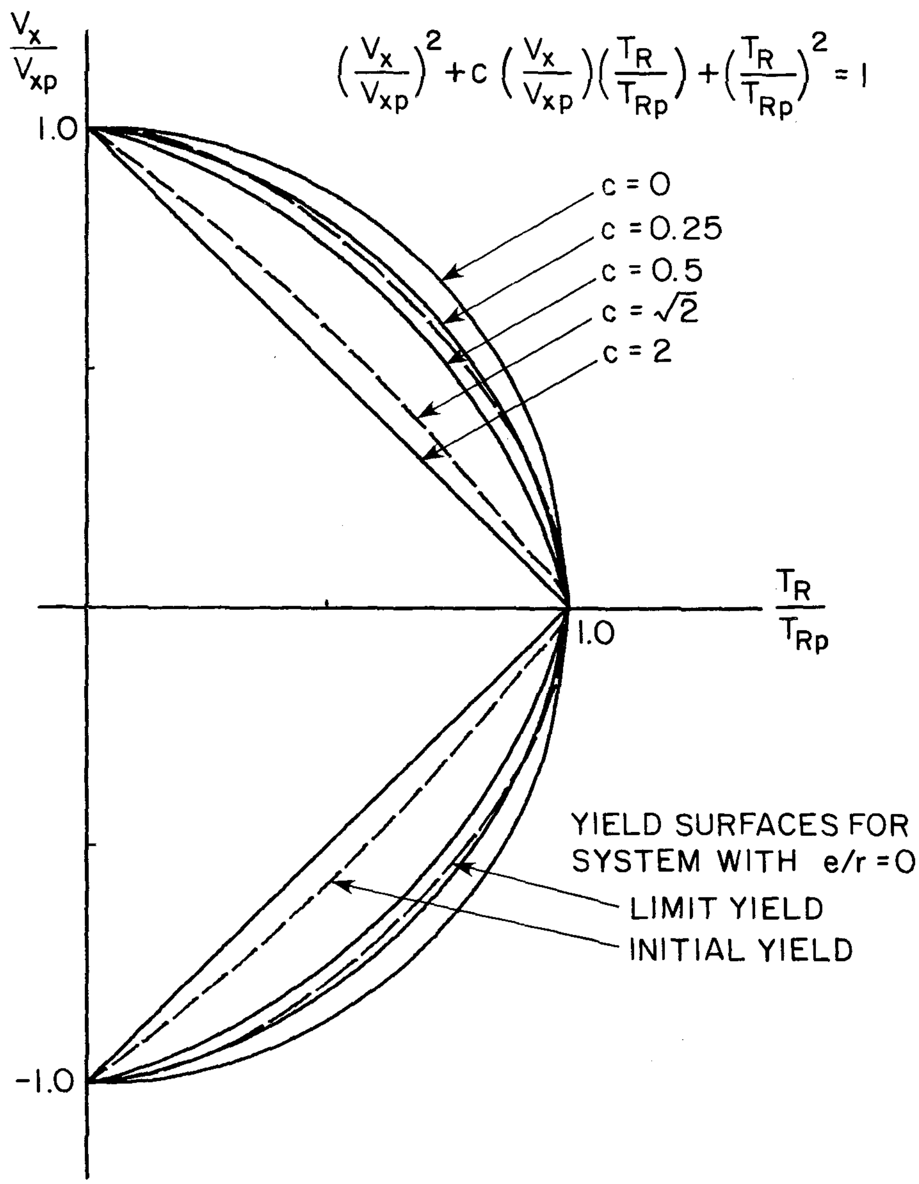

FIG. 3.4 YIELD SURFACES FOR FOUR-ELEMENT SYSTEMS WITH e/r = 0

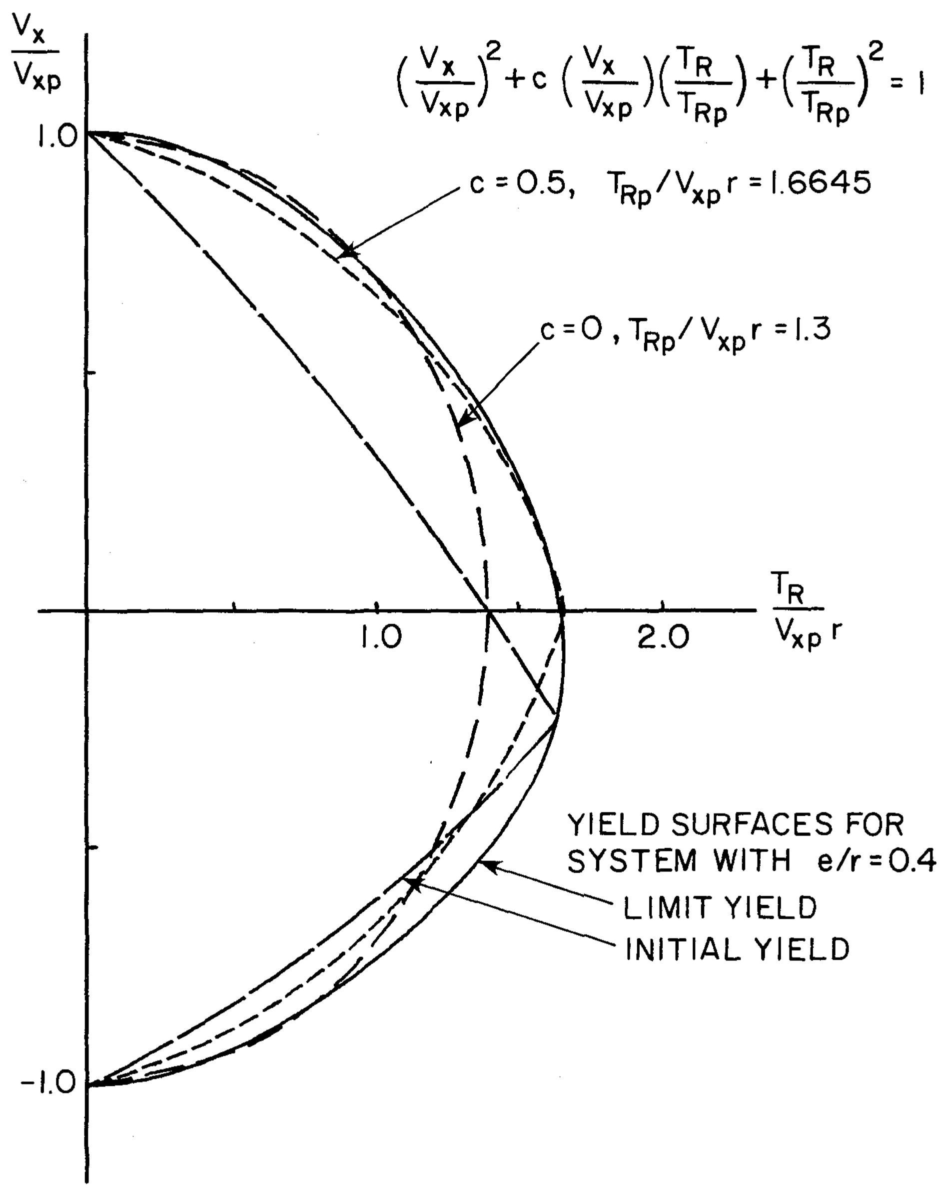

FIG. 3.5 YIELD SURFACES FOR FOUR-ELEMENT SYSTEMS WITH e/r = 0.4

differences between initial and limit yield surfaces of multi-element systems will be ignored and a single yield surface will be employed to define the boundary between elastic and plastic states. Such an idealization of the single-element model is equivalent to the assumption of elastic-perfectly-plastic behavior. If an appropriate single yield surface lying between the initial and limit yield surfaces is selected, based on earlier work [27], the response of the single-element model is expected to provide a satisfactory approximation to the response of multi-element systems.

3.4 Single-Element Model: Equations of Motion

The equations of motion of the single-element model defined in its linear range of behavior as shown in Fig. 2.2 and having a yield surface given by Eq. 3.7 are the same as for the multi-element system (Eqs. 3.1-3.4) except that $\underset{\sim}{K}_c$ is no longer given by Eq. 3.5. For the single-element model in the linearly elastic state, $\underset{\sim}{K}_c$ is a zero matrix; in the plastic state it is given by Eq. 3.8 (Appendix III-B):

$$\underset{\sim}{K}_c = \frac{1}{G}\begin{bmatrix} B_x^2 & B_x B_t \\ B_x B_t & B_t^2 \end{bmatrix} \tag{3.8a}$$

in which

$$\begin{aligned} G &= K_x H_x^2 + K_{tR} H_t^2 \\ B_x &= K_x H_x \\ B_t &= K_{tR} H_t - (e/r)\, K_x H_x \end{aligned} \tag{3.8b}$$

where

$$K_{tR} = (K_\theta - e^2 K_x)/r^2$$

$$\begin{aligned} H_x &= \frac{1}{V_{xp}}\left(2\frac{V_x}{V_{xp}} + c\,\frac{T_R}{T_{Rp}}\right) \\ H_t &= \frac{r}{T_{Rp}}\left(2\frac{T_R}{T_{Rp}} + c\,\frac{V_x}{V_{xp}}\right) \end{aligned} \tag{3.8c}$$

3.5 Systems, Ground Motions and Method of Analysis

Numerical results of earthquake responses of four-element systems and corresponding single-element models are presented in the next section with the purpose of evaluating the single-element models. In this section, properties of these systems and the method of analysis employed in analyzing them are summarized.

3.5.1 Systems. The four-element systems selected have the following properties: Elastic stiffness $K_x = (4\pi^2/T_x^2)$ m, where $T_x = 2\pi/\omega_x$ is the uncoupled period of lateral vibration. Yield shear $V_{xp} = mS_a$, where S_a is obtained from the response spectrum of Fig. 3.7 for elastic-perfectly-plastic systems, corresponding to the selected ductility factor of $\mu = 5$. Values for V_{xp} are listed in Table 1 for several values of T_x. For each column, the stiffnesses in the x and y directions are the same, i.e., $k_{ix} = k_{iy}$. Columns located symmetrically about the y-axis are assumed to have the same stiffness so that the C.R. is on the y-axis but the unsymmetric distribution of stiffness about the x-axis depends on e/r. The yield shears of each column in the x and y directions are assumed the same, i.e., $V_{ixp} = V_{iyp}$. Yield shears of individual columns are proportional to their stiffnesses. Yielding properties including the yield surface of individual columns were described in Sec. 3.1.

The specific parameter values chosen are: $\omega_\theta/\omega_x = \sqrt{3}$, which is consistent with what was implied above: the system has equal stiffness in the x and y directions; e/r = 0.4, which represents an eccentricity of 16.3% of the plan dimension in the y direction; and $\xi = 0.02$; several values for $T_x = 2\pi/\omega_x$ in the range 0.5 to 2.5 sec. are considered.

The single-element model to be compared with a four-element system is assigned the same values of ω_θ/ω_x, e/r, T_x and ξ. Two different yield surfaces are considered: (1) Eq. 3.7 for c = 0.5 with yield shear V_{xp} and yield torque T_{Rp} same as that for the four-element system; (2) Eq. 3.7 for c = 0 with the same yield shear V_{xp} but yield torque $T_{Rp}/(rV_{xp}) = 1.3$. Both the yield surfaces are potentially appropriate as they lie between the initial and limit yield surfaces of the four-element system (Fig. 3.5).

In the latter yield surface, the yield shear is the same as for the four-element system, whereas the yield torque is smaller. This reduction

Table 1. Yield Shears for Inelastic Systems

Uncoupled Period T_x, sec.	Yield Shear, $V_{xp} \div mg$
0.5	0.1381
0.6	0.1634
0.7	0.1752
0.8	0.1551
0.9	0.1187
1.0	0.0913
1.2	0.0685
1.4	0.0543
1.6	0.0466
1.8	0.0424
2.0	0.0390
2.25	0.0305
2.5	0.0240

in yield torque was necessary to have a yield surface intermediate between the initial and limit yield surface (Fig. 3.5). Alternatively, the yield shear could have been reduced to achieve a similar effect; however, that would not be appropriate because yielding in torsionally coupled systems is controlled primarily by the yield shear. This was confirmed by examining the history of responses of four-element systems, indicating that yielding occurs predominantly on portions of the yield surface in the neighborhood of $V_x/V_{xp} = 1$ or -1 (Fig. 3.8).

3.5.2 Ground Motion. The ground motion considered is the first 30 seconds of the S00E component of the El Centro record obtained during the Imperial Valley earthquake of May 18, 1940. The ground acceleration history presented in Fig. 3.6 is the most recent digitization with "standard" base line correction [14]. However, the response spectra of Fig. 3.7 from which the yield shears were obtained (Sec. 3.5.1) is based on an earlier digitization of the record with parabolic base line correction.

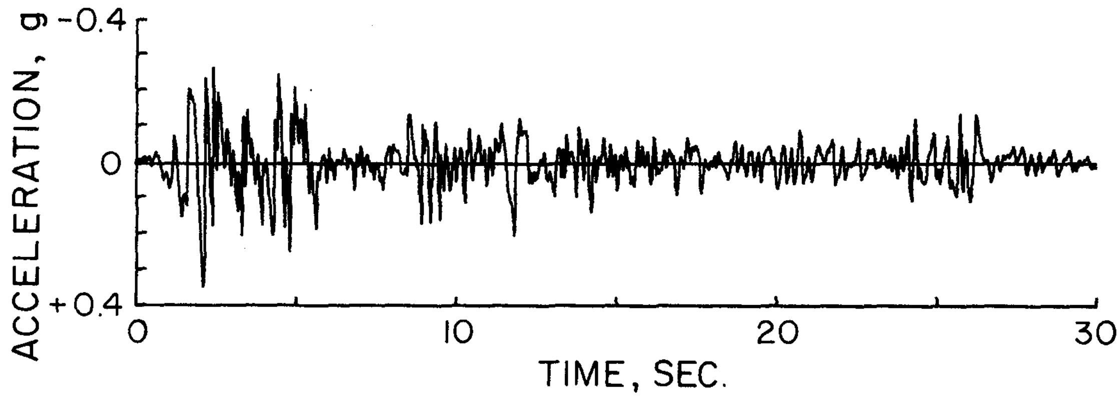

FIG. 3.6 SOOE COMPONENT OF IMPERIAL VALLEY EARTHQUAKE, MAY 18, 1940, EL CENTRO, IMPERIAL VALLEY IRRIGATION DISTRICT

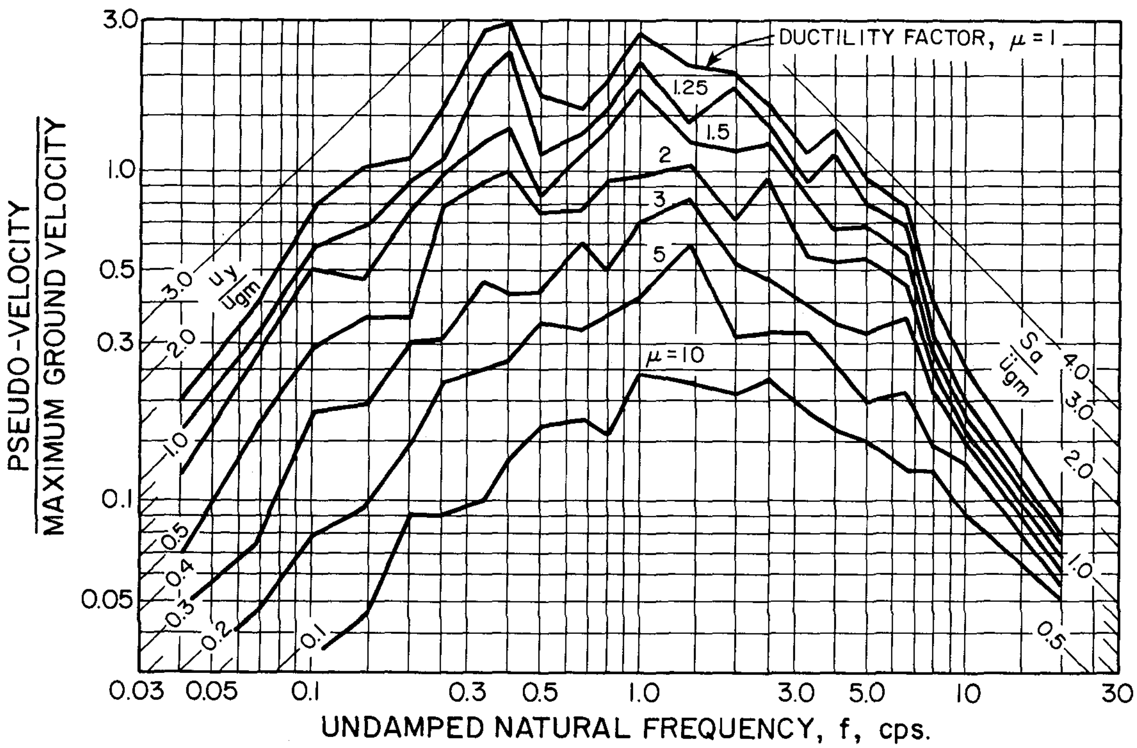

FIG. 3.7 DEFORMATION SPECTRA FOR ELASTIC-PERFECTLY PLASTIC SYSTEMS WITH 2% CRITICAL DAMPING SUBJECTED TO THE EL CENTRO EARTHQUAKE (FROM REF. 36). MAXIMUM GROUND DISPLACEMENT, u_{gm} = 8.28 in.; MAXIMUM GROUND VELOCITY = 13.68 in./sec.; MAXIMUM GROUND ACCELERATION, $\ddot{u}_{gm}$ = 0.32 g; u_y = YIELD DISPLACEMENT.

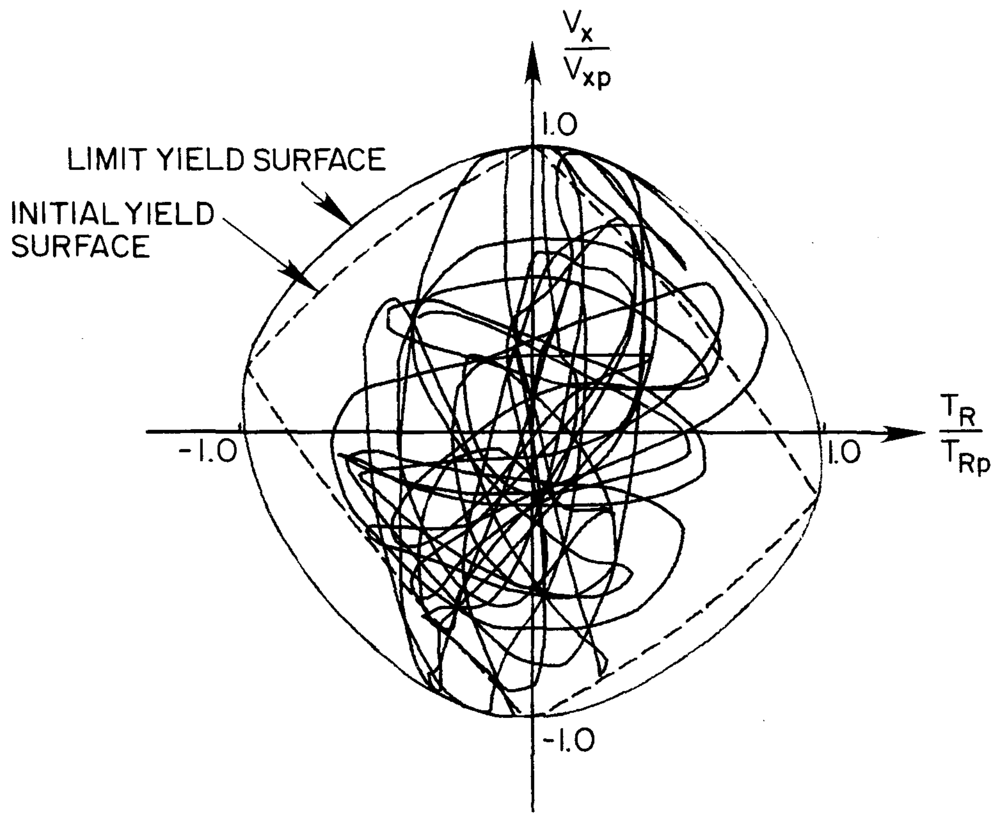

FIG. 3.8 LOCUS OF RESPONSE FORCES FOR FOUR-ELEMENT SYSTEM SUBJECTED TO THE EL CENTRO EARTHQUAKE. SYSTEM PARAMETERS ARE: T_x = 2 sec., $\omega_\theta/\omega_x = \sqrt{3}$, e/r = 0.4.

3.5.3 Method of Analysis. Earthquake responses of each four-element system and corresponding single-element models are determined by solving the equations of motion presented in Sec. 3.2 and Sec. 3.4 by a numerical integration procedure (Appendix III-D). The time scale is discretized into equal time intervals, small enough (0.02 sec. or less) to define the earthquake accelerogram accurately and no more than a small fraction (1/20th) of the shorter natural period of linearly elastic vibration of the system. Within each small time interval, the lateral and torsional accelerations of the deck were assumed to vary linearly. For the time intervals during which transition from elastic to plastic state or from one plastic state to another occurred, the tangent stiffness was re-evaluated and a predictor-corrector iteration procedure was used to reduce force unbalances created by the numerical approximation to an acceptably small value. Analysis of the four-element system and single-element model differ mainly in the formulation of the tangent stiffness in the plastic state, Eq. 3.5 vs. Eq. 3.8.

3.6 Evaluation of Single-Element Models

The response of a four-element system and the two corresponding single-element models to the El Centro ground motion record are presented in Fig. 3.9. Responses of the three systems are very similiar, except for different plastic drifts and maximum deformations. These differences are the result of slightly different yielding properties of single-element models compared to the multi-element systems. When considered over a wide range of periods, the differences in maximum deformations, u_{xm} in translation and $u_{\theta m}$ in rotation, however, are not large (Fig. 3.10). Based on these results, and additional results — not included here — for systems with different parameters, both single-element models may be suitable for studying inelastic response of four-element systems.

It is apparent from Figs. 3.9 and 3.10 that response of the single-element model is relatively insensitive to differences in the two yield surfaces. Note that the second yield surface is circular in the normalized coordinate system: V_x/V_{xp}, T_R/T_{Rp}. Considering that it offers computation advantages — simpler expression for $\underline{K}_c$ and hence for the tangent stiffness matrix (Eq. 3.8) and slope is continuous across the two coordinate axes (Fig. 3.5) — a circular yield surface is chosen for the single-element model.

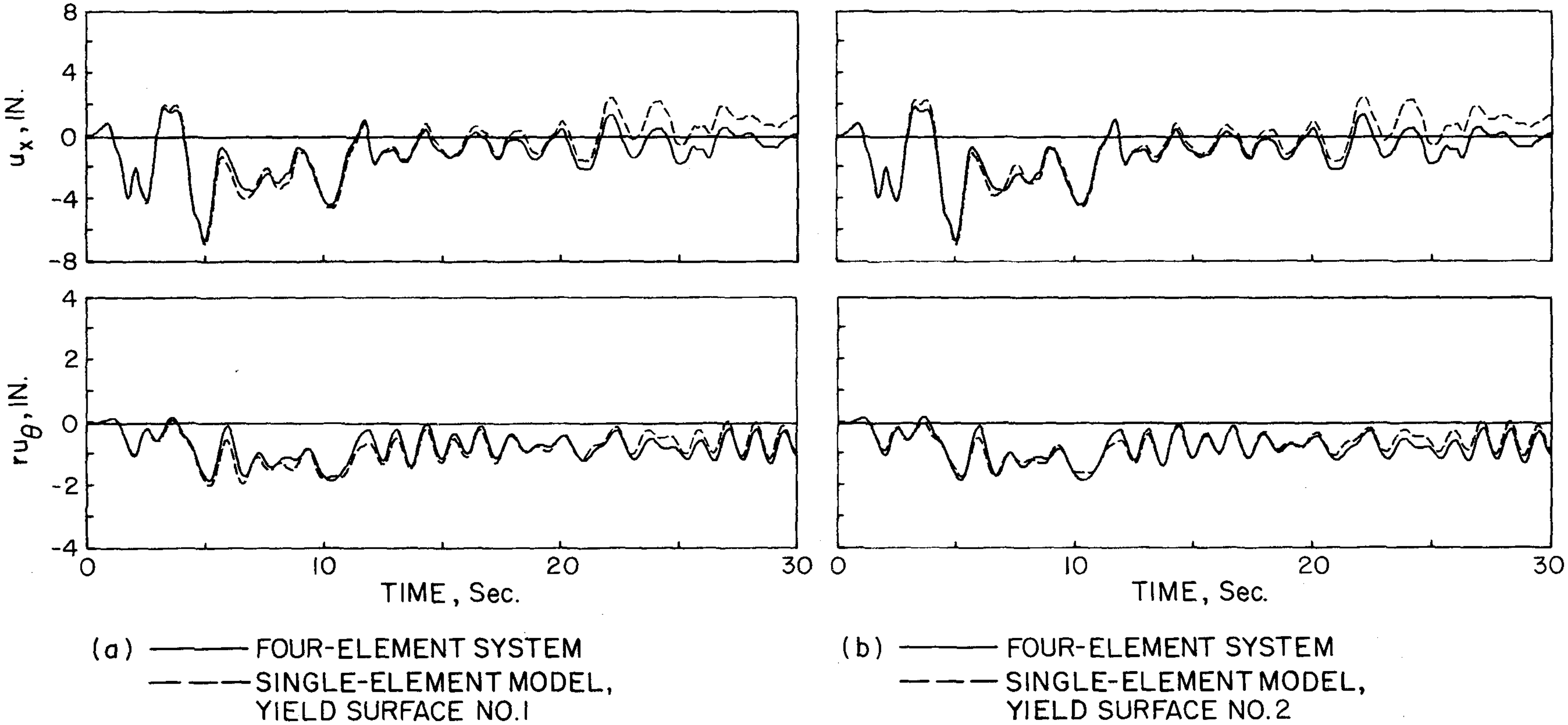

FIG. 3.9 DISPLACEMENT-TIME RESPONSE OF INELASTIC TORSIONALLY COUPLED SYSTEMS TO THE EL CENTRO EARTHQUAKE. SYSTEM PARAMETERS: T_x = 2 sec., $\omega_\theta/\omega_x = \sqrt{3}$, e/r = 0.4 AND ξ = 2%.

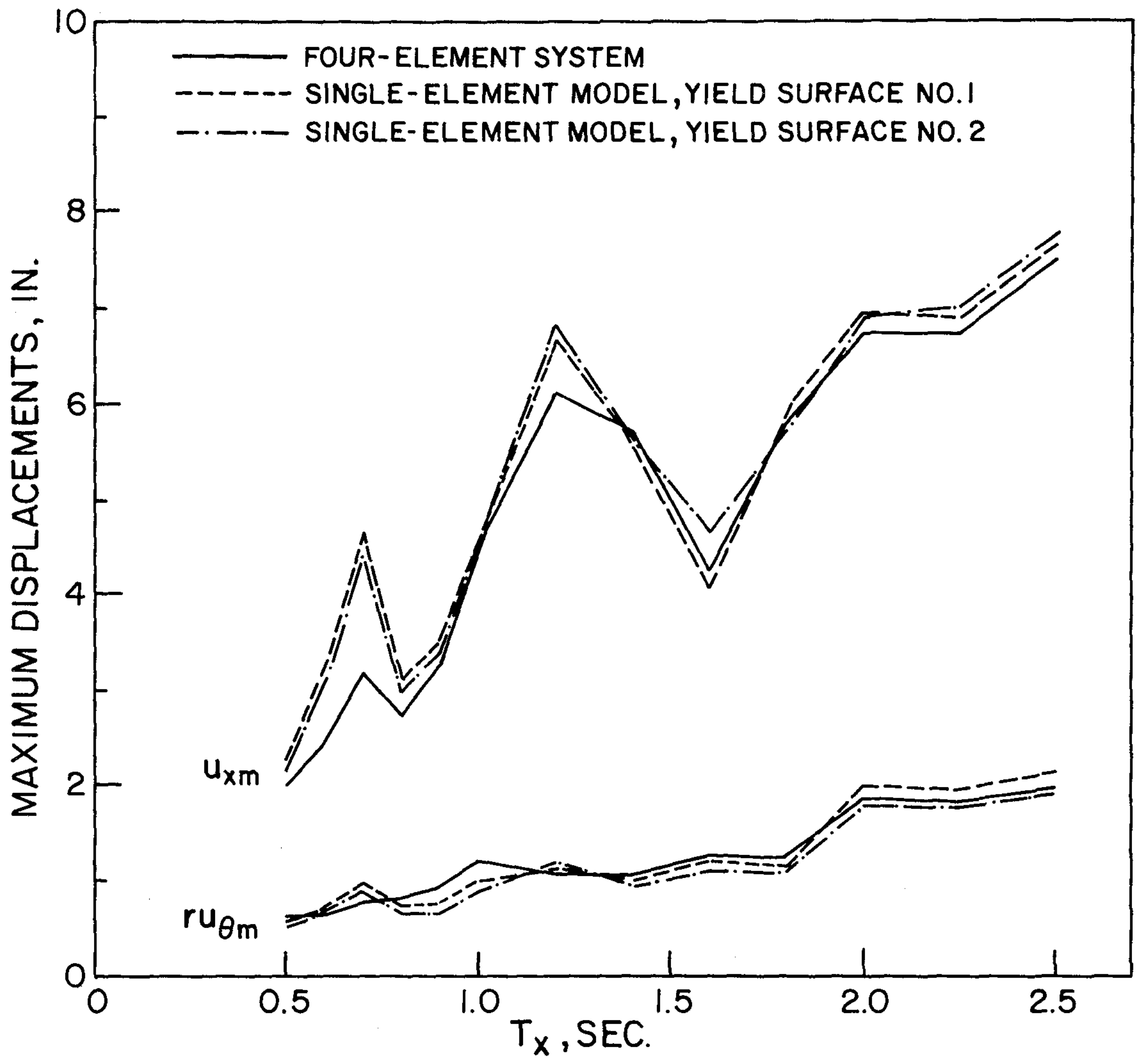

FIG. 3.10 MAXIMUM DISPLACEMENTS OF INELASTIC TORSIONALLY COUPLED SYSTEMS SUBJECTED TO THE EL CENTRO EARTHQUAKE. SYSTEM PROPERTIES: $\omega_\theta/\omega_x = \sqrt{3}$; $e/r = 0.4$; and $\xi = 2\%$.

The principal disparity between a multi-element system and the corresponding single-element model is in their yielding properties. Force combinations between the initial and limit yielding surfaces imply yielding of some of the resisting elements, resulting in migration of the center of resistance; a phenomenon which is not present in the single-element model. The center of resistance migrates most abruptly and through greatest distance in the four-element system of Fig. 3.2, compared to systems of Fig. 2.1 with larger number of resisting elements. Consequently, the single-element system, shown to be a suitable model for four-element systems, should be even more appropriate for systems with larger number of resisting elements.

3.7 Single-Element Model: Yield Shear and Torque

Having selected for the single-element model a yield surface that is circular in the normalized coordinate system: V_x/V_{xp} and T_R/T_{Rp}, only the yield shear V_{xp} and yield torque T_{Rp} remain to be specified. Values for these should be selected so that the resulting yield surface lies between the initial and limit yield surfaces of the original multi-element system.

Consider a multi-element system with eight identical columns located in plan as shown in Fig. 3.11. The initial and limit yield surfaces for this multi-element system were determined (Appendix III-E) and are presented in the first quadrant (Fig. 3.11); they are symmetrical about both shear and torque axes. The initial yield surface (in the first quadrant) is almost a straight line; for systems with more elements, it would be even closer to a straight line. The limit yield surface is similar to and enclosed by a circle. If the yield displacements for all the resisting elements are the same, which was the case for the system of Fig. 3.11, the initial yield shear is identical to the limit yield shear. Thus, it is appropriate to assign the same value to the yield shear of the single-element model. In contrast to what was observed for a four-column system (Fig. 3.4), the initial yield torque is different from the limit yield torque (Fig. 3.11). The yield torque for the single-element model should be chosen as intermediate between those two values so that the yield surface would lie between the initial and limit yield surfaces.

Consider the four-element system of Fig. 3.2 with the yield displacement for all resisting elements assumed to be the same. The stiffness properties

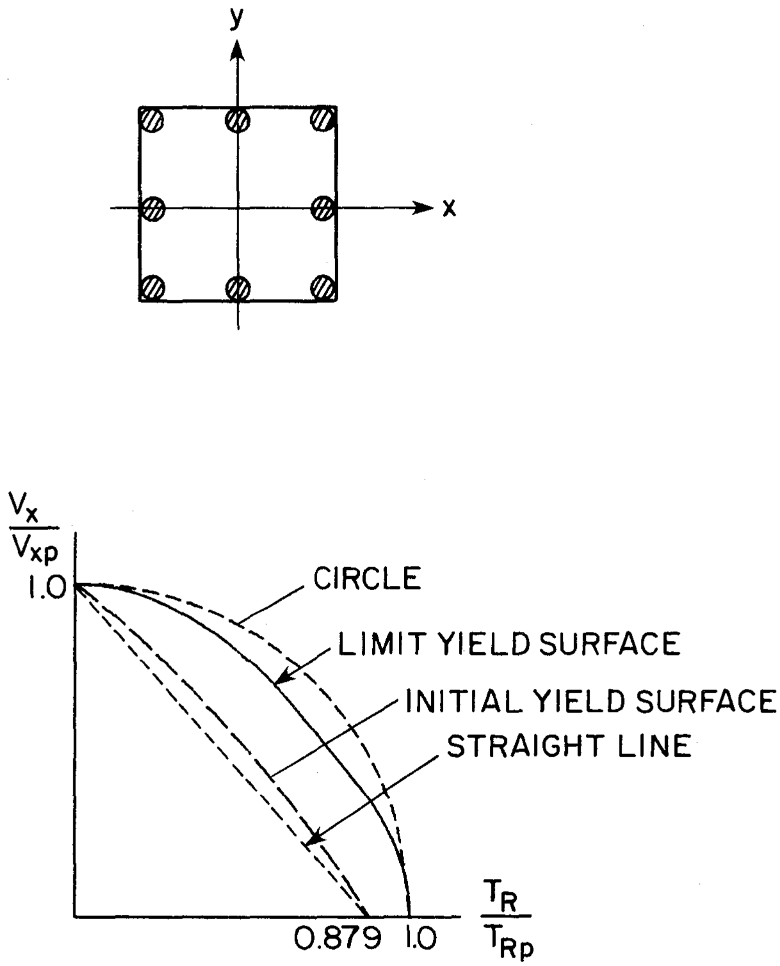

FIG. 3.11 YIELD SURFACES FOR 8-COLUMN SYSTEM (e/r = 0)

of individual elements of such a system can be determined from the yield shear V_{xp} for the system, the frequency ratio ω_θ/ω_x and eccentricity ratio e/r. The initial and limit yield torques are identical; they can be determined from these element properties, and hence are related only to V_{xp}, ω_x/ω_θ, and e/r. The initial and limit yield torques for systems with more than four resisting elements are not identical but each of them is related to V_{xp}, ω_x/ω_θ, and e/r in a manner similar to the four-element system. This relationship may be expressed empirically in the following dimensionless form:

$$\frac{T_{Rp}}{V_{xp}\ r} = q\left[\left(\frac{\omega_\theta}{\omega_x}\right)^2 - \left(\frac{e}{r}\right)^2\right] \tag{3.9}$$

where q is a coefficient that depends on the number, type and location of resisting elements in the structure.

It can be shown (see Appendix III-F) that for systems with rectangular plans, Eq. 3.9 with $q = 1/\sqrt{3} = 0.577$ provides a lower bound for the initial yield torque; with $q = 0.86$ it leads to an upper bound (valid for systems with 100 resisting elements or less) for the limit yield torque. A value of q between the bounds of 0.577 and 0.86 is, therefore, appropriate to define the yield torque in the circular yield surface for the single-element model.

3.8 Single-Element Model: Summary

The inelastic response of a multi-element system, with same yield displacements for all resisting elements, can be determined to a useful degree of approximation by analyzing a single-element system with the following properties: parameters ω_x, ω_θ, e/r and ξ in the linearly elastic range of behavior are the same as for the multi-element system; a single yield surface, circular in the normalized coordinate system, with yield shear same as for the multi-element system and yield torque given by Eq. 3.9 with q having a value between 0.577 and 0.86. This range of q is appropriate for systems with eight or more resisting elements.

4. EFFECTS OF TORSIONAL COUPLING ON DEFORMATIONS

4.1 Introductory Note

The effects of torsional coupling are studied by comparing deformation responses of single-element models (Chapter 3) of torsionally coupled ($e \neq 0$) and corresponding torsionally uncoupled ($e = 0$) one-story systems. Results obtained by the procedures described are presented for systems analyzed under the assumption of linear and nonlinear behavior. The excitation selected is the first 30 sec. of the S00E component of the El Centro record obtained during the Imperial Valley earthquake of May 18, 1940 (Fig. 3.6).

4.2 System Properties

The basic parameters controlling linear response of idealized one-story systems (Fig. 2.1) are ω_x (or $T_x = 2\pi/\omega_x$), ω_θ/ω_x, e/r and ξ. The following values were selected for these parameters: T_x = several values in the range 0.5 to 2.0 sec.; ω_θ/ω_x = 0.8, 0.9, 1.0, 1.25, 1.5 and 2.0; e/r = 0, 0.2 and 0.4, and $\xi = 0.02$. The first of the e/r values indicates no torsional coupling and provides a basis for evaluating the effects of torsional coupling.

The selected values for T_x span a range of vibration periods which would include many multi-story buildings. Measured natural frequencies of vibration of buildings [11] indicate that the ratio of the natural frequency of the lowest torsion-dominant mode to that of the lowest translation-dominant mode of vibration varies between 1.0 and 1.8. If these measurements were for the system of Fig. 2.1, based on Eq. 2.7 it could be concluded that ω_θ/ω_x values would be within the range of 1.0 and 1.8. Considering the one-story system of Fig. 2.1 to be a three degree-of-freedom model to represent the three lowest vibration modes of a multi-story building, the above conclusion forms the basis for the chosen range of values for ω_θ/ω_x. Because $\omega_\theta/\omega_x < 1$ is uncommon unless the major resistance to lateral loads is provided by a central core, and $\omega_\theta/\omega_x > 2$ implies negligible torsional coupling [18], values for ω_θ/ω_x were chosen in the range 0.8 to 2.0. The chosen eccentricity ratios e/r = 0.2 and 0.4 represent significant eccentricities between the centers of mass and resistance (for a rectangular building plan, e/r = 0.4 represents eccentricity of 11.5 to 16.3% of the longer plan dimension) and e/r = 0 represents the corresponding torsionally uncoupled system. Because effects of torsional coupling decrease as damping increases [18], the damping ratio was assigned a value which is on the low side but yet reasonable for many buildings.

Corresponding to each linearly elastic system with specified parameters ω_x (or $T_x = 2\pi/\omega_x$), ω_θ/ω_x, e/r and ξ, an inelastic system is defined to have the same properties in its linear range of behavior. The yield shear in translation is specified in Table 1 as the base shear determined from Fig. 3.7, corresponding to the natural period T_x of the corresponding torsionally-uncoupled system and ductility factor $\mu = 5$. Yield torque for a system is specified as the torque determined from Eq. 3.9 with $q = 0.75$.

4.3 Response Characteristics

Response histories for a torsionally-coupled system and the corresponding system with no torsional coupling, analyzed for two different assumptions, linearly elastic and elastic-perfectly-plastic, of force-deformation behavior, are presented in Fig. 4.1.

Whereas systems, elastic or inelastic, with no torsional coupling respond only in translation, torsionally-coupled systems deform in translation as well as in torsion. Deformations of elastic systems, with or without torsional coupling, are oscillators about the initial equilibrium position. On the other hand, responses of inelastic systems are characterized by several increments in the plastic part of the deformation, each causing a shift in the equilibrium position about which the system oscillates until the next increment in plastic part of the deformation occurs. The oscillatory part of the lateral deformation as well as drift of the equilibrium position due to plastic deformation are affected by torsional coupling.

Torsional coupling affects the response of elastic systems to a greater degree compared to corresponding inelastic systems. It modifies the natural vibration periods and hence response amplitude and predominant frequencies of elastic systems. In the latter case, the response is strongly influenced by yielding properties of the system, and even with torsional coupling, yielding of the system is controlled primarily by the yield shear because the response is primarily in translation and the system is relatively strong in torsion. Consequently, after initial yielding, the system has a tendency to yield further primarily in translation and behave more and more like an

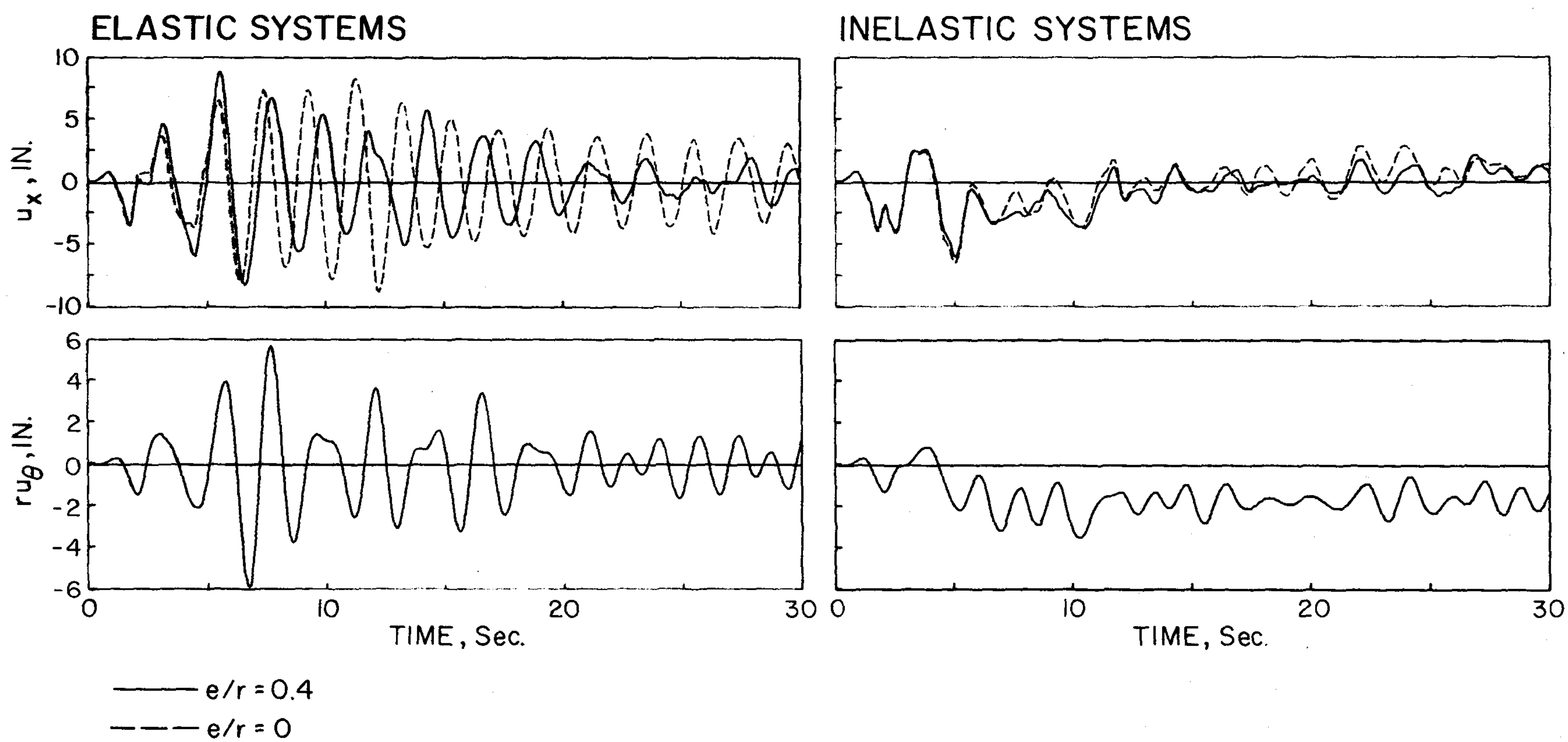

FIG. 4.1 RESPONSE OF ELASTIC AND INELASTIC SYSTEMS TO THE EL CENTRO EARTHQUAKE. SYSTEM PROPERTIES: T_x = 2 sec., ω_θ/ω_x = 1.25 AND ξ = 2%.

inelastic, single degree-of-freedom (SDOF) system, responding primarily in translation; thus, torsional deformations and effects of torsional coupling on translational deformations are not as large as they were for elastic systems.

4.4 Maximum Deformations

For each single-element system defined in Sec. 4.2, a complete set of results, including variation of response with time, were obtained by numerical integration of the equations of motion. However, only the maximum lateral and torsional deformations are presented. They are presented as a function of T_x for the three values of e/r in Figs. 4.2-4.7; each figure is for systems with fixed values of ω_θ/ω_x. In Figs. 4.8-4.9 they are presented as functions of T_x for varying values of ω_θ/ω_x but a fixed value of e/r.

In order to interpret these results, it is useful to summarize selected conclusions from an earlier study based on maximum responses of linearly elastic systems determined for two idealized response spectra, flat (or period independent) pseudo-acceleration spectrum and hyperbolic pseudo-acceleration spectrum (or flat pseudo-velocity spectrum) [18]:

1. Torsional coupling results in torque (and torsional deformation); and smaller values for base shear (and lateral deformation).
2. As e/r increases, torsional coupling has increased effect: shear (and lateral deformation) decreases, torque (and torsional deformation) increases.
3. The effects of torsional coupling depend strongly on ω_θ/ω_x, the ratio of uncoupled frequencies of the system. For systems with smaller values of e/r (less than 0.4), this effect is most pronounced when $\omega_\theta = \omega_x$.
4. For systems with uncoupled frequency in torsion much higher than in translation, $\omega_\theta > 2\omega_x$, torsional coupling results in essentially no reduction in base shear; furthermore the torque is essentially proportional to e/r, indicating little dynamic amplification.

When actual ground motions, instead of idealized response spectra, are considered, responses of elastic as well as inelastic systems exhibit some,

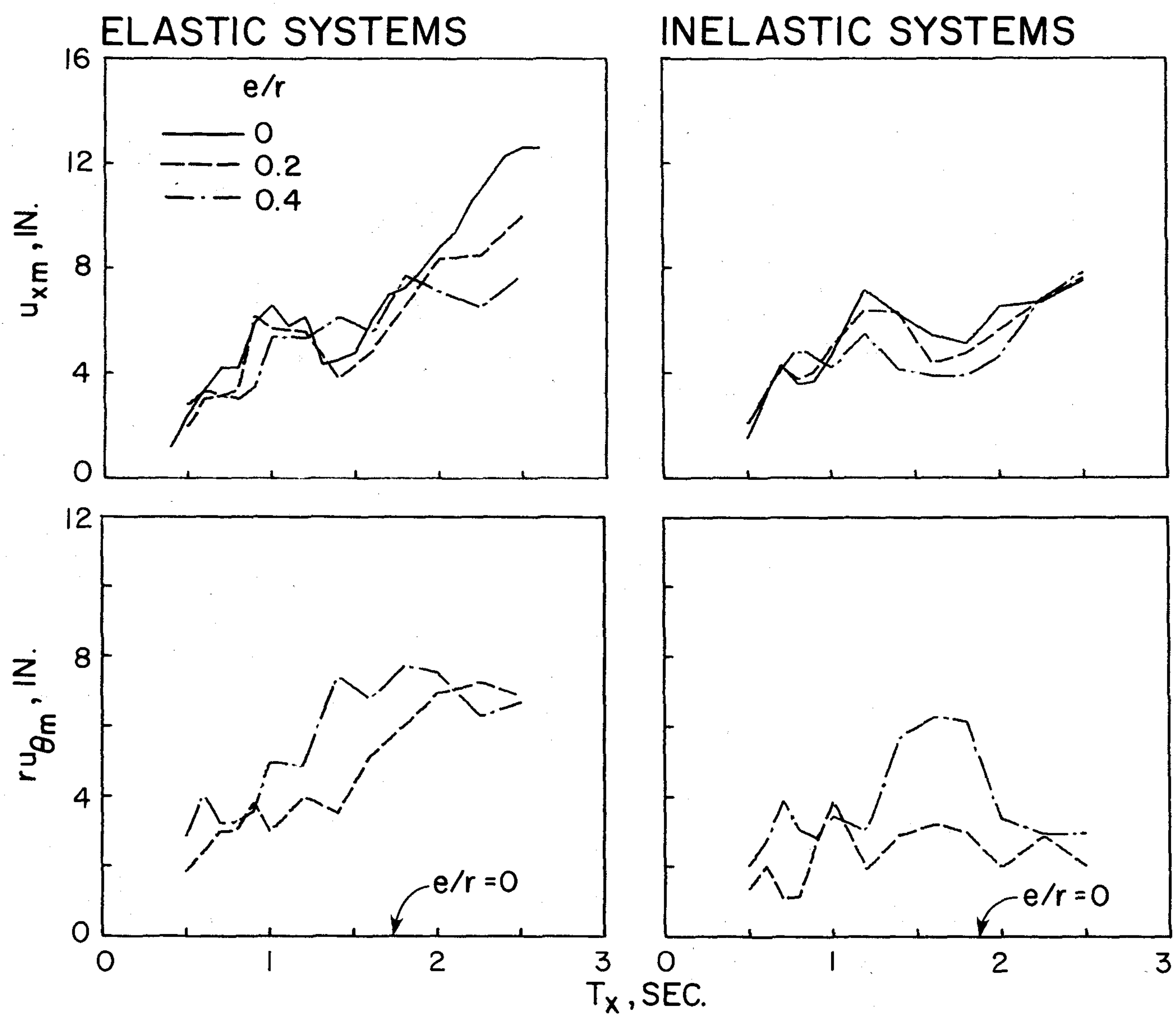

FIG. 4.2 MAXIMUM LATERAL AND TORSIONAL DISPLACEMENTS FOR ELASTIC AND INELASTIC SYSTEMS WITH ω_θ/ω_x = 0.8 SUBJECTED TO THE EL CENTRO EARTHQUAKE

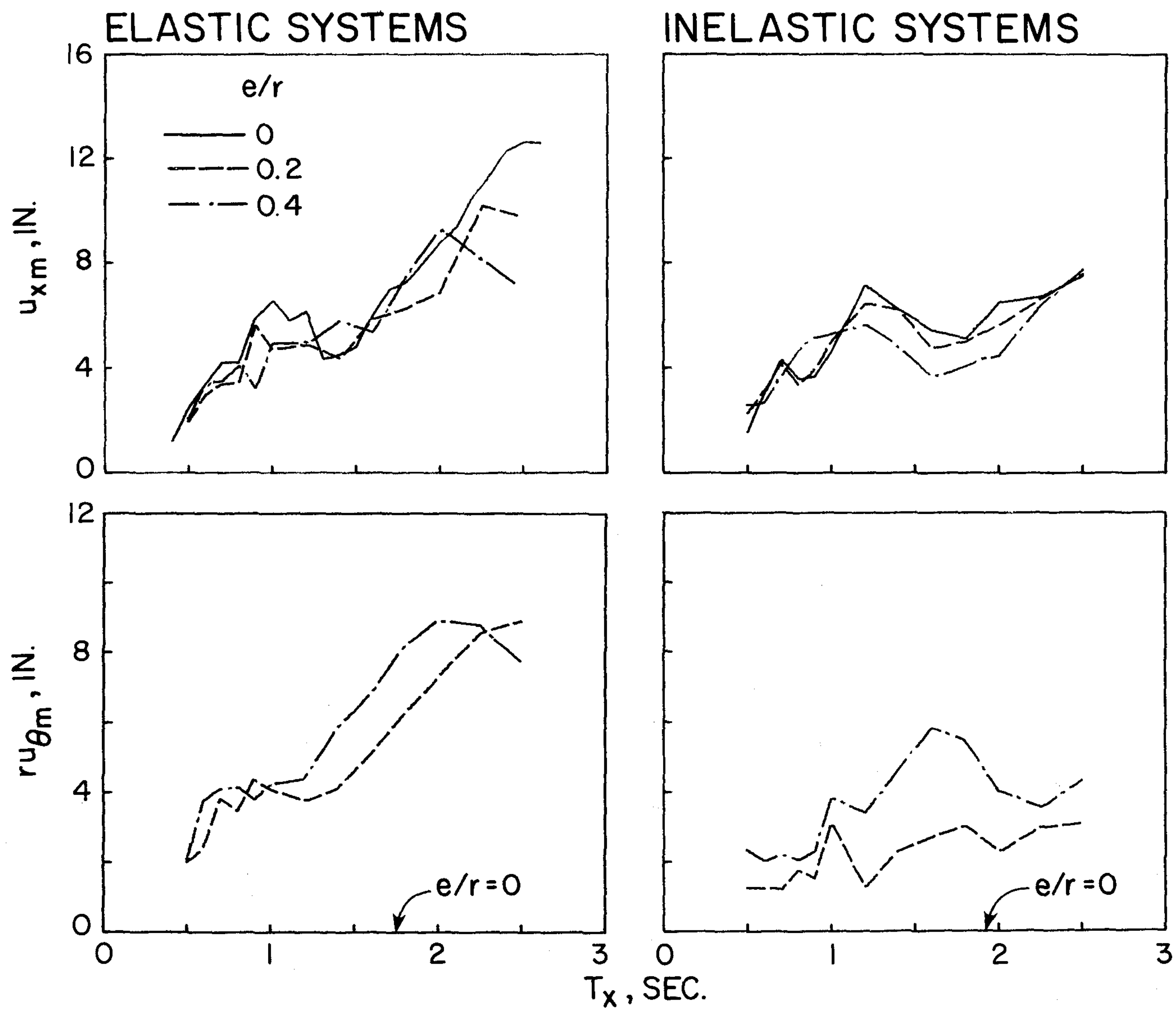

FIG. 4.3 MAXIMUM LATERAL AND TORSIONAL DISPLACEMENTS FOR ELASTIC AND INELASTIC SYSTEMS WITH ω_θ/ω_x = 0.9 SUBJECTED TO THE EL CENTRO EARTHQUAKE

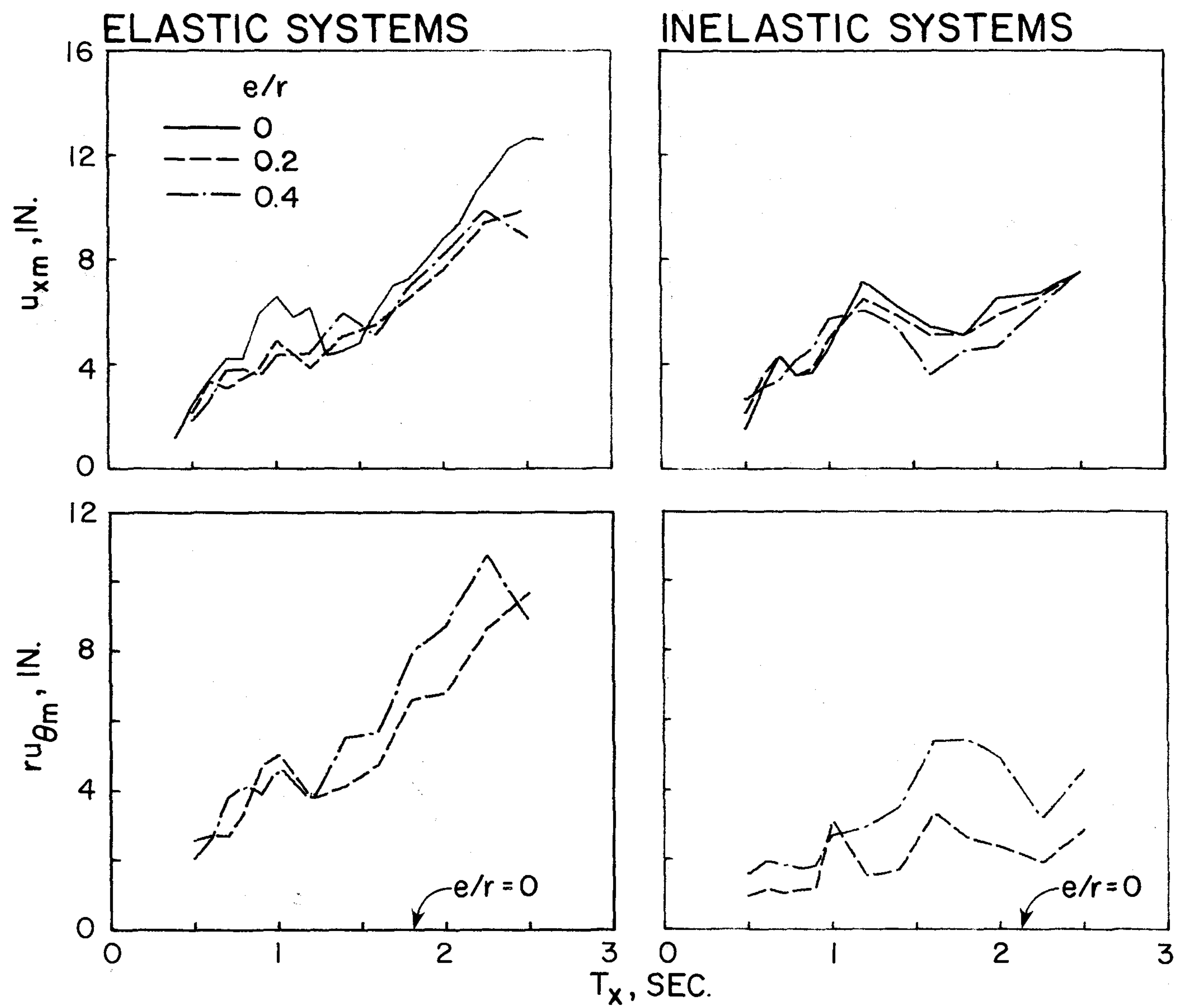

FIG. 4.4 MAXIMUM LATERAL AND TORSIONAL DISPLACEMENTS FOR ELASTIC AND INELASTIC SYSTEMS WITH ω_θ/ω_x = 1 SUBJECTED TO THE EL CENTRO EARTHQUAKE

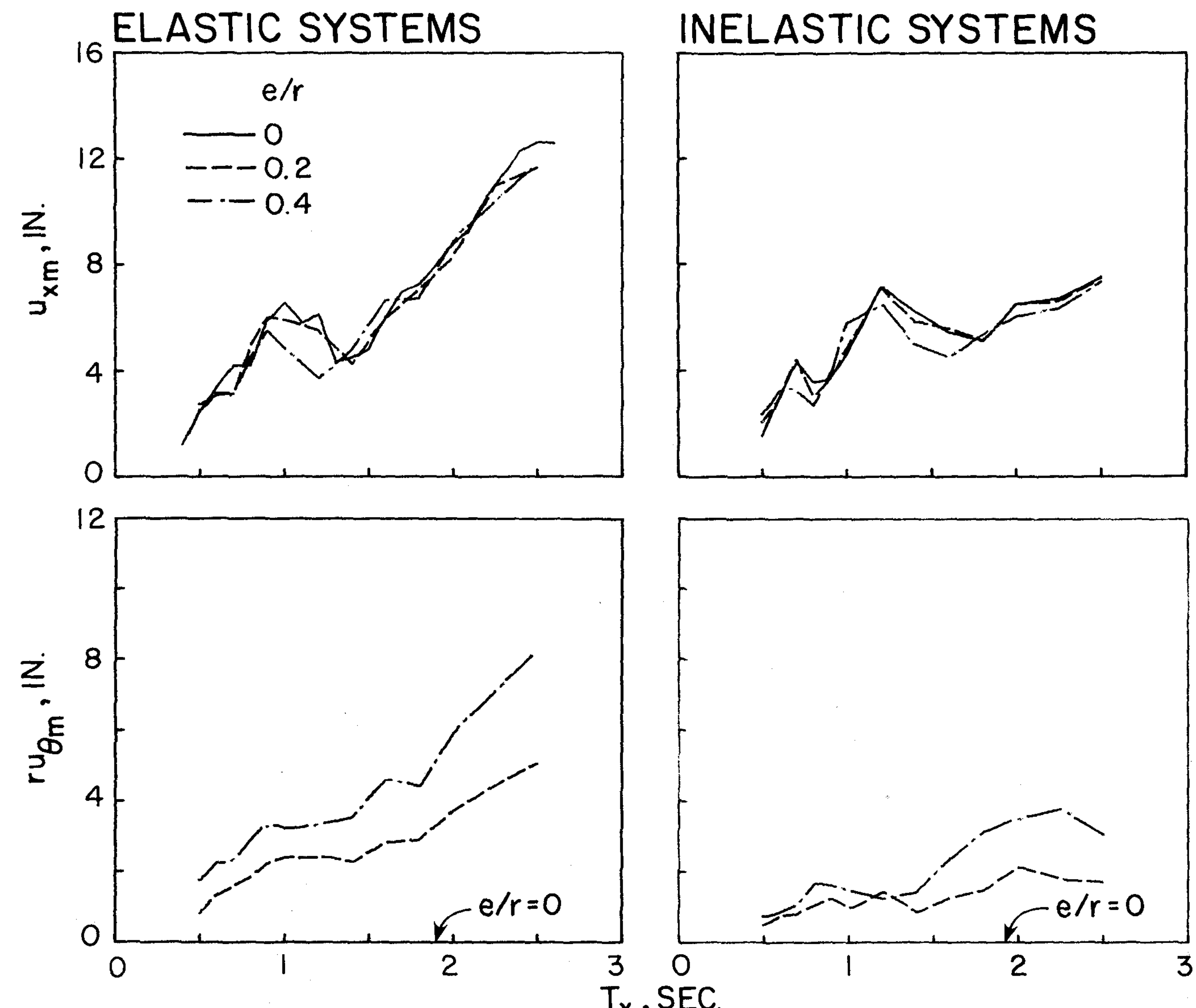

FIG. 4.5 MAXIMUM LATERAL AND TORSIONAL DISPLACEMENTS FOR ELASTIC AND INELASTIC SYSTEMS WITH ω_θ/ω_x = 1.25 SUBJECTED TO THE EL CENTRO EARTHQUAKE

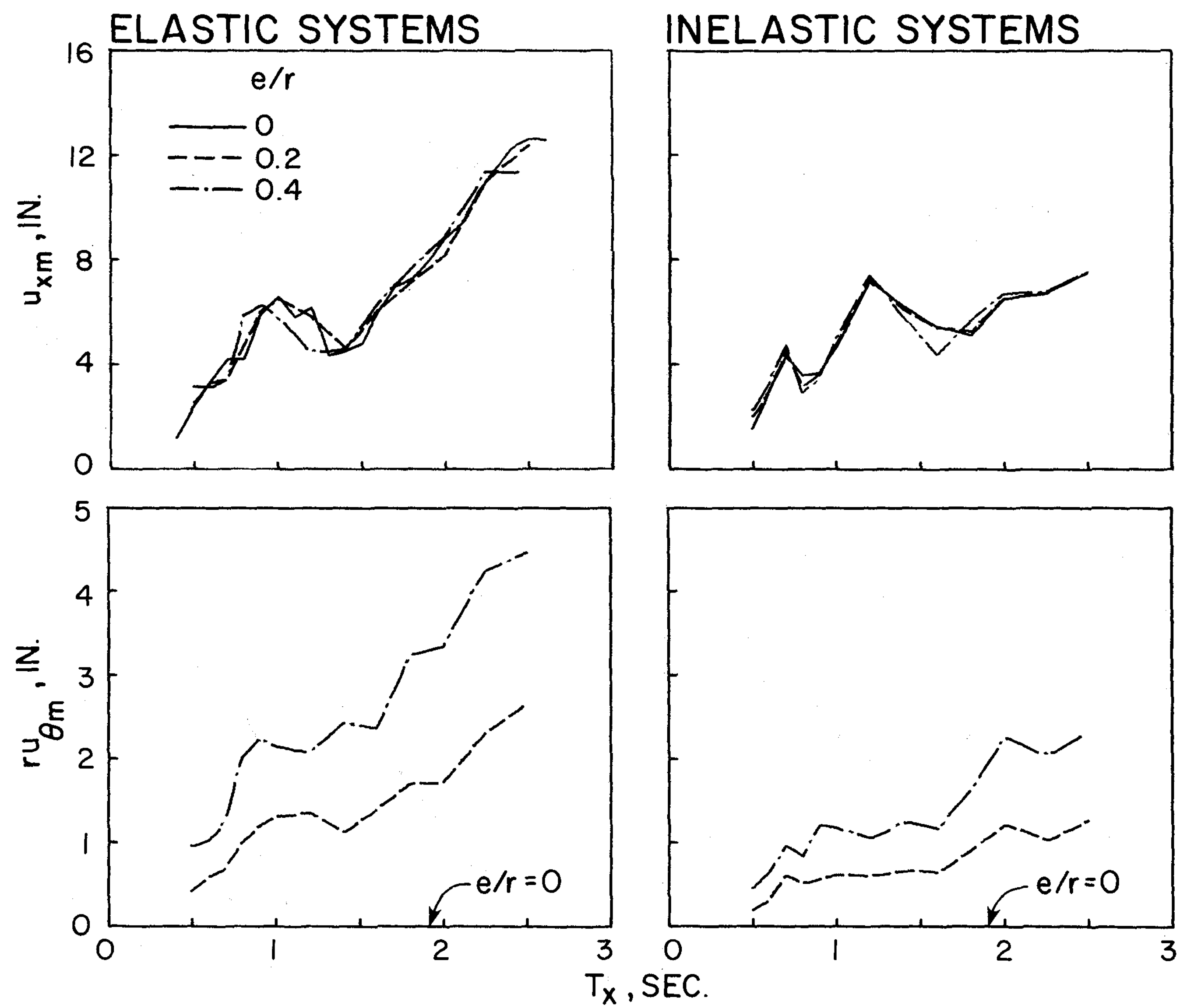

FIG. 4.6 MAXIMUM LATERAL AND TORSIONAL DISPLACEMENTS FOR ELASTIC AND INELASTIC SYSTEMS WITH ω_θ/ω_x = 1.5 SUBJECTED TO THE EL CENTRO EARTHQUAKE

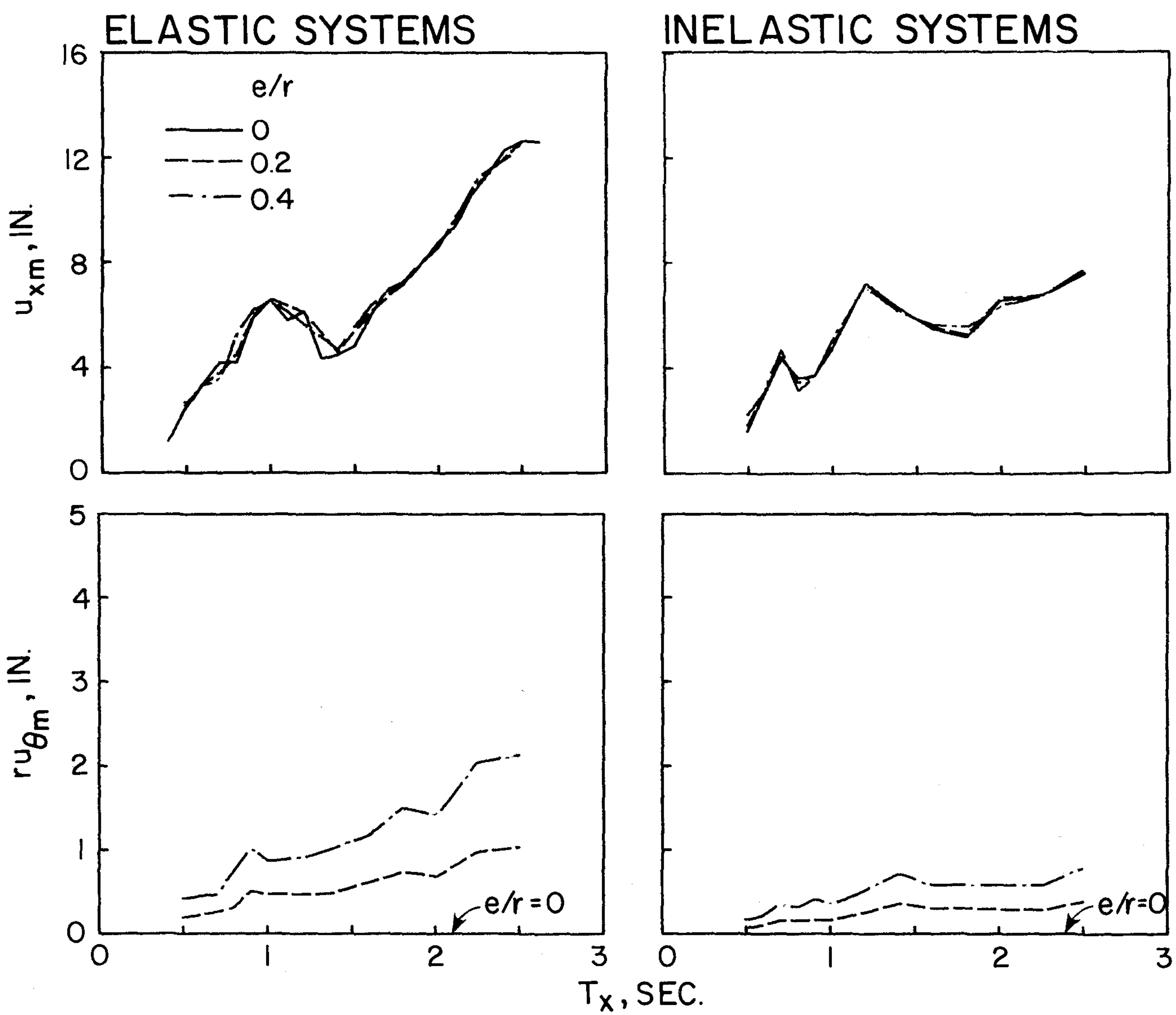

FIG. 4.7 MAXIMUM LATERAL AND TORSIONAL DISPLACEMENTS FOR ELASTIC AND INELASTIC SYSTEMS WITH $\omega_\theta/\omega_x = 2$ SUBJECTED TO THE EL CENTRO EARTHQUAKE

but not all, of the results summarized above:

1. Torsional coupling causes torsional deformations and modifies lateral deformations, reduction for some values of T_x but increase for others (Figs. 4.2-4.7).
2. As e/r increases, the effects of torsional coupling may or may not increase; lateral deformations decrease for some values of T_x but increase for other values; torsional deformations increase for all, except very few, values of T_x (Figs. 4.2-4.7).
3. For systems with $\omega_\theta/\omega_x = 2$, torsional coupling produces little modification in the lateral deformation and the torsional deformation is essentially proportional to e/r, indicating no dynamic amplification (Fig. 4.7).
4. The effects of torsional coupling — change in lateral deformation and increase in torsional deformation — depend on ω_θ/ω_x (Fig. 4.8-4.9) but not as strongly, nor in as simple a manner, as was mentioned above for idealized response spectra. As ω_θ/ω_x approaches 1 from above, the torsional deformation of elastic systems, and almost all inelastic systems, increases over the entire range of T_x considered; however, there is no consistent variation in the lateral deformation, decreasing for some values of T_x and increasing for others. As ω_θ/ω_x approaches 1 from below, the effects of torsional coupling vary with ω_θ/ω_x in not a simple manner.

The general impression that emerges from the above results is that effects of torsional coupling on earthquake response are similar but not as simple as were observed from maximum responses determined for idealized response spectra. Complications arise basically because the response spectrum of an actual ground motion is rather irregular compared to the flat or hyperbolic shapes assumed for the idealized acceleration response spectrum. Torsional coupling affects the natural periods of vibration of the system and hence the corresponding spectrum ordinates. Depending on the variation of the response spectrum in the neighborhood of T_x, these ordinates may increase or decrease by varying degrees, resulting in another factor influencing the differences between the responses of torsionally coupled and uncoupled systems.

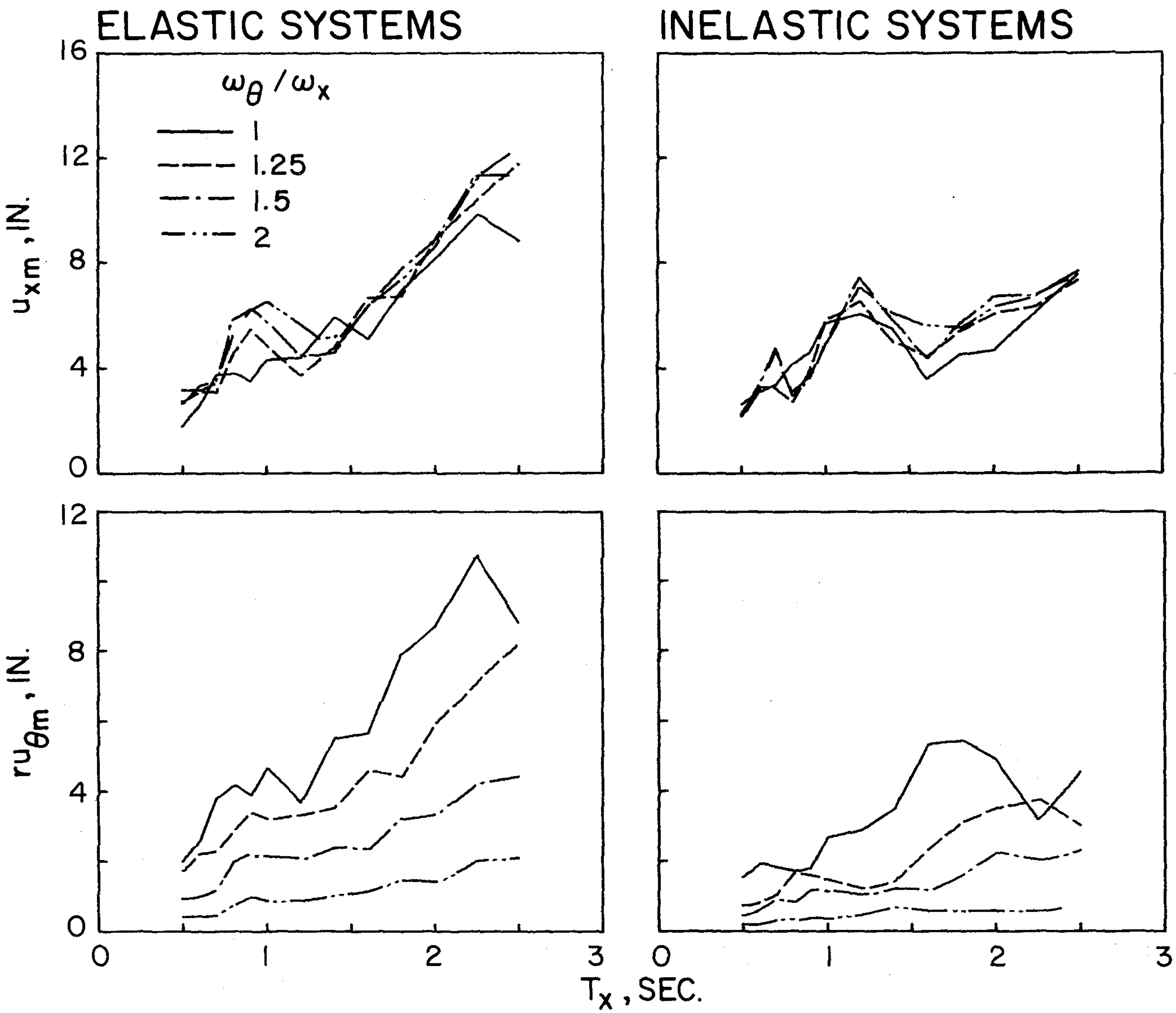

FIG. 4.8 MAXIMUM LATERAL AND TORSIONAL DISPLACEMENTS FOR ELASTIC AND INELASTIC TORSIONALLY COUPLED SYSTEMS WITH e/r = 0.4 SUBJECTED TO THE EL CENTRO EARTHQUAKE

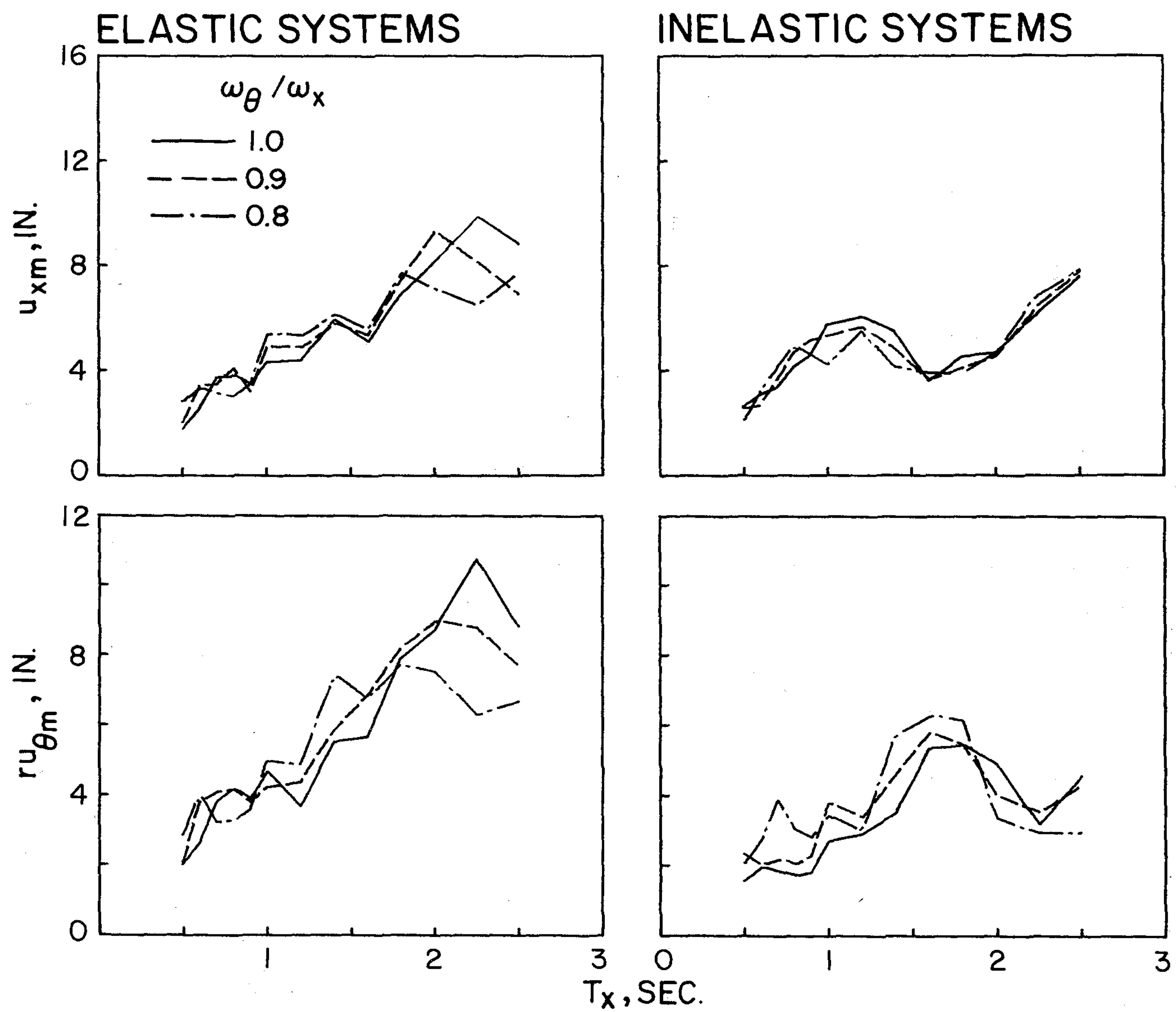

FIG. 4.9 MAXIMUM LATERAL AND TORSIONAL DISPLACEMENTS FOR ELASTIC AND INELASTIC TORSIONALLY COUPLED SYSTEMS WITH e/r = 0.4 SUBJECTED TO THE EL CENTRO EARTHQUAKE

Torsional coupling influences the maximum deformation response of inelastic systems to a lesser degree compared to linearly elastic systems (Figs. 4.2-4.9), for reasons mentioned in Sec. 4.3. Except for that one difference, inelastic and elastic systems are affected similarly by torsional coupling.

5. EFFECTS OF TORSIONAL COUPLING ON COLUMN DEFORMATIONS

5.1 Introductory Note

The deformation of a resisting element results from the combined effect of lateral and torsional displacements at the C.M. Having studied in Chapter 4 the effects of torsional coupling on displacement response at the C.M., results for the deformations of corner columns are presented and interpreted in this section. Recall that the displacements at the C.M. of a torsionally coupled system were determined from analysis of a single-element model of the system. For a specified set of system parameters, the plan geometry does not affect these results but, of course, influences the deformations of corner columns.

5.2 Column Deformations and Displacements at Center of Mass

Considering rectangular plans with several resisting elements, including columns at the four corners (Fig. 5.1), u_{ix} and u_{iy}, the x and y components of the deformation of column i (displacement of the top of the column relative to its bottom) can be expressed in terms of u_x and u_θ, the lateral and torsional displacements at the C.M., simply from the geometry of displacement (Fig. 5.1):

$$\begin{aligned}
\frac{u_{ix}}{u_x} &= 1 - \frac{a}{r}\left(\frac{ru_\theta}{u_x}\right) & i &= 1,2 \\
\frac{u_{ix}}{u_x} &= 1 + \frac{a}{r}\left(\frac{ru_\theta}{u_x}\right) & i &= 3,4 \\
\frac{u_{iy}}{u_x} &= \frac{b}{r}\left(\frac{ru_\theta}{u_x}\right) & i &= 1,4 \\
\frac{u_{iy}}{u_x} &= -\frac{b}{r}\left(\frac{ru_\theta}{u_x}\right) & i &= 2,3
\end{aligned} \tag{5.1}$$

The total vector-deformation of the column i

$$u_i = \sqrt{u_{ix}^2 + u_{iy}^2} \tag{5.2}$$

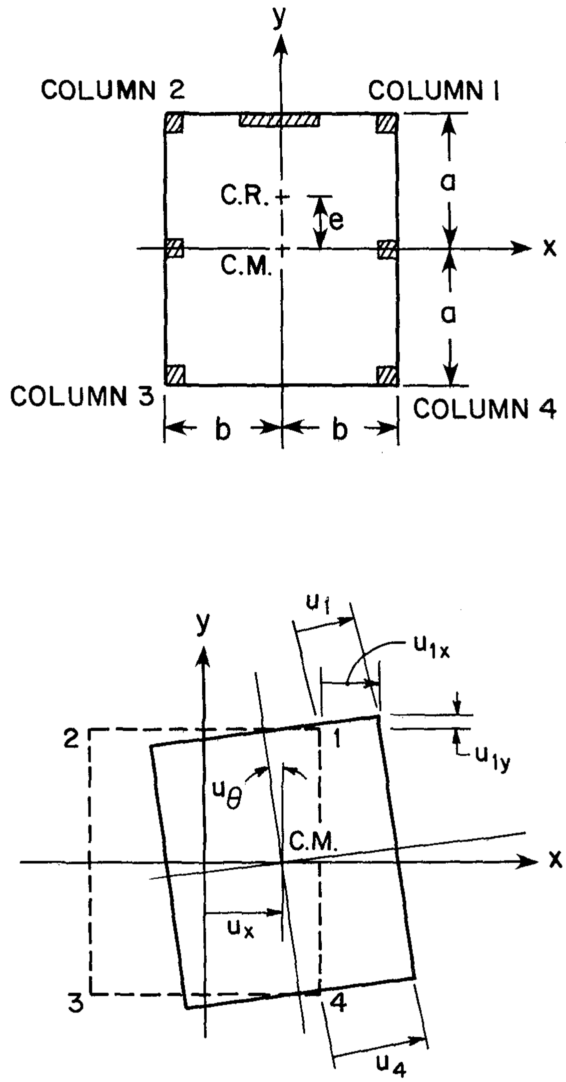

FIG. 5.1 RECTANGULAR PLAN AND ITS DISPLACED CONFIGURATION

It is necessary to examine the results for only two columns, say 1 and 4, because from Eqs. 5.1 and 5.2

$$u_1 = u_2 \quad \text{and} \quad u_3 = u_4 \tag{5.3}$$

Column 1 is located closer to C.R. compared to column 4.

5.3 Response to Static Lateral Force

To aid in interpreting the results to be presented later for column deformations in torsionally-coupled systems subjected to earthquake ground motion, it will be useful to consider first the effects of a static lateral force, V_x, applied at the C.M. The deformations u_i of the four columns expressed as ratios with u_x are given by Eqs. 5.1 and 5.2, wherein (it can be easily shown)

$$\frac{ru_\theta}{u_x} = \frac{e}{r}\left(\frac{\omega_x}{\omega_\theta}\right)^2 \tag{5.4}$$

Furthermore, for rectangular plans

$$\frac{a}{r} = \sqrt{\frac{3}{1 + (b/a)^2}} \quad \text{and} \quad \frac{b}{r} = \frac{b}{a}\left(\frac{a}{r}\right) \tag{5.5}$$

Consequently, ratios u_i/u_x depend only on the dimensionless parameters e/r, ω_θ/ω_x, and a/b. They are presented as functions of ω_θ/ω_x for selected values of e/r and a/b (Fig. 5.2). If the system is torsionally uncoupled $u_i/u_x = 1$; differences between this value and those presented in Fig. 5.2 may, therefore, be interpreted as effects of torsional coupling on column deformations. Torsional coupling causes an increase in the deformation in the column farthest from the C.R. but generally a decrease in the deformation of the column nearest the C.R. Torsional coupling has increased effects, i.e., u_4/u_x increases and u_1/u_x decreases, with increasing e/r for fixed a/b; and with increasing a/b for fixed e/r.

5.4 Earthquake Responses

Responses of an elastic and corresponding inelastic single-element system

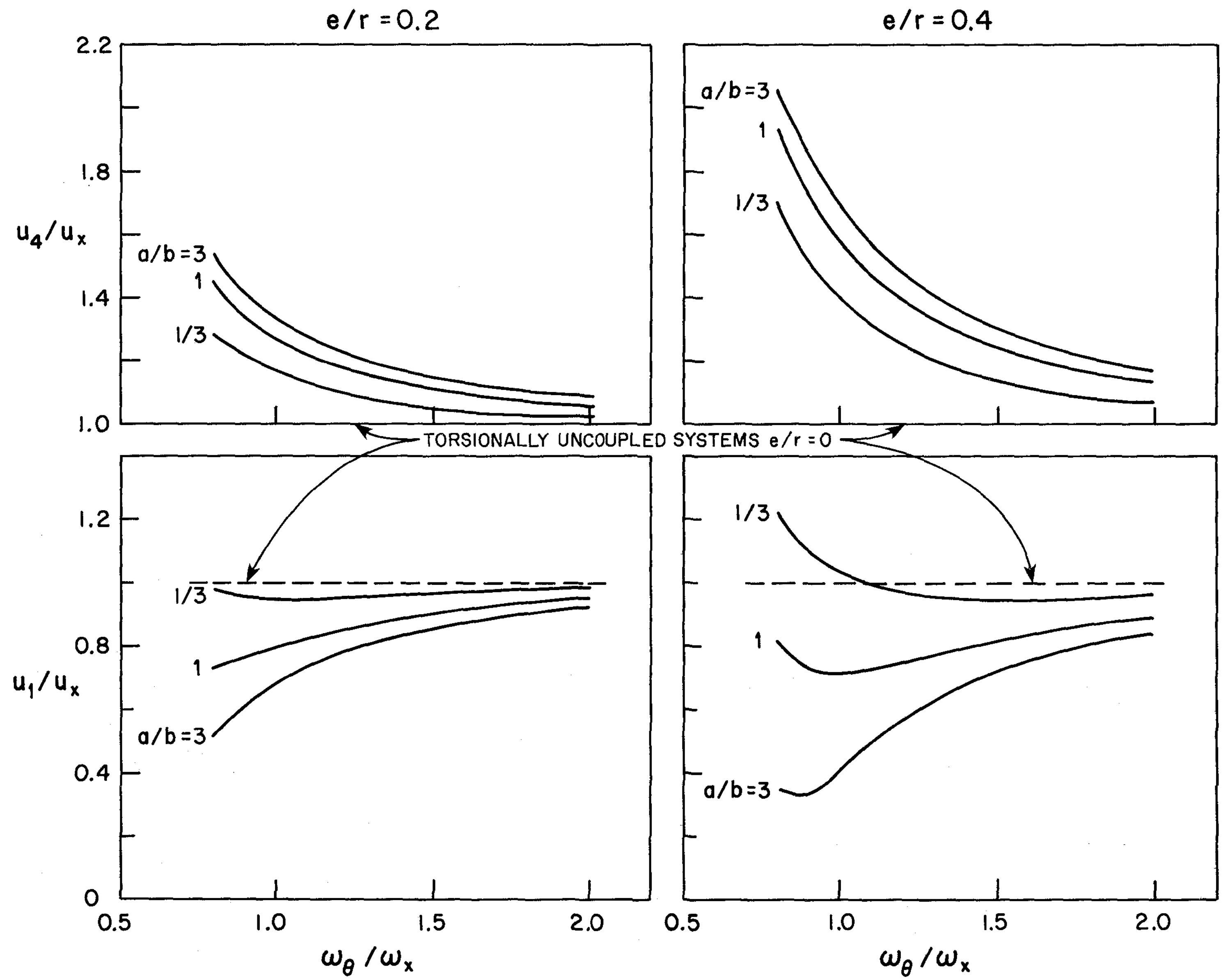

FIG. 5.2 RATIOS OF CORNER COLUMN DEFORMATIONS TO LATERAL DISPLACEMENT AT C.M. FOR A STATIC SHEAR FORCE APPLIED AT C.M.

to the El Centro earthquake acting along the x-axis were obtained in Chapter 4 for several values of the system parameters: T_x, ω_θ/ω_x, and e/r. From the history of displacements at C.M. of each system (specified T_x, ω_θ/ω_x and e/r) deformations of corner columns were determined by applying Eqs. 5.1 and 5.2 at each instant of time. Ratios u_{im}/u_{xm}, where u_{im} and u_{xm} are respectively the maximum values of displacements during the earthquake at column i and at C.M., were then computed for several different values of the aspect ratio a/b of the rectangular plan.

Results for systems with $\omega_\theta/\omega_x = 2$ are presented as functions of T_x for a fixed value of a/b but two values of e/r (Fig. 5.3) and for a fixed value of e/r but three values of a/b (Fig. 5.4). Also shown superimposed for elastic systems are the u_i/u_x values from Fig. 5.2 associated with a static lateral force acting at the C.M. Whereas these are independent of T_x, the u_{im}/u_{xm} values obtained from response to earthquake ground motion are not. This dependence on T_x is, however, weak and is associated with changes in earthquake responses due to changes in vibration periods caused by torsional coupling. Similar to the conclusions for systems subjected to static force, torsional coupling causes increase and decrease in the deformations of columns farthest and nearest, respectively, from the C.R. (Figs. 5.3 and 5.4); and effects of torsional coupling increase with increasing e/r (Fig. 5.3) and increasing a/b (Fig. 5.4). It is therefore concluded that for systems with $\omega_\theta/\omega_x = 2$ the effects of torsional coupling on column deformations are similar whether the deformations are induced by earthquake motion or static lateral force. This observation is consistent with the one of Sec. 4.4, indicating that for systems with $\omega_\theta/\omega_x \geq 2$ effects of torsional coupling on displacements at C.M. are similar whether they are due to earthquake motion or static lateral force.

In Figs. 5.3-5.4, the effects of torsional coupling on deformations of corner columns are less for inelastic systems than for elastic systems. Because the yield torque increases with the square of ω_θ/ω_x (Eq. 3.9), systems with $\omega_\theta/\omega_x = 2$ are relatively strong in torsion. As a result, it is the yield shear that controls the initial yielding, and subsequently the system has a tendency to yield further primarily in translation and behave more and more like an inelastic, single degree-of-freedom system, responding primarily in translation; thus the effects of torsional coupling on column

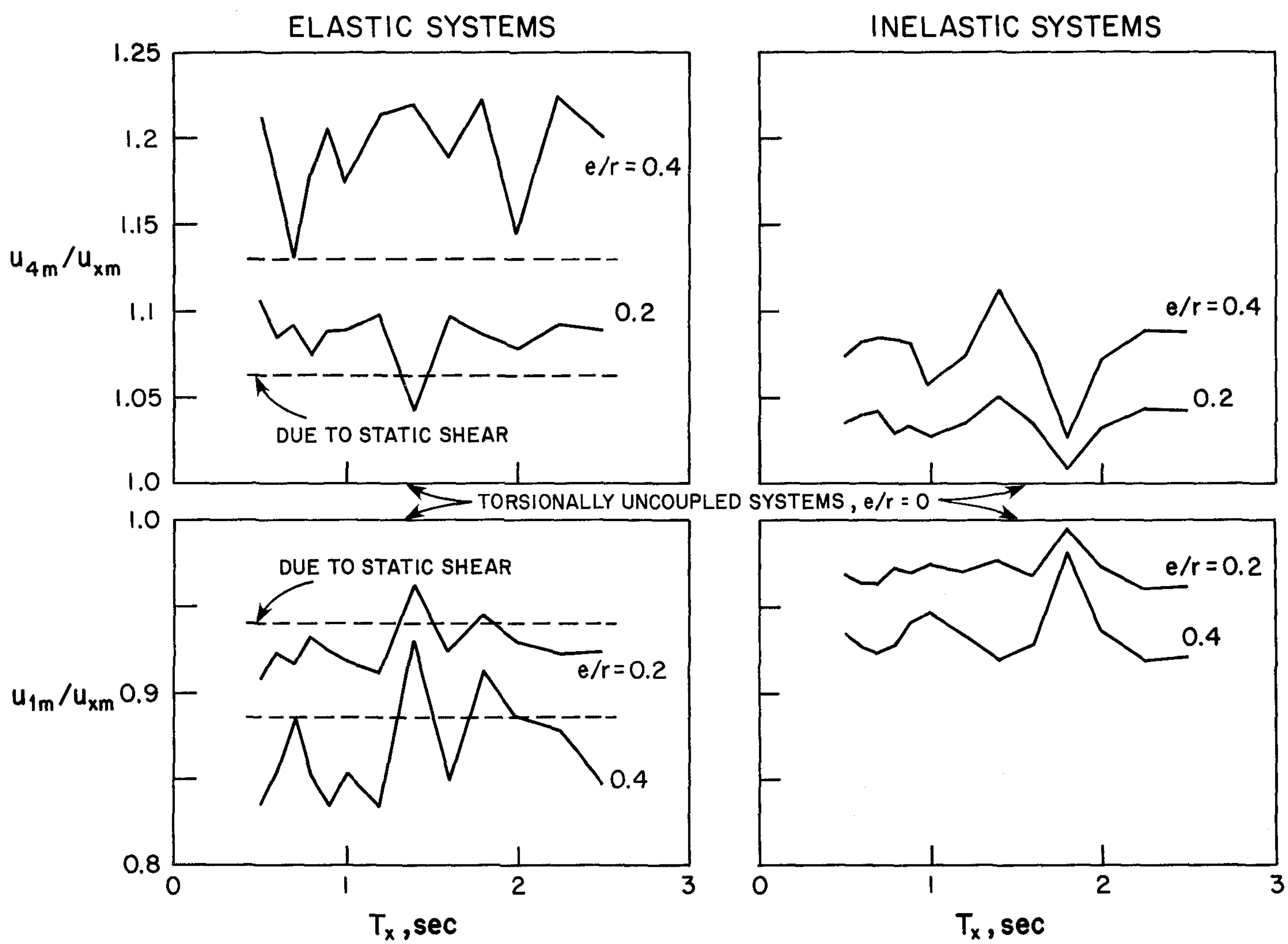

FIG. 5.3 RATIOS OF CORNER COLUMN DEFORMATION u_{im} TO LATERAL DISPLACEMENT AT C.M. u_{xm} FOR SYSTEMS WITH $a/b = 1$ and $\omega_\theta/\omega_x = 2$ SUBJECTED TO THE EL CENTRO EARTHQUAKE

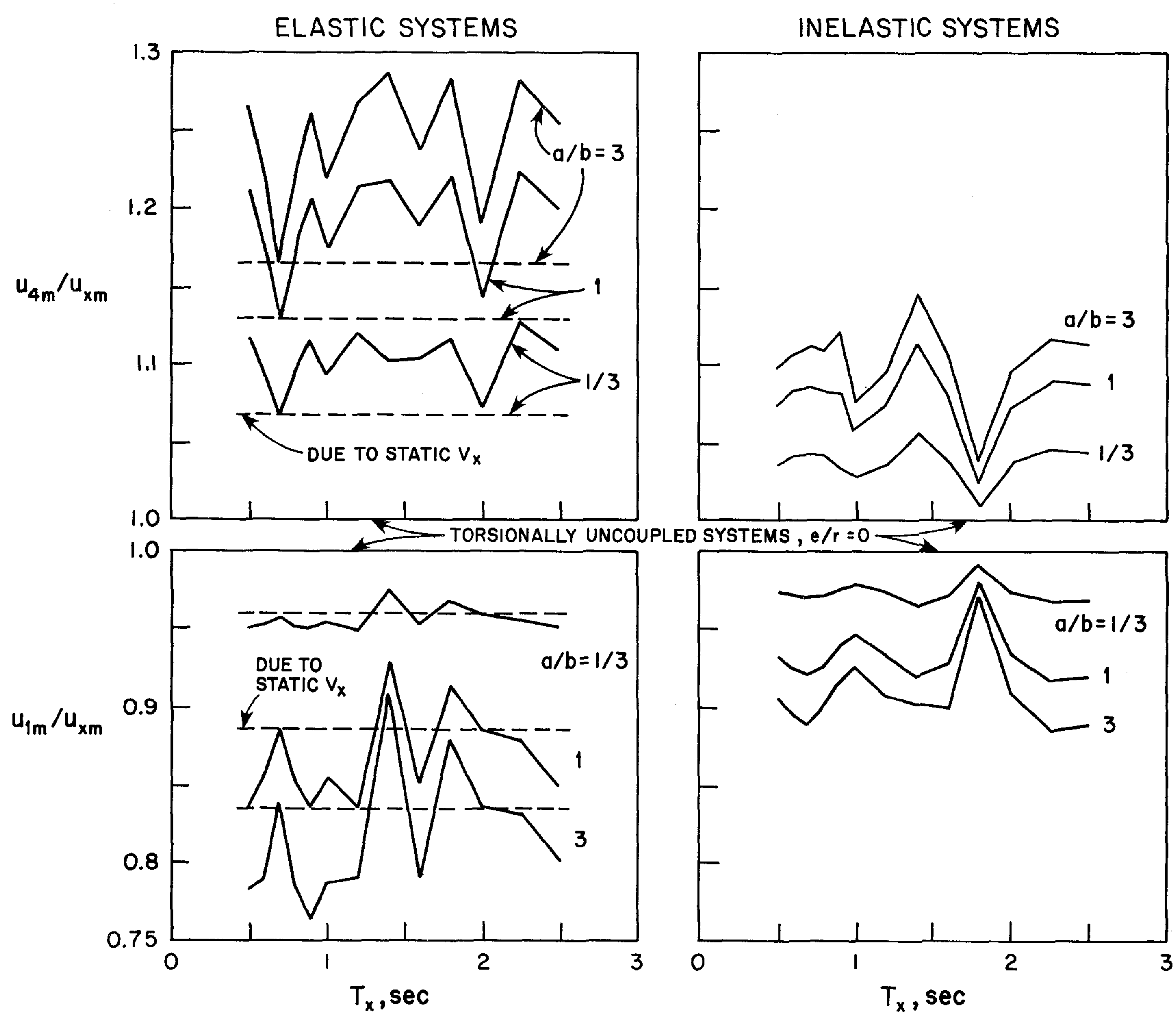

FIG. 5.4 RATIOS OF CORNER COLUMN DEFORMATION u_{im} TO LATERAL DISPLACEMENT AT C.M. u_{xm} FOR SYSTEMS WITH $\omega_\theta/\omega_x = 2$ AND $e/r = 0.4$ SUBJECTED TO THE EL CENTRO EARTHQUAKE

deformations are not as large as they are for elastic systems.

The deformation ratios u_{im}/u_{xm} are presented for systems with $\omega_\theta/\omega_x = 1$ as functions of T_x for a fixed value of a/b but two values of e/r (Fig. 5.5) and for a fixed value of e/r but several values of a/b (Fig. 5.6). As discussed in Sec. 4.4, the effects of torsional coupling are especially pronounced for systems with $\omega_\theta = \omega_x$, and this is reflected in the results for column deformations: u_{im}/u_{xm} are considerably different than 1, the value with no torsional coupling. It is of interest to compare the ratio u_i/u_x obtained from deformations due to (1) a static lateral force through the C.M. (Fig. 5.2) and (2) earthquake ground motion (Figs. 5.5-5.6). Whereas in the former case the u_1/u_x ratio is typically smaller than 1 and $u_4 > u_1$ (Fig. 5.2), in the latter case $u_1/u_x > 1$ and for some systems $u_4 < u_1$, a consequence of the large earthquake-induced torques in systems with $\omega_\theta/\omega_x = 1$. The deformation ratios u_{im}/u_{xm} tend to increase with e/r (Fig. 5.5) and also have some, but not consistent, tendency to increase with a/b (Fig. 5.6).

For systems with parameter values $\omega_\theta/\omega_x = 1$ and e/r = 0.2, torsional coupling affects column deformations in inelastic systems to a lesser degree compared to elastic systems (Fig. 5.5). This result is similar to the one observed earlier for systems with $\omega_\theta/\omega_x = 2$ (Figs. 5.3-5.4). However, inelastic systems can be affected to a greater degree; witness the large peak in the neighborhood of $T_x = 1.6$ sec. for systems with e/r = 0.4. This very pronounced effect of torsional coupling is a consequence of especially unfavorable phasing of u_x and u_θ resulting in their maximum values to occur almost simultaneously.

As discussed in Sec. 4.4, the effects of torsional coupling on u_x and u_θ, the lateral and torsional displacements of C.M., depend on ω_θ/ω_x in a complicated manner. Because column deformations u_i depend on u_x and u_θ, variation of deformation ratios u_{im}/u_{xm} with ω_θ/ω_x is similarly complicated (Fig. 5.7). Because of torsional coupling, column deformations can be considerably amplified, by a factor as large as 2 to 3 for systems with $\omega_\theta/\omega_x = 1$ (Fig. 5.7).

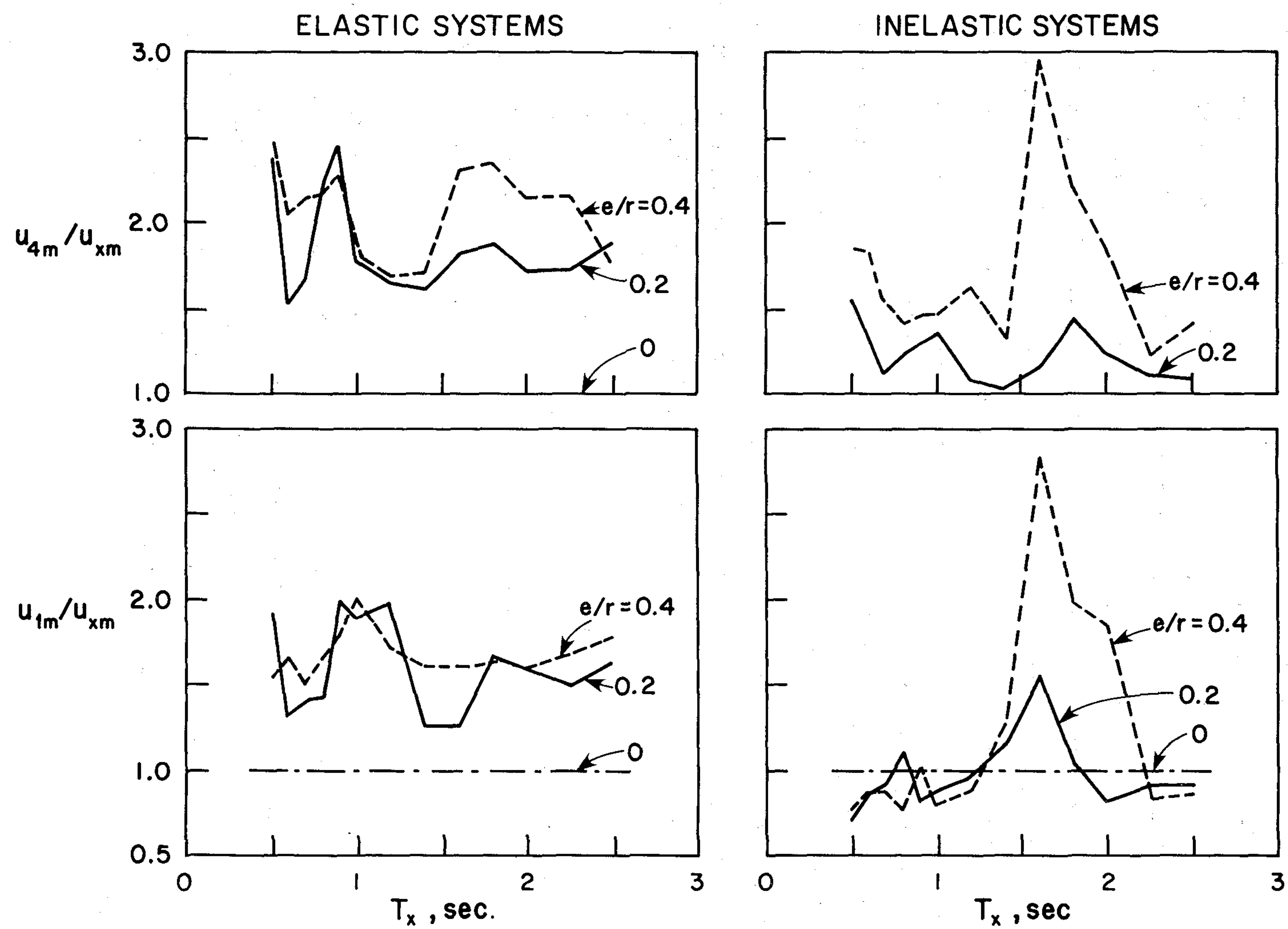

FIG. 5.5 RATIOS OF CORNER COLUMN DEFORMATION u_{im} TO LATERAL DISPLACEMENT AT C.M. u_{xm} FOR SYSTEMS WITH $a/b = 1$ AND $\omega_\theta/\omega_x = 1$ SUBJECTED TO THE EL CENTRO EARTHQUAKE

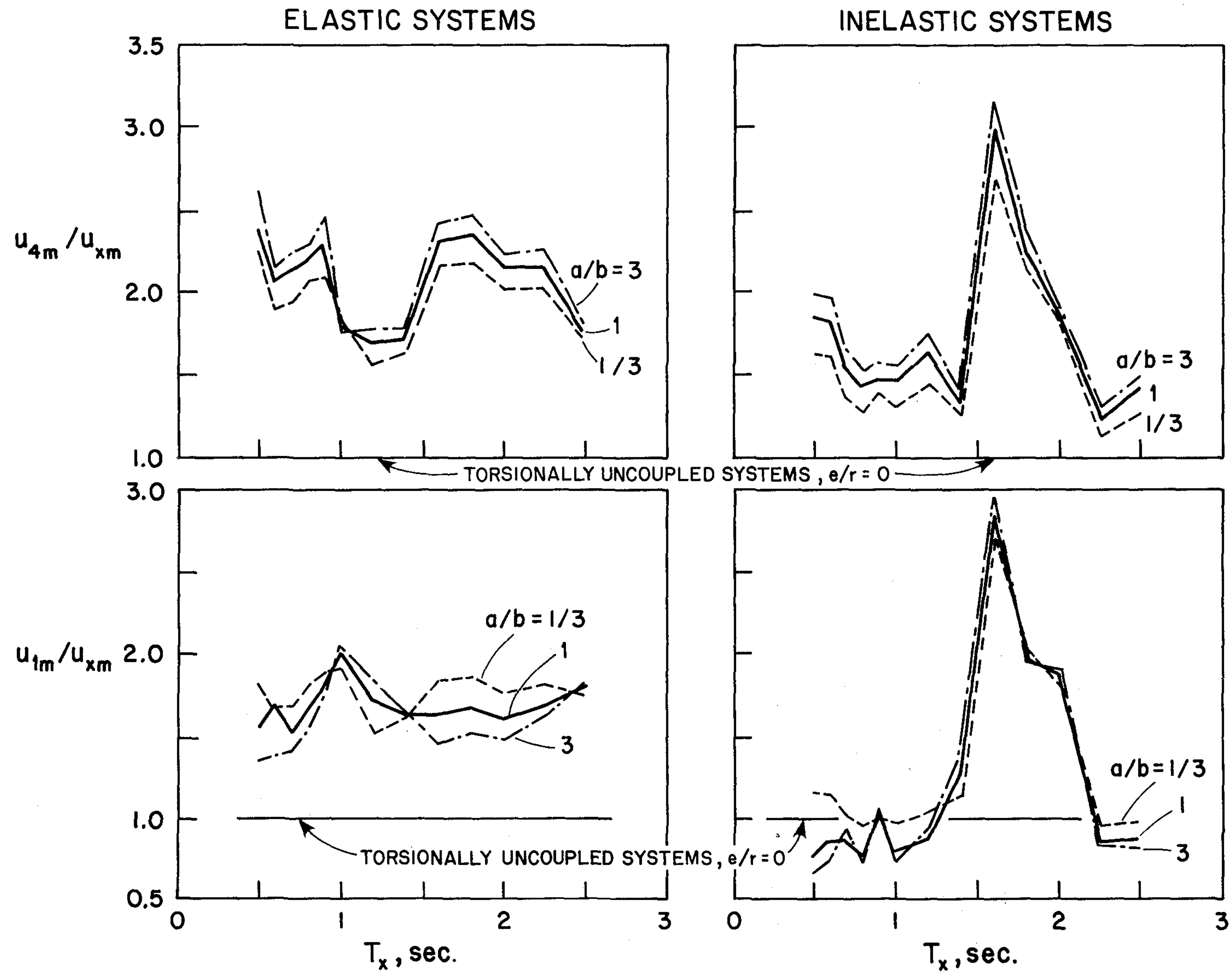

FIG. 5.6 RATIOS OF CORNER COLUMN DEFORMATION u_{im} TO LATERAL DISPLACEMENT AT C.M. u_{xm} FOR SYSTEMS WITH $\omega_\theta/\omega_x = 1$ AND $e/r = 0.4$ SUBJECTED TO THE EL CENTRO EARTHQUAKE.

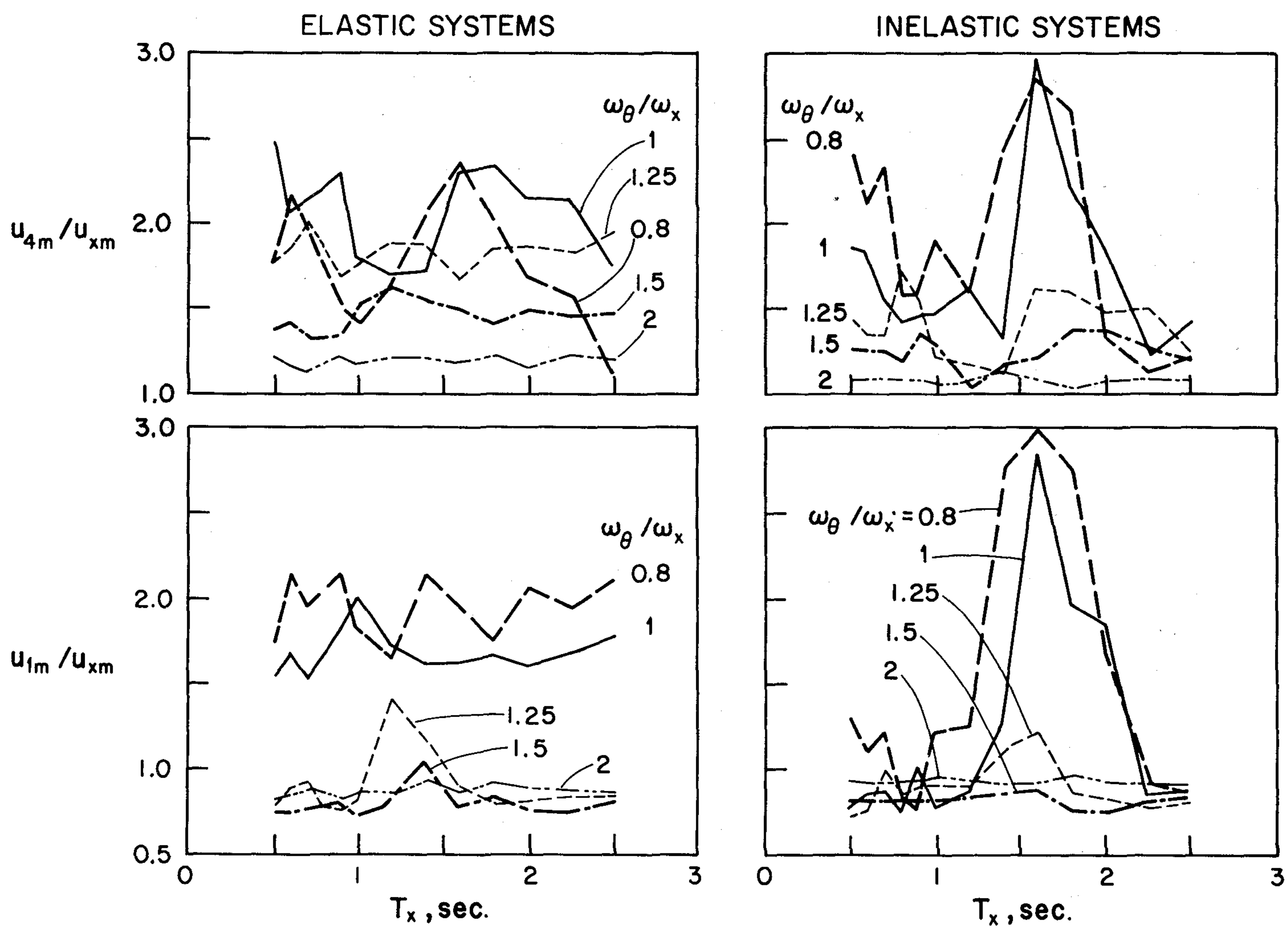

FIG. 5.7 RATIOS OF CORNER COLUMN DEFORMATION u_{im} TO LATERAL DISPLACEMENT AT C.M. u_{xm} FOR SYSTEMS WITH a/b = 1 AND e/r = 0.4 SUBJECTED TO THE EL CENTRO EARTHQUAKE.

6. ESTIMATION OF MAXIMUM COLUMN DEFORMATIONS

6.1 Introductory Note

The deformation of a resisting element, such as a column, results from the combined effect of lateral and torsional displacements at the C.M., and it will be largest for an element at a corner. At any instant of time, u_{ix} and u_{iy}, the x and y components of the deformation of column i, can be expressed in terms of u_x and u_θ, the lateral and torsional displacements at the C.M., at the same time, simply from the geometry of displacement (Eq. 5.1). Thus, the complete history of u_x and u_θ is needed to calculate the history and, subsequently, the maximum values of column deformations. As will be seen in Chapter 7, u_{xm} and $u_{\theta m}$, the maximum values of $u_x(t)$ and $u_\theta(t)$, can be estimated for elastic as well as inelastic systems by using the appropriate response spectrum. Presented in this chapter is a procedure for estimating the maximum value of deformation in a column directly from the maximum values of displacements, u_{xm} and $u_{\theta m}$, at the C.M.

6.2 Upper Bounds

An upper bound for maximum column deformations may be obtained by assuming that the maximum lateral and torsional displacements at the C.M. occur simultaneously. If u_{xm} and $u_{\theta m}$ denote the absolute value of these maxima, and the building plan is rectangular (Fig. 5.1), an upper bound for the x-component of the deformation of any column is

$$U_x = u_{xm} + \left(\frac{a}{r}\right) ru_{\theta m} \tag{6.1}$$

and the maximum value of the y-component of the deformation of any column is

$$U_y = \left(\frac{b}{r}\right) ru_{\theta m} \tag{6.2}$$

Thus, an upper bound estimate for the total vector-deformation of any column is

$$U = \sqrt{\left[u_{xm} + \left(\frac{a}{r}\right) ru_{\theta m}\right]^2 + \left(\frac{b}{r}\right)^2 (ru_{\theta m})^2} \tag{6.3}$$

This is an upper bound for the largest of the maximum deformations of individual columns.

An estimate obtained from Eq. 6.3 is compared with the larger of the "exact" maximum deformations in columns 1 and 4 obtained in Chapter 5 from a complete response history analysis. The "exact" values of u_{xm} and $ru_{\theta m}$, obtained in Chapter 4 from a response history analysis of the single-element model, were substituted in Eq. 6.3 to obtain the estimate. The ratio of estimated to "exact" values of maximum column deformation is presented for several elastic and inelastic systems as a function of T_x; $a/b = 1$, i.e., the plan is square, and $e/r = 0.4$ for all systems but several different values of ω_θ/ω_x are considered (Fig. 6.1). This ratio is always greater than 1 because the estimate obtained from Eq. 6.3 is an upper bound value. The quality of the estimate is about the same, independent of whether the system is elastic or inelastic. The estimated values are close to the "exact" values in many cases, but they may be larger by as much as 50% (Fig. 6.1).

6.3 Estimated Values

With the aim of improving the quality of the estimates, Eq. 6.3 is modified by dropping the least significant of the three terms on the right side. The contribution of the first term, u_{xm}, is always significant, but, depending on the ratio a/b of plan dimensions, the second or third term may be relatively insignificant. Between the two terms, the second term is less significant if a/b is much smaller than 1; whereas the third term is less significant if a/b is much larger than 1. Thus, the maximum value of total vector deformation of any column may be estimated from

$$U = u_{xm} + (a/r)\, ru_{\theta m} \qquad \text{if } a/b \geq 1 \tag{6.4}$$

and

$$U = \sqrt{u_{xm}^2 + (b/r)^2\,(ru_{\theta m})^2} \qquad \text{if } a/b < 1 \tag{6.5}$$

The ratios of estimates obtained from Eq. 6.4 to the "exact" values of maximum column deformations are also presented (Fig. 6.1). Eq. 6.4 provides better — compared to Eq. 6.3 — estimates for maximum column deformations

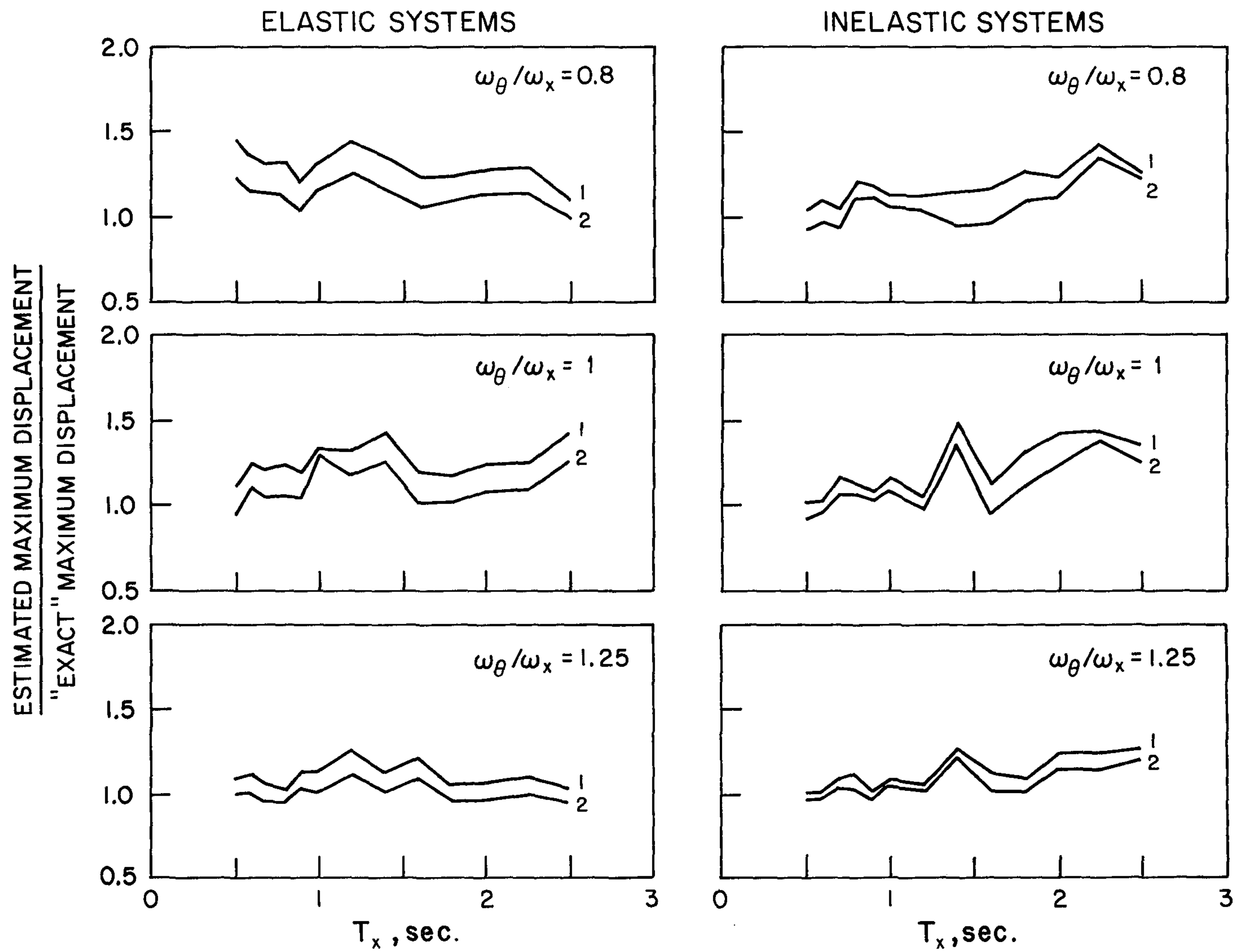

FIG. 6.1 RATIOS OF ESTIMATED TO "EXACT" MAXIMUM COLUMN DEFORMATION FOR SYSTEMS WITH a/b = 1 AND e/r = 0.4 SUBJECTED TO THE EL CENTRO EARTHQUAKE. ESTIMATES FROM EQ. 6.3 LEAD TO CURVE 1 AND EQ. 6.4 TO CURVE 2.

in systems with a/b = 1 for most of the system parameters considered. Improvements in the estimated values are similar for elastic and inelastic systems.

Similar results are presented for building plans with a/b = 3 and 1/3. The ratios of estimated values, obtained from Eq. 6.4 when a/b = 3 and Eq. 6.5 when a/b = 1/3, to the "exact" values are presented in Fig. 6.2. It is apparent from Figs. 6.1 and 6.2 that Eqs. 6.4 and 6.5 can provide useful estimates for maximum column deformation. The quality of these estimates appears to deteriorate for systems with a/b much larger than 1. These estimates are usually conservative and, when they are nonconservative, the errors do not exceed 20%. The quality of these estimates is similar for elastic and inelastic systems.

Based on the results presented above, the maximum values of column deformations may be estimated to a useful degree of approximation from Eqs. 6.4 and 6.5. In addition to the dimensions a and b of the rectangular plan, the maximum values of lateral and torsional displacements at the C.M. are required in computing column deformations. A procedure for estimation of displacements at C.M. for linearly elastic and for inelastic systems is presented in Chapter 7.

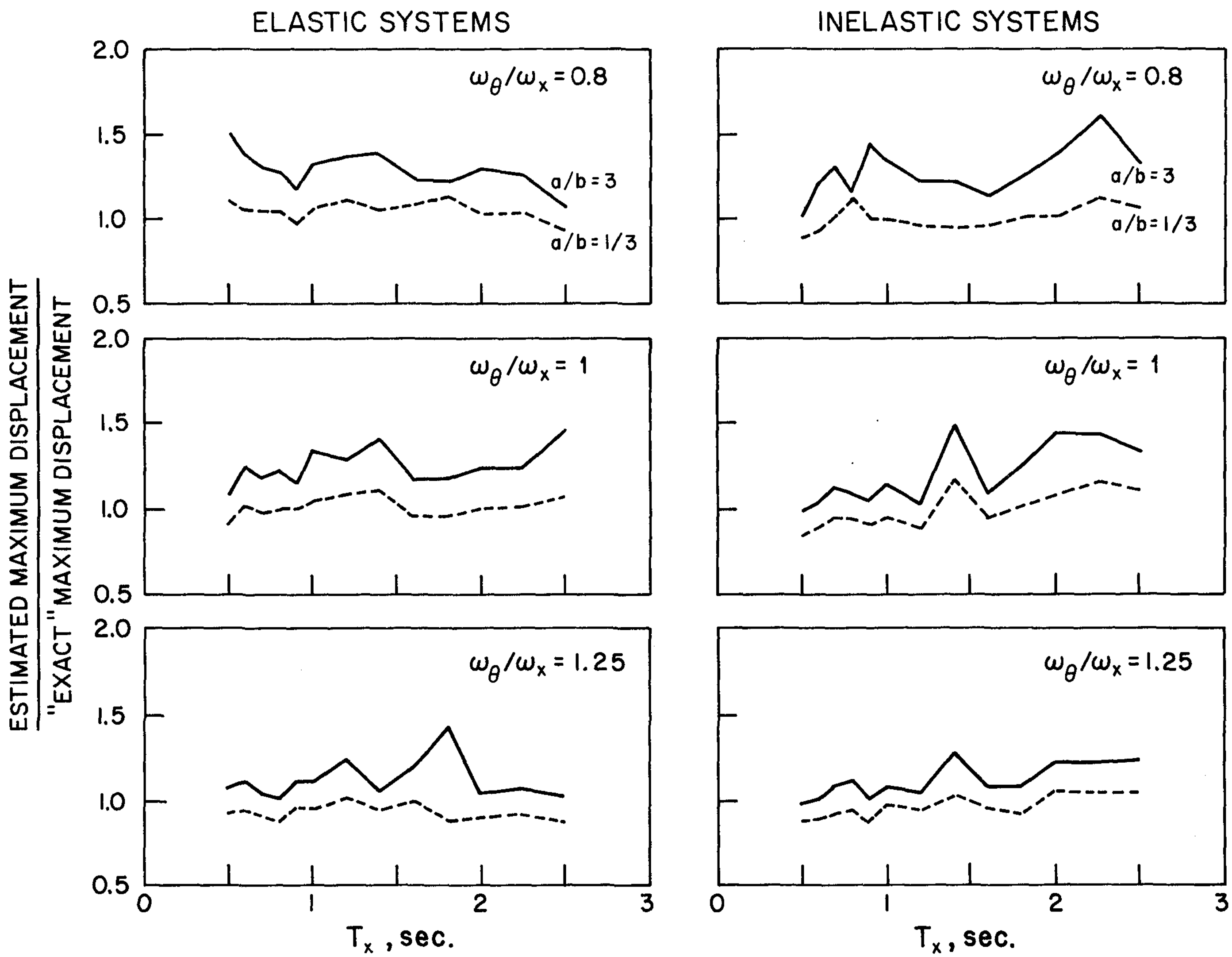

FIG. 6.2 RATIOS OF ESTIMATED TO "EXACT" MAXIMUM COLUMN DEFORMATION FOR SYSTEMS WITH e/r = 0.4 SUBJECTED TO THE EL CENTRO EARTHQUAKE. ESTIMATES FOR SYSTEMS WITH a/b = 3 WERE OBTAINED FROM EQ. 6.4 AND FOR SYSTEMS WITH a/b = 1/3 FROM EQ. 6.5.

7. ESTIMATION OF MAXIMUM RESPONSES FROM RESPONSE SPECTRA

7.1 Linear Systems

Consider the one-story torsionally-coupled system of Fig. 2.1 with linearly elastic properties subjected to earthquake ground motion along the x-principal axis of resistance. For this two degree-of-freedom system, an estimate of the maximum value of any response quantity r may be obtained by combining the modal maximum r_1 and r_2 — determined from the modal equations and the elastic response spectrum for the excitation — according to [26]

$$r^2 = r_1^{\,2} + r_2^{\,2} + 2\,\frac{r_1 r_2}{1 + \varepsilon^2} \tag{7.1}$$

where

$$\varepsilon = \frac{\sqrt{1 - \xi^2}}{\xi}\;\frac{\omega_2 - \omega_1}{\omega_2 + \omega_1} \tag{7.2}$$

and r_n is to be taken with a proper sign, the sign that its unit impulse response function has when it attains its maximum numerical value. The first two terms in Eq. 7.1 represent the more commonly used combination rule: square root of the sum of the squares of the modal maxima. The third term is important under certain conditions, in particular when the two natural frequencies of the structure are close. As this is often the case for the torsionally coupled system considered here, the third term is included in the analysis.

For the one-story system, the two force responses of interest are: base shear in x-direction V_x, and torque T defined at the C.M. or T_R at C.R. It can be shown that V_{xn} and T_n, the maximum values — with proper signs for use in Eq. 7.1 — of V_x and T in the n^{th} mode of vibration, are [17]:

$$\begin{aligned} V_{xn}/m &= \alpha_{xn}^2\, S_a(\omega_n,\xi) \\ T_n/mr &= \alpha_{xn}\alpha_{\theta n}\, S_a(\omega_n,\xi) \end{aligned} \tag{7.3}$$

wherein the mode shapes (Eq. 2.6) have been normalized so that $\underline{\alpha}_n^T\,\underline{\alpha}_n = 1$ and $S_a(\omega_n,\xi)$ is the ordinate of the pseudo-acceleration response spectrum at natural circular frequency ω_n for damping ratio ξ. By statics, the maximum value of the torque T_R at the C.R. in the n^{th} mode of vibration is

$$T_{Rn}/mr = T_n/mr + (e/r)(V_{xn}/m) \tag{7.4}$$

Similarly, the modal maxima, with proper signs, for displacements u_x and u_θ at the C.M. are

$$\begin{aligned} u_{xn} &= \alpha_{xn}^2 \frac{S_a(\omega_n,\xi)}{\omega_n^2} \\ ru_{\theta n} &= \alpha_{xn}\, \alpha_{\theta n} \frac{S_a(\omega_n,\xi)}{\omega_n^2} \end{aligned} \tag{7.5}$$

The sequence of steps in the modal analysis procedure for estimation of maximum responses of the one-story system (Fig. 2.1) to ground motion along the x-principal axis of resistance are summarized:

1. Analyze the vibration frequencies ω_n and mode shapes $\underline{\alpha}_n$ of the two natural modes by solving the eigenvalue problem of Eq. 2.6.
2. Corresponding to the vibration frequencies ω_n obtained in Step 1 and assumed damping ratio ξ, obtain $S_a(\omega_n,\xi)$ from the response spectrum for the ground motion.
3. From the mode shapes determined in Step 1 and the spectrum ordinates in Step 2, compute for each mode of vibration the maximum value of each force from Eqs. 7.3 and 7.4 and each displacement from Eq. 7.5.
4. Compute the total value of any response quantity — force or displacement — from the modal maxima obtained in Step 3 in accordance with Eqs. 7.1-7.2.

The accuracy of this approximate procedure may be evaluated by comparing the resulting estimate of maximum response with the "exact" values, obtained from complete response history analysis presented in Sec. 4.4. The estimates were obtained from Eqs. 7.3-7.5 and the elastic response spectrum of Fig. 3.7 for ξ = 2%. The ratio of estimated and "exact" values of maximum responses, force and displacements, is presented as a function of T_x for four values of ω_θ/ω_x (Figs. 7.1-7.2). The approximate procedure overestimates the displacements for the system parameters considered, underestimates the base shear from some values of the system parameters, and overestimates it for others. The relation between estimated and "exact" values of torque depends strongly on ω_θ/ω_x with the estimated value being relatively small if $\omega_\theta/\omega_x = 0.8$, about the same if $\omega_\theta/\omega_x = 1$, somewhat larger if $\omega_\theta/\omega_x = 1.25$ and substantially large if $\omega_\theta/\omega_x = 1.5$. The approximate procedure generally underestimates the torque for systems with $\omega_\theta/\omega_x \leq 1$ but overestimates it for systems with $\omega_\theta/\omega_x > 1$. The differences between estimated and "exact" values generally increase as ω_θ/ω_x decreases below or increases above $\omega_\theta/\omega_x = 1$. The differences between estimated and "exact" values of responses observed in Figs. 7.1-7.2 are similar in magnitude to those reported in earlier studies [25] of multi-degree-of-freedom systems.

7.2 Nonlinear Systems

Strictly speaking, the modal analysis procedure described in Sec. 7.1, which is applicable only to analysis of linear response, cannot be used for calculation of maximum responses of nonlinear systems. However, it has been suggested [25] that satisfactory approximations to the design forces and deformations can be obtained from the modal method by using the response spectrum for nonlinear systems instead of the elastic response spectrum. For elastic-perfectly-plastic systems, response spectra have been obtained that define the yield resistance required to limit the maximum deformation to a prescribed ductility factor μ, the ratio of the maximum earthquake-induced deformation to the yield displacement (Fig. 3.7).

Thus, with the following modifications, the modal analysis procedure of Sec. 7.1 may be employed as an approximate procedure for analysis of nonlinear responses:

1. In Eq. 7.3, replace $S_a(\omega_n,\xi)$, the ordinate of the pseudo-acceleration spectrum for a linearly elastic system with vibration frequency ω_n and damping ratio ξ_n, by $S'_a(\omega_n,\xi)$, the corresponding value for a nonlinear system with the same frequency of small amplitude vibration and damping ratio, determined from the inelastic response spectrum

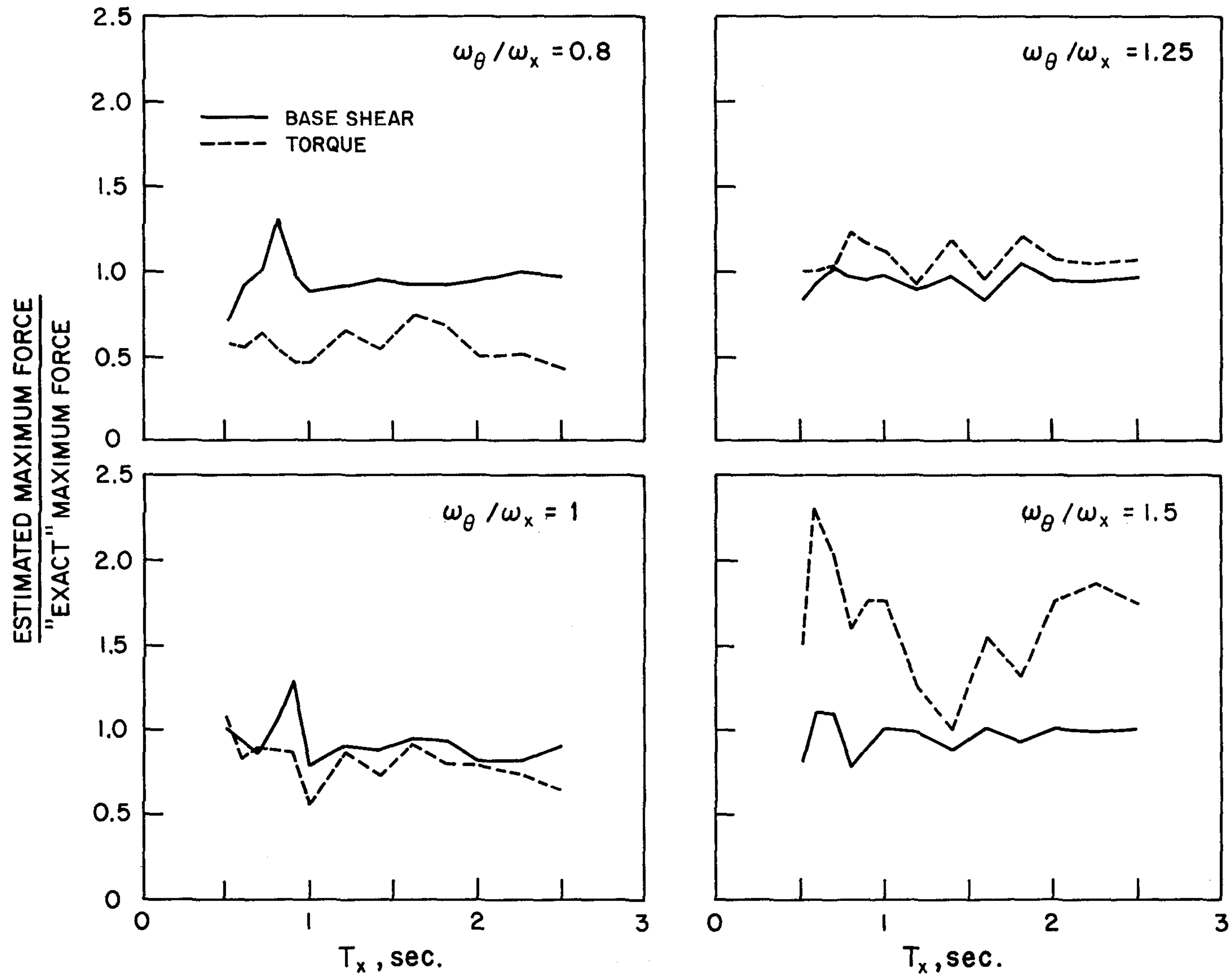

FIG. 7.1 RATIOS OF ESTIMATED TO "EXACT" MAXIMUM RESPONSE FORCES FOR ELASTIC SYSTEMS WITH e/r = 0.4 SUBJECTED TO THE EL CENTRO EARTHQUAKE.

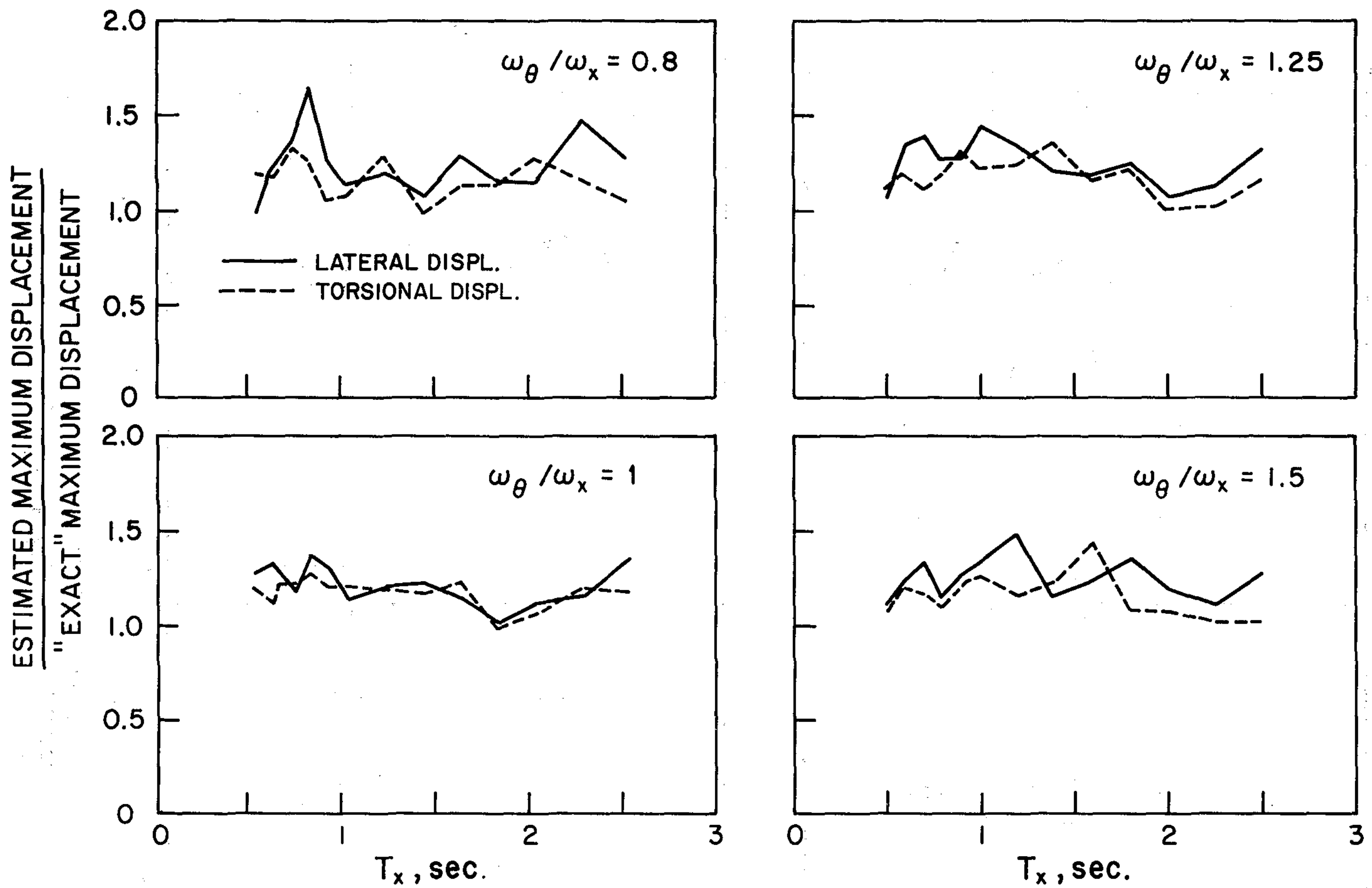

FIG. 7.2 RATIOS OF ESTIMATED TO "EXACT" MAXIMUM DISPLACEMENTS FOR ELASTIC SYSTEMS WITH e/r = 0.4 SUBJECTED TO THE EL CENTRO EARTHQUAKE.

(e.g., Fig. 3.7) for the specified μ:

$$
\begin{aligned}
V_{xn}/m &= \alpha_{xn}^2 \, S_a'(\omega_n,\xi) \\
T_n/mr &= \alpha_{xn}\alpha_{\theta n} \, S_a'(\omega_n,\xi)
\end{aligned}
\tag{7.6}
$$

2. Multiply displacements calculated from Eq. 7.5 by μ:

$$
\begin{aligned}
u_{xn} &= \mu \, \alpha_{xn}^2 \, \frac{S_a'(\omega_n,\xi)}{\omega_n^2} \\
ru_{\theta n} &= \mu \, \alpha_{xn}\alpha_{\theta n} \, \frac{S_a'(\omega_n,\xi)}{\omega_n^2}
\end{aligned}
\tag{7.7}
$$

The following approach was used to evaluate the accuracy of this approximate procedure for analysis of torsionally-coupled systems. Yield forces were determined from Eq. 7.6 for several systems all having $e/r = 0.4$, damping ratio $\xi = 2\%$, four different values for ω_θ/ω_x: 0.8, 1.0, 1.25, and 1.5, and several values for T_x in the range 0.5 to 2.5 secs. For each set of system properties, the yield forces were determined for two selected values of ductility factor: $\mu = 3$ and 5, from Eq. 7.6 and the inelastic response spectrum of Fig. 3.7. Each system so defined was analyzed by the procedures of Sec. 3.5.3 to obtain its displacement response-history for the El Centro ground motion, and the "exact" values of the maximum displacements were determined. Estimates were also obtained for these quantities from Eq. 7.7 and the inelastic response spectrum of Fig. 3.7. The ratio of estimated to "exact" values of maximum displacements is presented as a function of T_x (Figs. 7.3 and 7.4). The approximate procedure overestimates or underestimates the displacements, depending in no apparently systematic way on the system parameters. Discrepancies are larger in the estimated values of torsional displacements and they may be as much as twice the "exact" values. Although the errors in the approximate procedure may be significant, the results suggest that the design forces may be calculated from Eq. 7.6, corresponding to the allowable ductility factor μ. The structure should then be designed

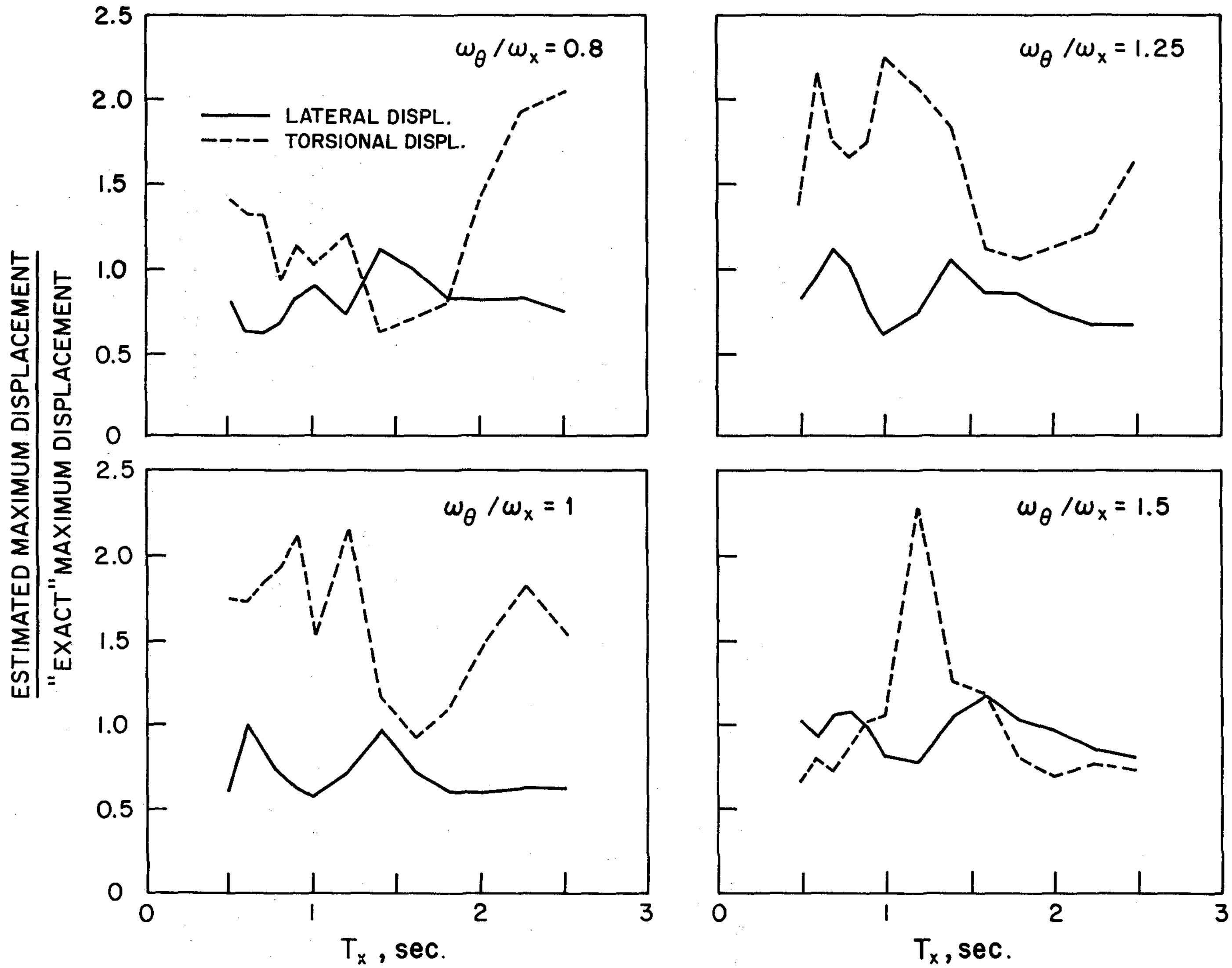

FIG. 7.3 RATIOS OF ESTIMATED TO "EXACT" MAXIMUM DISPLACEMENTS FOR INELASTIC SYSTEMS WITH e/r = 0.4 SUBJECTED TO THE EL CENTRO EARTHQUAKE. YIELD FORCES BASED ON INELASTIC RESPONSE SPECTRUM FOR μ = 5.

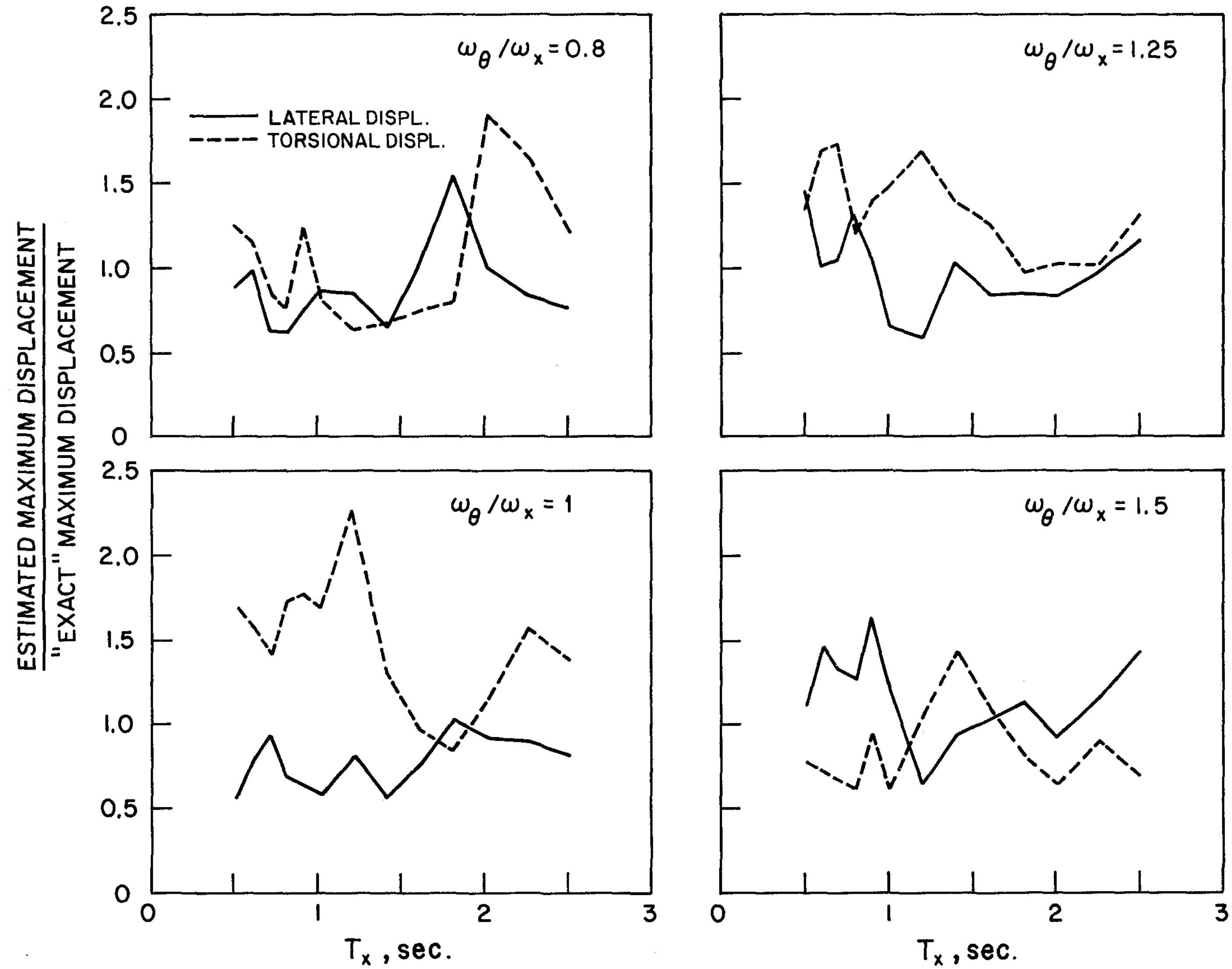

FIG. 7.4 RATIOS OF ESTIMATED TO "EXACT" MAXIMUM DISPLACEMENTS FOR INELASTIC SYSTEMS WITH $e/r = 0.4$ SUBJECTED TO THE EL CENTRO EARTHQUAKE. YIELD FORCES BASED ON INELASTIC RESPONSE SPECTRUM FOR $\mu = 3$.

to withstand these forces within allowable stresses and to be capable of mobilizing the assumed level of ductility. The design displacements may be roughly estimated by Eq. 7.7.

In evaluating discrepancies between estimated and "exact" values of maximum displacements of inelastic systems, it should be noted that four sources of approximation are involved in the estimation procedure. Firstly, the inelastic response spectrum of Fig. 3.7 is not precise because it could not be obtained directly and was the result of interpolation of responses of systems with different yield strengths. Secondly, errors are inherent in reading from Fig. 3.7 the spectrum ordinates used in Eqs. 7.6 and 7.7. The "exact" ductility factors (maximum deformation from response history analysis ÷ yield displacement) for an elastic-perfectly-plastic SDOF system with yield shears listed in Table 1 are presented in Fig. 7.5. Since these yield shears were obtained from Fig. 3.7 for $\mu = 5$, the differences between $\mu = 5$ and the "exact" values of μ indicate the combined effect of the two sources of approximation mentioned above. These approximations, according to Fig. 7.5, appear to be the source of a significant part of the errors in results from the approximate procedure presented in Figs. 7.3 and 7.4. Combining modal maxima by Eq. 7.1 is the third source of approximation which introduces significant errors even in the response of elastic systems (Figs. 7.1 and 7.2). Lastly, the application of modal analysis procedures to computation of response of inelastic systems is strictly not valid and is another source of discrepancy. It is because of these several sources of approximation that the analysis procedure provides estimates of maximum response of inelastic systems (Figs. 7.3 and 7.4) considerably worse than those for linearly elastic systems (Figs. 7.1 and 7.2).

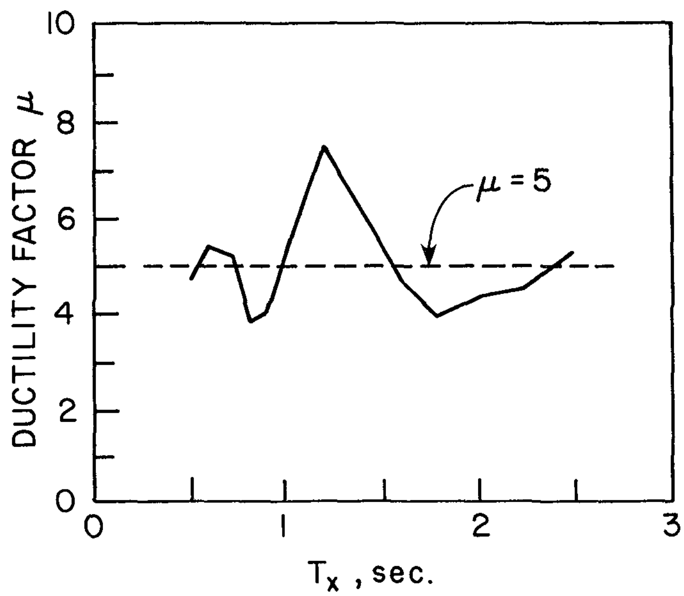

FIG. 7.5 "EXACT" DUCTILITY FACTORS FOR ELASTIC-PERFECTLY-PLASTIC SDOF SYSTEMS SUBJECTED TO THE EL CENTRO EARTHQUAKE. YIELD SHEARS BASED ON INELASTIC RESPONSE SPECTRUM FOR μ = 5.

8. CONCLUSIONS

The principal conclusions of this study concerned with coupled lateral (x) - torsional (θ) response of one-story structures, symmetric about the y-principal axis of resistance, to ground motion along the x-axis may be summarized as follows.

The linear response — lateral and torsional deformations (displacements of the center of mass relative to the ground) and associated total shear and torque — depends on the system parameters ω_x, ω_θ, e/r and ξ but not independently on the number, location and stiffness of the individual resisting elements, nor the plan geometry.

Response in the inelastic range of behavior is controlled by the yield shear and torque in addition to the basic parameters of the corresponding linear system. The inelastic response of a multi-element system, with yield displacements same for all resisting elements, can be determined to a useful degree of approximation by analyzing a single-element model with the following properties: parameters ω_x, ω_θ, e/r and ξ in the linearly elastic range of behavior same as for the multi-element system, a single yield surface with the yield shear same as for the multi-element system and the yield torque such that the yield surface is intermediate between the initial and limit yield surfaces of that multi-element system.

The effects of torsional coupling on the maximum deformation response of inelastic systems are, in general qualitative terms, similar to those for elastic systems. These effects depend in a complicated manner on the system parameters with few apparent systematic trends. The more important of these effects may be summarized as follows:

1. Torsional coupling causes torsional deformation in the system and modifies, increases or decreases, the lateral deformation of the system. Deformation of an individual column is also modified compared to the lateral deformation of the system, the column deformation in torsionally uncoupled systems.
2. The effects of torsional coupling depend significantly on ω_θ/ω_x, being most pronounced for systems with this ratio close to 1. Variation of these effects with ω_θ/ω_x is rather complicated in a

neighborhood of $\omega_\theta/\omega_x = 1$, representative of properties of many buildings, and generalizations do not appear possible. It is only for the relatively larger values of ω_θ/ω_x that these effects are rather simple and easily generalized. For systems with $\omega_\theta/\omega_x \geq 2$, lateral deformation is essentially unaffected, torsional deformation is essentially proportional to e/r, indicating no dynamic amplifications; deformations are increased and decreased, respectively, in columns farthest and nearest from the center of resistance.

3. For systems with $\omega_\theta/\omega_x \geq 2$, these effects of torsional coupling on system and column deformations increase with increasing e/r and a/b. For systems with smaller values of ω_θ/ω_x, the effects of torsional coupling depend on these parameters in a complicated manner with no apparent systematic trends.

Because the response is primarily in translation and most buildings are strong in torsion, yielding of the system is controlled primarily by the yield shear; after initial yielding the system has a tendency to yield further primarily in translation and behave more and more like an inelastic single-degree-of-freedom system, responding primarily in translation. Thus, torsional coupling generally affects maximum deformations in inelastic systems to a lesser degree compared to corresponding linearly elastic systems.

The maximum response of a linear system can be estimated to a useful degree of approximation by combining the modal maxima, computed from the response spectrum for the ground motion, in accordance with Eqs. 7.1 and 7.2. As is well known, such estimates of response may err on either — conservative or unconservative — side, depending on the system parameters, in particular on ω_θ/ω_x. The errors are similar in magnitude to those reported in earlier studies of multi-degree-of-freedom systems without torsional coupling.

Using an inelastic response spectrum, this estimation procedure may be employed to determine estimates of maximum response of inelastic systems. The errors in these results depend in no apparent systematic way on the system parameters. The errors are significantly larger than those for linear systems.

The maximum column deformations may be estimated to a useful degree of approximation from Eqs. 6.4 and 6.5 requiring, in addition to the plan dimensions, the maximum lateral and torsional displacements at the C.M. of the system. As mentioned above, the latter can be estimated from the modal properties and the response spectrum, elastic or inelastic, as appropriate.

APPENDIX I - REFERENCES

1. Ayre, R. S., "Interconnection of Translational and Torsional Vibrations in Buildings," Bulletin of the Seismological Society of America, Vol. 28, No. 2, April 1938, pp. 89-130.

2. Ayre, R. S., "Experimental Response of an Asymmetric, One-Story Building Model to an Idealized Transient Ground Motion," Bulletin of the Seismological Society of America, Vol. 33, No. 2, April 1943, pp. 91-119.

3. Ayre, R. S., "Methods for Calculating the Earthquake Response of 'Shear' Buildings," Proceedings of the World Conference on Earthquake Engineering, Berkeley, California, June 1956, pp. 13-1 to 13-24.

4. Arze, E., "Torsion en Planta de Edificios," Primeras Jornadas Chilenas de Sismologia e Ingenieria Antisismica, Vol. 2, Chile, July 1963, pp. B3.1-1 to B3.1-13.

5. Berg, G. V., "Earthquake Stresses in Tall Buildings with Setbacks," Second Symposium on Earthquake Engineering, Section IV, Roorkee, India, 1962, pp. 267-284.

6. Bustamante, J. I. and Rosenblueth, E., "Building Code Provisions on Torsional Oscillations," Proceedings of the Second World Conference on Earthquake Engineering, Vol. 2, Tokyo, Japan, 1960, pp. 879-894.

7. Douglas, B. M. and Trabert, T. E., "Coupled Torsional Dynamic Analysis of a Multistory Building," Bulletin of the Seismological Society of America, Vol. 63, No. 3, June 1973, pp. 1025-1039.

8. Elorduy, J. and Rosenblueth, E., "Torsiones Sismicas en Edificios de Un Piso," Segundo Congreso Nacional de Ingenieria Sismica, Veracruz, Mexico, 1968.

9. Erdik, M. O., "Torsional Effects in Dynamically Excited Structures," Ph.D. Thesis, Rice University, Houston, Texas, May 1975.

10. Gibson, R. E., Moody, M. L., and Ayre, R. S., "Free Vibration of an Unsymmetrical Multistoried Building Modelled as a Shear-Flexible Cantilever Beam," Bulletin of the Seismological Society of America, Vol. 62, No. 1, February 1972, pp. 195-213.

11. Hart, G. C., DiJulio, R. M., Jr., and Lew, M., "Torsional Response of High-Rise Buildings," Journal of the Structural Division, ASCE, Vol. 101, No. ST2, Proc. Paper 11126, February 1975, pp. 397-416.

12. Hoerner, J. B., "Modal Coupling and Earthquake Response of Tall Buildings," Report No. EERL 71-07, Earthquake Engineering Research Laboratory, California Institute of Technology, Pasadena, California, May 1971.

13. Housner, G. W. and Outinen, H., "The Effects of Torsional Oscillations on Earthquake Stresses," Bulletin of the Seismological Society of America, Vol. 48, No. 2, July 1958, pp. 221-229.

14. Hudson, D. E. and Brady, A. G., "Strong Motion Earthquake Accelerograms," Report No. EERL 71-50, Earthquake Engineering Research Laboratory, California Institute of Technology, Pasadena, California, September 1971.

15. Jhaveri, D. P., "Three-Dimensional Dynamic Analysis of High-Rise Buildings," Report JAB-99-36, John A. Blume and Associates, Research Division, San Francisco, California, August 1968.

16. Jurukovoki, D. and Bickovski, V., "Dynamic Response to Torsional and Shear Vibrations," Proceedings of the Third European Symposium on Earthquake Engineering, Sofia, Bulgaria, September 1970, pp. 673-683.

17. Kan, C. L. and Chopra, A. K., "Coupled Lateral-Torsional Response of Buildings to Ground Shaking," Report No. EERC 76-13, Earthquake Engineering Research Center, University of California, Berkeley, California, May 1976.

18. Kan, C. L. and Chopra, A. K., "Effects of Torsional Coupling on Earthquake Forces in Buildings," Journal of the Structural Division, ASCE, Vol. 103, ST4, Proc. Paper 12876, April 1977, pp. 805-819.

19. Kan, C. L. and Chopra, A. K., "Elastic Earthquake Analysis of a Class of Torsionally Coupled Buildings," Journal of the Structural Division, ASCE, Vol. 103, ST4, Proc. Paper 12877, April 1977, pp. 821-838.

20. Kan, C. L. and Chopra, A. K., "Elastic Earthquake Analysis of Torsionally Coupled Buildings," International Journal of Earthquake Engineering and Structural Dynamics, Vol. 5, No. 4, October 1977, pp. 395-412.

21. Mazilu, P., Sandi, H., and Teodorescu, D., "Analysis of Torsional Oscillations," Proceedings of the Fifth World Conference on Earthquake Engineering, Vol. 1, Rome, Italy, 1973, pp. 153-162.

22. Medearis, K., "Coupled Bending and Torsional Oscillations of a Modern Skyscraper," Bulletin of the Seismological Society of America, Vol. 56, No. 4, August 1966, pp. 937-946.

23. Mondkar, D. P. and Powell, G. H., "Static and Dynamic Analysis of Nonlinear Structures," Report No. EERC 75-10, Earthquake Engineering Research Center, University of California, Berkeley, California, March 1975.

24. Newmark, N. M., "Torsion in Symmetrical Buildings," Proceedings of the Fourth World Conference on Earthquake Engineering, Vol. 2, Santiago, Chile, 1969, pp. A3-19 to A3-32.

25. Newmark, N. M., "Current Trends in the Seismic Analysis and Design of High-Rise Structures," Earthquake Engineering, Prentice-Hall, Englewood Cliffs, New Jersey, 1970, pp. 403-424.

26. Newmark, N. M. and Rosenblueth, E., Fundamentals of Earthquake Engineering, Prentice-Hall, Englewood Cliffs, New Jersey, 1971.

27. Nigam, N. C., "Inelastic Interactions in the Dynamic Response of Structures," Ph.D. Thesis, California Institute of Technology, Pasadena, California, June 1967.

28. Porter, F. L. and Powell, G. H., "Static and Dynamic Analysis of Inelastic Frame Structures," Report No. EERC 71-3, Earthquake Engineering Research Center, University of California, Berkeley, California, June 1971.

29. Skinner, R. I., Skilton, D.W.C., and Laws, D. A., "Unbalanced Buildings and Buildings With Light Towers Under Earthquake Forces," Proceedings of the Third World Conference on Earthquake Engineering, Vol. 2, Auckland and Wellington, New Zealand, 1965, pp. 586-602.

30. Shepherd, R. and Donald, R.A.H., "Seismic Response of Torsionally Unbalanced Buildings," Journal of Sound and Vibration, Vol. 6, No. 1, 1967, pp. 20-37.

31. Shibata, A., Onose, J. and Shiga, T., "Torsional Response of Buildings to Strong Earthquake Motions," Proceedings of the Fourth World Conference on Earthquake Engineering, Vol. 2, Santiago, Chile, 1969, pp. A4-123 to A4-138.

32. Shiga, T., "Torsional Vibrations of Multi-Storied Buildings," Proceedings of the Third World Conference on Earthquake Engineering, Vol. 2, Auckland and Wellington, New Zealand, 1965, pp. 569-584.

33. Shiga, T., Shibata, A., and Onose, J., "Torsional Response of Buildings to Strong Motion Earthquakes," Proceedings of the Japan Earthquake Engineering Symposium, Tokyo, Japan, 1966, pp. 209-214.

34. Tso, W. K., "Induced Torsional Oscillations in Symmetrical Structures," International Journal of Earthquake Engineering and Structural Dynamics, Vol. 3, 1975, pp. 337-346.

35. Tso, W. K. and Asmis, K. G., "Torsional Vibration of Symmetrical Structures," Proceedings of the First Canadian Conference on Earthquake Engineering, Vancouver, Canada, 1971, pp. 178-186.

36. Veletsos, A. S. and Newmark, N. M., "Design Procedures for Shock Isolation Systems of Underground Protective Structures," Report RTD-TDR-63-3096, Vol. 3, Air Force Weapons Laboratory, Albuquerque, New Mexico, June 1964.

37. Veletsos, A. S., Erdik, M. O., and Kuo, P. T., "Response of Structures to Propagating Ground Motions," Structural Research Report No. 22, Department of Civil Engineering, Rice University, Houston, Texas, April 1975.

APPENDIX II - NOTATION

The following symbols are used in this paper:

a,b	dimensions of the rectangular building plan
B_x, B_t	parameters defined in Eq. 3.8b
B_{ix}, B_{iy}	parameters defined in Eq. 3.6b
c	scalar defining shape of the yield surface for the single-element model
e	static eccentricity, the distance measured from the center of mass to the center of resistance
e_x, e_y	static eccentricities, distances measured from the center of mass along the x and y axes to the center of resistance
$\underline{F}$	vector of restoring forces
G	parameter defined in Eq. 3.8b
G_i	parameter defined in Eq. 3.6b
g	gravitational constant
H_x, H_t	parameters defined in Eq. 3.8c
h_{ix}, h_{iy}	parameters defined in Eq. 3.6c
$\underline{K}_c$	contribution to the tangent stiffness matrix due to yielding
$\underline{K}_e$	elastic stiffness matrix
$\underline{K}_t$	tangent stiffness matrix
K_{tR}	$K_{\theta R}/r^2$
K_x	translational stiffness of the structure in the x direction
K_θ	torsional stiffness of the structure defined at the center of mass
$K_{\theta R}$	torsional stiffness of the structure defined at the center of resistance
$\underline{k}_{ic}$	contribution of member i to the matrix $\underline{K}_c$
k_{ix}, k_{iy}	lateral stiffnesses of the i-th resisting element in the x and y directions

m	mass of the deck
q	coefficient relating yield torque to yield shear (Eq. 3.9)
r	radius of gyration of the deck
$\mathcal{r}$	response quantity
S_a	pseudo-acceleration for an elastic system
S_a'	pseudo-acceleration for an inelastic system
T	torque defined at the center of mass
T_n	torque defined at the center of mass due to the n-th mode alone
T_R	torque defined at the center of resistance
T_{Rn}	torque defined at the center of resistance due to the n-th mode
T_{Rp}	plastic torque defined at the center of resistance
T_x	uncoupled translational period in the x direction
U	estimate of the largest maximum deformation of individual columns
U_x	upper bound for the x component of column deformations
U_y	upper bound for the y component of column deformations
$\ddot{u}_g$	ground acceleration along the x axis
u_i	displacement of column i
u_{ix}, u_{iy}	displacements of column i in the x and y directions
u_x	horizontal displacement of the center of mass, relative to the ground, in the x direction
u_{xm}	maximum value of u_x
u_{xy}	yield displacement in translation
u_θ	rotation of the deck about the vertical axis
$u_{\theta m}$	maximum value of u_θ
$u_{\theta y}$	yield displacement in rotation
V_{ix}, V_{iy}	shear forces on member i in the x and y directions
V_{ixp}, V_{iyp}	plastic shear forces of member i in the x and y directions

V_x	base shear of the structure in the x direction
V_{xn}	base shear due to the n-th mode
V_{xp}	plastic shear of the structure
x_i, y_i	distances of the i-th resisting element from the mass center
$\underline{\alpha}_n$	n-th mode shape
$\alpha_{xn}, \alpha_{\theta n}$	coefficients in the n-th mode shape
ε	parameter defined in Eq. 7.2
μ	ductility factor
ξ	viscous damping factor
ω_n	natural circular frequency of the n-th mode
ω_x	uncoupled translational circular frequency
ω_θ	uncoupled torsional circular frequency

Subscripts:

i	column or resisting element number
m	maximum
n	mode number
p	plastic
x,y	principal axes of resistance
θ	rotation

APPENDIX III

MATHEMATICAL AND NUMERICAL DETAILS

A. INDIVIDUAL ELEMENT PROPERTIES FOR FOUR-ELEMENT SYSTEM

Consider the system in Fig. 3.2, which consists of a square deck supported by four elements, one at each corner. When the ratio of the translational stiffnesses of each element in the y and x directions

$$k_{iy}/k_{ix} = \gamma \tag{A-1}$$

is assumed to be independent of the element number i, the stiffnesses of the individual elements are given by

$$\begin{aligned} k_{1x} &= k_{2x} = \frac{K_x}{4}\left(1 + \sqrt{\frac{2}{3}}\,\frac{e}{r}\right) \\ k_{3x} &= k_{4x} = \frac{K_x}{4}\left(1 - \sqrt{\frac{2}{3}}\,\frac{e}{r}\right) \\ \gamma &= \frac{2}{3}\left(\frac{\omega_\theta}{\omega_x}\right)^2 - 1 \\ k_{iy} &= \gamma k_{ix} \end{aligned} \tag{A-2}$$

Assume also that the yield displacements of all the elements in both the x and y directions to be the same, given by u_p where

$$u_p = V_{xp}/K_x \tag{A-3}$$

Then the yield shears of element i are

$$\begin{aligned} V_{ixp} &= k_{ix}u_p = (k_{ix}/K_x)V_{xp} \\ V_{iyp} &= k_{iy}u_p = \gamma V_{ixp} \end{aligned} \tag{A-4}$$

It should be noted from Eq. (A-2) that when ω_θ/ω_x is $\sqrt{3/2}$, γ, and hence k_{iy}, become zero. The parameter ω_θ/ω_x cannot have a value less than $\sqrt{3/2}$ for the four-element system; this is one of the major restrictions of the four-element system.

B. INELASTIC TANGENT STIFFNESS MATRICES

B.1 General Formulation for an Elasto-Plastic Member

The force-deformation relationship of an elastic-perfectly-plastic member i may be expressed, in the member coordinate system, by

$$\underline{dS}_i = \underline{k}_{it}\,\underline{dv}_i \tag{B-1}$$

where $\underline{dS}_i$ is the vector of incremental member forces, $\underline{dv}_i$ the vector of incremental member displacements, and $\underline{k}_{it}$ the tangent stiffness of the elasto-plastic member. Furthermore, the yield surface of the member may be written as

$$\phi_i(S_i) = 1 \tag{B-2}$$

where ϕ_i is a function of the member forces S_i.

Then, according to Ref. 28, the tangent stiffness of the member may be written as

$$\underline{k}_{it} = \underline{k}_{ie} - \underline{k}_{ip} \tag{B-3}$$

where $\underline{k}_{ie}$ is the conventional elastic stiffness matrix for the member, and $\underline{k}_{ip}$ represents the modification to the stiffness due to yielding of the member. If the element is elastic, $\underline{k}_{ip}$ is a zero matrix. If the element is in a plastic condition, then $\underline{k}_{ip}$ is given by (Ref. 28)

$$\underline{k}_{ip} = \underline{D}_i^T\,\underline{E}_i^{-1}\,\underline{D}_i \tag{B-4a}$$

where

$$\left.\begin{aligned}\underline{D}_i &= \underline{\phi}_{i,S}^T\,\underline{k}_{ie}\\ \underline{E}_i &= \underline{\phi}_{i,S}^T\,\underline{k}_{ie}\,\underline{\phi}_{i,S}\end{aligned}\right\} \tag{B-4b}$$

and $\phi_{i,S}$ is a vector of partial derivatives of $\phi_i(S_i)$ with respect to the forces S_i.

It should be noted that Eqs. (B-1) to (B-4) are expressed in the member coordinate system. The stiffness $\underline{k}_{it}$ when obtained should be transformed to the global coordinates and assembled into the structure stiffness.

B.2 Multi-Element Systems

Consider the multi-element system in Fig. 2.1, where each element has a yield surface, as shown in Fig. 3.1, given by

$$\phi_i(V_{ix},V_{iy}) = \left(\frac{V_{ix}}{V_{ixp}}\right)^2 + \left(\frac{V_{iy}}{V_{iyp}}\right)^2 \tag{B-5}$$

When the member forces are given by

$$\underline{S}_i = \begin{Bmatrix} V_{ix} \\ V_{iy} \end{Bmatrix} \tag{B-6}$$

and the displacements by

$$\underline{v}_i = \begin{Bmatrix} u_{ix} \\ u_{iy} \end{Bmatrix} \tag{B-7}$$

the elastic stiffness matrix of the member is

$$\underline{k}_{ie} = \begin{bmatrix} k_{ix} & 0 \\ 0 & k_{iy} \end{bmatrix} \tag{B-8}$$

and the vector of partial derivatives $\underline{\phi}_{i,S}$ is given by

$$\underline{\phi}_{i,S} = \begin{Bmatrix} 2h_{ix} \\ 2h_{iy} \end{Bmatrix} \tag{B-9}$$

where

$$h_{ix} = \frac{V_{ix}}{V^2_{ixp}} \quad \text{and} \quad h_{iy} = \frac{V_{iy}}{V^2_{iyp}} \tag{B-10}$$

Substitution of Eqs. (B-8) and (B-9) into Eq. (B-4) gives

$$\underline{k}_{ip} = \frac{1}{G_i} \begin{bmatrix} B^2_{ix} & B_{ix}C_{iy} \\ B_{ix}C_{iy} & C^2_{iy} \end{bmatrix} \tag{B-11a}$$

where

$$\begin{aligned} G_i &= k_{ix}h^2_{ix} + k_{iy}h^2_{iy} \\ B_{ix} &= k_{ix}h_{ix} \\ C_{iy} &= k_{iy}h_{iy} \end{aligned} \tag{B-11b}$$

Now the tangent stiffness matrix of the whole structure is given by

$$\underline{K}_t = \sum_i \underline{A}_i^T \, \underline{k}_{it} \, \underline{A}_i \tag{B-12}$$

where the coordinate transformation matrix $\underline{A}_i$ (from member coordinates to global coordinates) for member i is

$$\underline{A}_i = \begin{bmatrix} 1 & -y_i/r \\ 0 & x_i/r \end{bmatrix} \tag{B-13}$$

Substitution of Eqs. (B-8) and (B-11) into Eq. (B-3), and the resulting expression for $\underline{k}_{it}$ with Eq. (B-13) into Eq. (B-12) gives

$$\underline{K}_t = \underline{K}_e - \underline{K}_c \tag{B-14}$$

where $\underline{K}_e$ is given by Eq. (3.4) and $\underline{K}_c$ by Eqs. (3.5) and (3.6).

B.3 Single-Element Model

Consider the single-element system in Fig. 2.2, where the yield surface, according to Eq. (3.7), is given by

$$\phi = \left(\frac{V_x}{V_{xp}}\right)^2 + c\left(\frac{V_x}{V_{xp}}\right)\left(\frac{T_R}{T_{Rp}}\right) + \left(\frac{T_R}{T_{Rp}}\right)^2 \tag{B-15}$$

The forces on the single member may be written as

$$\underline{S} = \begin{Bmatrix} V_x \\ T_R/r \end{Bmatrix} \tag{B-16}$$

The corresponding displacements are

$$\underline{v} = \begin{Bmatrix} u_x - (e/r)(ru_\theta) \\ ru_\theta \end{Bmatrix} \tag{B-17}$$

and the elastic stiffness of the member, with respect to the center of resistance, is

$$\underline{k}_e = \begin{bmatrix} K_x & 0 \\ 0 & K_{tR} \end{bmatrix} \tag{B-18}$$

where

$$K_{tR} = (K_\theta - e^2 K_x)/r^2 ,$$

and the vector of partial derivatives $\underline{\phi}_{,S}$ is given by

$$\underline{\phi}_{,S} = \begin{Bmatrix} H_x \\ H_t \end{Bmatrix} \tag{B-19a}$$

where

$$H_x = \frac{1}{V_{xp}} \left(2 \frac{V_x}{V_{xp}} + c \frac{T_R}{T_{Rp}} \right)$$

$$H_t = \frac{r}{T_{Rp}} \left(2 \frac{T_R}{T_{Rp}} + c \frac{V_x}{V_{xp}} \right) \tag{B-19b}$$

Substitution of Eqs. (B-18) and (B-19) into Eq. (B-4) gives

$$\underline{k}_p = \frac{1}{G} \begin{bmatrix} B_x^2 & B_x C_t \\ B_x C_t & C_t^2 \end{bmatrix} \tag{B-20a}$$

where

$$G = K_x H_x^2 + K_{tR} H_t^2$$

$$B_x = K_x H_x \tag{B-20b}$$

$$C_t = K_{tR} H_t$$

and the subscript i has been dropped from Eq. (B-4) since there is only one element.

Now the tangent stiffness matrix of the structure with respect to the center of mass is

$$\underline{K}_t = \underline{A}^T \underline{k}_t \underline{A} \tag{B-21}$$

where

$$\underline{k}_t = \underline{k}_e - \underline{k}_p \tag{B-22}$$

and

$$\underline{A} = \begin{bmatrix} 1 & -e/r \\ 0 & 0 \end{bmatrix} \tag{B-23}$$

Substitution of Eqs. (B-18) and (B-20) into Eq. (B-22), and the resulting expression for $\underline{k}_t$ with Eq. (B-23) into Eq. (B-21) gives

$$\underset{\sim}{K}_t = \underset{\sim}{K}_e - \underset{\sim}{K}_c \tag{B-24}$$

where $\underset{\sim}{K}_e$ is given by Eq. (3.4) and $\underset{\sim}{K}_c$ by Eq. (3.8).

C. YIELD SURFACES FOR FOUR-ELEMENT SYSTEM

The equations of the yield surfaces, initial yield and limit yield are derived for the four-element system (Fig. 3.2) for which $k_{iy} = k_{ix}$ (i = 1, 2,3,4) or $\gamma = 1$. Furthermore, each element i is assumed to have equal stiffness k_{ix} and the same plastic yield displacement u_p in any horizontal direction. These assumptions are equivalent to assuming that each element consists of a thin tube with similar properties in any horizontal direction.

C.1 Displacement Relationships

For the square deck of Fig. 3.2, the dimension a is related to the radius of gyration of the deck by

$$a = \sqrt{\frac{3}{2}}\, r \tag{C-1}$$

and u_{ix} and u_{iy}, the x and y components of the deformation of element i, are related to the displacements at the C.M. by

$$\begin{aligned} u_{1x} &= u_{2x} = u_x - au_\theta \\ u_{3x} &= u_{4x} = u_x + au_\theta \\ u_{1y} &= u_{4y} = au_\theta \\ u_{2y} &= u_{3y} = -au_\theta \end{aligned} \tag{C-2}$$

The total vector-displacement of element i is

$$u_i = \sqrt{u_{ix}^2 + u_{iy}^2} \tag{C-3}$$

It is clear from Eqs. (C-2) and (C-3) that

$$u_1 = u_2 \quad \text{and} \quad u_3 = u_4 \tag{C-4}$$

Element 2 yields or unloads from a plastic state at the same time as element 1; and element 3 yields or unloads simultaneously with element 4. So in describing yielding in the system, it is sufficient to describe it only in terms of u_1 and u_4 instead of the displacements of all the elements.

C.2 Initial Yield Surface

Yielding in the four-element system is initiated when u_1 or u_4 first reaches a value equal to u_p. Whether u_1 or u_4 first reaches that value depends on the relative signs of u_x and u_θ.

(a) If u_x and u_θ both have the same sign, u_4, according to Eqs. (C-2) and (C-3), is larger than u_1. So yielding is initiated when

$$u_4 = u_p \tag{C-5}$$

Substitution of Eqs. (C-2) and (C-3) into Eq. (C-5) gives

$$s_x^2 + 2s_x s_t + 2s_t^2 = 1 \tag{C-6}$$

where

$$\begin{aligned} s_x &= u_x/u_p \\ s_t &= au_\theta/u_p \end{aligned} \tag{C-7}$$

Eq. (C-6) may be reduced further to

$$s_t = \frac{1}{2}\left(-s_x + \sqrt{2 - s_x^2}\right), \qquad 0 \le s_x \le 1 \tag{C-8}$$

(b) If u_x and u_θ have opposite signs, yielding is initiated when

$$u_1 = u_p \tag{C-9}$$

Substitution of Eqs. (C-2) and (C-3) into Eq. (C-9) gives

$$s_x^2 - 2s_x s_t + 2s_t^2 = 1 \tag{C-10}$$

which may be reduced further to

$$s_t = \frac{1}{2}\left(s_x + \sqrt{2 - s_x^2}\right), \quad -1 < s_x < 0 \qquad \text{(C-11)}$$

Now, in the linear range, the forces on the structure are related to the displacements at the C.M. by

$$\begin{Bmatrix} V_x \\ \\ T/r \end{Bmatrix} = \begin{bmatrix} K_x & -(e/r)K_x \\ \\ -(e/r)K_x & K_\theta/r^2 \end{bmatrix} \begin{Bmatrix} u_x \\ \\ ru_\theta \end{Bmatrix} \qquad \text{(C-12)}$$

and

$$T_R/r = T/r + (e/r)V_x \; .$$

And, for the assumption that $\gamma = 1$,

$$K_\theta/(K_x r^2) = (\omega_\theta/\omega_x)^2 = 3 \qquad \text{(C-13)}$$

Substitution of Eqs. (A-3), (C-1), (C-7), and (C-13) into Eq. (C-12) gives

$$\begin{aligned} V_x/V_{xp} &= s_x - \sqrt{\tfrac{2}{3}}\,(e/r)s_t \\ T/(V_{xp}r) &= -(e/r)s_x + \sqrt{6}\,s_t \qquad \text{(C-14)} \\ T_R/(V_{xp}r) &= T/(V_{xp}r) + (e/r)(V_x/V_{xp}) \end{aligned}$$

The initial yield surface of the four-element system is then given by the parametric equations (C-8), (C-11), and (C-14).

C.3 Limit Yield Surface

The system reaches limit yield when all its elements have yielded, i.e. when both u_1 and u_4 are equal to or greater than u_p. Whether element 1 or element 4 is the last element to yield under a certain displacement configuration depends on the relative sings of u_x and u_θ.

(a) If u_x and u_θ both have the same sign, u_4 is always greater than u_1; and the structure may be considered to have reached limit yield when

$$u_1 = u_p \tag{C-15}$$

Substitution of Eqs. (C-2) and (C-3) into Eq. (C-15) gives

$$s_x^2 - 2s_x s_t + 2s_t^2 = 1 \tag{C-16}$$

which may be reduced to

$$s_t = \frac{1}{2}\left(s_x + \sqrt{2 - s_x^2}\right), \quad 0 \le s_x \le \sqrt{2} \tag{C-17}$$

(b) If u_x and u_θ have opposite signs, the structure reaches limit yield when

$$u_4 = u_p \tag{C-18}$$

Substitution of Eqs. (C-2) and (C-3) into Eq. (C-19) gives

$$s_x^2 + s_x s_t + 2s_t^2 = 1 \tag{C-19}$$

which may be reduced to

$$s_t = \frac{1}{2}\left(-s_x + \sqrt{2 - s_x^2}\right), \quad -\sqrt{2} \le s_x \le 0 \tag{C-20}$$

When all the members have yielded, the vector shear force on each element i is

$$V_i = k_{ix} u_p = V_{ixp} \tag{C-21}$$

and V_{ix} and V_{iy}, the x and y components of the shear force on element i are

$$V_{ix} = (u_{ix}/u_i)V_i \quad \text{and} \quad V_{iy} = (u_{iy}/u_i)V_i \tag{C-22}$$

Now, by statics, the forces on the whole structure are given by

$$V_x = 2(V_{1x} + V_{4x})$$

$$T = 2a(V_{4x} + V_{4y} - V_{1x} + V_{1y}) \tag{C-23}$$

$$T_R = T + eV_x$$

Substitution of Eq. (C-1) into Eq. (C-23) gives

$$\begin{aligned} V_x/V_{xp} &= 2(V_{1x} + V_{4x})/V_{xp} \\ T_R/(V_{xp}r) &= \sqrt{6}\,(V_{4x} + V_{4y} - V_{1x} + V_{1y})/V_{xp} + (e/r)(V_x/V_{xp}) \end{aligned} \tag{C-24}$$

where, according to Eqs. (C-21), (C-22), and (A-4),

$$\begin{aligned} V_{ix}/V_{xp} &= (u_{ix}/u_i)(k_{ix}/K_x) \\ V_{iy}/V_{xp} &= (u_{iy}/u_i)(k_{ix}/K_x) \end{aligned} \tag{C-25}$$

and

$$\begin{aligned} u_{1x}/u_1 &= (s_x - s_t)/d_1 \\ u_{4x}/u_4 &= (s_x + s_t)/d_4 \\ u_{1y}/u_1 &= -s_t/d_1 \\ u_{4y}/u_4 &= s_t/d_4 \end{aligned} \tag{C-26}$$

where

$$\begin{aligned} d_1^2 &= (s_x - s_t)^2 + s_t^2 \\ d_4^2 &= (s_x + s_t)^2 + s_t^2 \end{aligned} \tag{C-27}$$

The limit yield surface of the system is then given by the parametric equations (C-17) and (C-20), together with Eqs. (C-24) to (C-27).

It should be noted that for cases in which k_{iy} is not equal to k_{ix} it becomes very difficult to obtain close-form equations for the limit yield surface of the system, and upper and lower bound theories have to be resorted to. It is for this reason that the yield surfaces are illustrated here only for the case in which $k_{iy} = k_{ix}$.

D. NUMERICAL INTEGRATION OF EQUATIONS OF MOTION

D.1 Discretized Differential Equations

The equations of motion (Eq. 3.1) of the torsionally coupled system may be written as

$$\underline{\ddot{u}} + \underline{C}\,\underline{\dot{u}} + \underline{F} = -\underline{\ddot{u}}_g \tag{D-1}$$

where

$$\underline{u} = \begin{Bmatrix} u_x \\ ru_\theta \end{Bmatrix} \quad \text{and} \quad \underline{\ddot{u}}_g = \begin{Bmatrix} \ddot{u}_g \\ 0 \end{Bmatrix} \tag{D-2}$$

The damping matrix $\underline{C}$ is given by

$$\underline{C} = \frac{2\xi}{\omega_1 + \omega_2} \begin{bmatrix} \omega_x^2 + \omega_1\omega_2 & -(e/r)\omega_x^2 \\ -(e/r)\omega_x^2 & \omega_\theta^2 + \omega_1\omega_2 \end{bmatrix} \tag{D-3}$$

and the force vector $\underline{F}$ by Eq. (3.2).

Assuming accelerations to vary linearly within each time increment Δt, the differential equations of Eq. (D-1) may be discretized (Ref. 23) as

$$\underline{\overline{K}}\,\underline{\Delta u} = \underline{\Delta P} \tag{D-4}$$

where

$$\begin{aligned} \underline{\overline{K}} &= \frac{6}{\Delta t^2}\underline{I} + \frac{3}{\Delta t}\underline{C} + \frac{1}{m}\underline{K}_t \\ \underline{\Delta P} &= -\underline{\ddot{u}}_g + \underline{A} + \underline{C}\,\underline{B} - \frac{1}{m}\underline{F}_t \end{aligned} \tag{D-5}$$

in which

$$\begin{aligned} \underline{A} &= \frac{6}{\Delta t}\underline{\dot{u}}_t + 2\underline{\ddot{u}}_t \\ \underline{B} &= 2\underline{\dot{u}}_t + \frac{\Delta t}{2}\underline{\ddot{u}}_t \end{aligned} \tag{D-6}$$

and $\underline{I}$ is an identity matrix, and $\underline{F}_t$ is the force vector $\underline{F}$ at time t.

With the displacements, velocities, accelerations, and forces known at time t, Eq. (D-4) may be solved numerically for the incremental displacements $\underline{\Delta u}$, from which the displacements, velocities, and accelerations at time t+Δt may be obtained:

$$\begin{aligned} \underline{u}_{t+\Delta t} &= \underline{u}_t + \underline{\Delta u} \\ \dot{\underline{u}}_{t+\Delta t} &= \frac{3}{\Delta t}\,\underline{\Delta u} - \underline{B} \\ \ddot{\underline{u}}_{t+\Delta t} &= \frac{6}{\Delta t^2}\,\underline{\Delta u} - \underline{A} \end{aligned} \qquad \text{(D-7)}$$

The solution is started by the initial conditions at time t = 0:

$$\begin{aligned} \underline{u}_{(t=0)} &= \dot{\underline{u}}_{(t=0)} = \underline{0} \\ \ddot{\underline{u}}_{(t=0)} &= -\ddot{\underline{u}}_{g(t=0)} \end{aligned} \qquad \text{(D-8)}$$

D.2 State Transitions

In solving Eq. (D-4), the tangent stiffness matrix is assumed to be constant during each time step. However, when one or more elements in the system pass from an elastic to a plastic state or from one plastic state to another, the stiffness of the system varies within the time step, dynamic equilibrium is violated, and unbalanced forces are introduced. The treatment of such state transitions together with the iterative schemes used are described below.

D.2.1 Plastic-to-Plastic State

An element is considered to be plastic when the element forces lie on its yield surface, i.e. $\phi_i = 1$, where

$$\phi_i = \left(\frac{V_{ix}}{V_{ixp}}\right)^2 + \left(\frac{V_{iy}}{V_{iyp}}\right)^2 \qquad \text{(D-9)}$$

for an element in the multi-element model (Fig. 2.1), and

$$\phi = \left(\frac{V_x}{V_{xp}}\right)^2 + c\left(\frac{V_x}{V_{xp}}\right)\left(\frac{T_R}{T_{Rp}}\right) + \left(\frac{T_R}{T_{Rp}}\right)^2 \qquad \text{(D-10)}$$

for the element in the single-element model (Fig. 2.2).

With the forces known at time t, the tangent stiffness matrix of the structure may be obtained from Eqs. (3.3) to (3.6) for the multi-element system or Eq. (3.8) for the single-element model. With this tangent stiffness matrix $\underline{K}_{t0}$ (in Eq. D-5), Eq. (D-4) may be solved for the incremental displacements $\underline{\Delta u}_0$. The corresponding unadjusted incremental forces for the system may be calculated from

$$\underline{\Delta F}_0 = \underline{K}_{t0}\,\underline{\Delta u}_0 \qquad \text{(D-11)}$$

If the system is found to be elastic both at the beginning and end of the time step, $\underline{\Delta u}_0$ and $\underline{\Delta F}_0$ are indeed the true incremental displacements and forces. But if an element in the system is already plastic at the beginning of the time step or passes to another plastic state at the end of the time step, $\underline{\Delta u}_0$ and $\underline{\Delta F}_0$ are first guesses for the incremental displacements and forces and should be corrected. The element forces obtained through the incremental forces of Eq. (D-11) may very well be found to lie outside the element yield surface (i.e. $\phi_i > 1$) and are therefore inadmissible. However, if the element forces are pulled back onto the yield surface, unbalanced forces are introduced. Different iterative schemes may be used for the reduction of such unbalanced forces. In the course of this study, three different procedures were examined and are described below.

(a) Newton-Raphson Iteration Scheme

(1) The state determination (finding the force increments when given the deformation increments) is performed by subdividing the incremental displacement $\underline{\Delta u}_0$ into subincrements $\underline{\delta u}$, which are applied one at a time to the system. The displacement subincrement $\underline{\delta u}$ is computed as a fraction of $\underline{\Delta u}_0$:

$$\underline{\delta u} = \frac{1}{n}\,\underline{\Delta u}_0 \qquad \text{(D-12)}$$

(Values used for n varied from 1 to 5. If n=1, no subdivision is made.)

Before each subincrement of displacement $\underline{\delta u}$ is applied to the system, the tangent stiffness matrix $\underline{K}_t$ is re-evaluated and the corresponding subincrement in force is calculated as

$$\underline{\delta F} = \underline{K}_t \, \underline{\delta u} \tag{D-13}$$

which is then added to the force vector of the system. After adding each force subincrement, the element forces $\underline{S}_i$ are re-evaluated. If, for an element that should be in a plastic state (i.e. unloading from plasticity is not detected), the element forces are not found to be on the yield surface, they are pulled back onto the yield surface. The element forces after such a pull-back are given by

$$\underline{S}_i' = \frac{1}{\sqrt{\phi_i}} \underline{S}_i \tag{D-14}$$

where ϕ_i is obtained from Eq. (D-9) or (D-10) with $\underline{S}_i$, the forces before the pull-back. The force vector on the system $\underline{F}$ is then re-evaluated by summing up the element forces.

(2) After finding the force vector $\underline{F}$ (after applying all the $\underline{\delta u}$'s), the unbalanced loads on the system are computed by

$$\underline{R} = \underline{F}_0 - \underline{F} \tag{D-15}$$

where

$$\underline{F}_0 = \underline{F}_t + \underline{\Delta F}_0$$

is the sum of the force vector at the beginning of the time step (at time t) and the unadjusted incremental forces (Eq. D-11). Convergence is then checked according to the following criteria:

$$||\underline{R}||/||m\underline{u}_{g(t+\Delta t)}|| \leq \text{tolerance}$$

(Depending on the value of n, a tolerance of 0.0005 or less was used.)

(3) If the convergence criteria is not satisfied, $\underline{\Delta u_1}$, the displacement corresponding to the unbalanced loads $\underline{R}$, is calculated from

$$\overline{\underline{K}}\,\underline{\Delta u_1} = \underline{R} \tag{D-16}$$

The tangent stiffness $\underline{K_t}$ for forming $\overline{\underline{K}}$ is evaluated for the forces $\underline{F}$ obtained at the end of step (1). Steps (1) and (2) are then repeated with $\underline{\Delta u_1}$ instead of $\underline{\Delta u_0}$, and with $\underline{\Delta u_2}$ and so on if necessary until the convergence criteria is satisfied. (For convergence within a reasonably small number of iterations, it may sometimes be necessary to reduce the time step increment Δt.)

(4) After the convergence criteria is satisfied, the total displacement increment for that time step is calculated as

$$\underline{\Delta u} = \underline{\Delta u_0} + \underline{\Delta u_1} + \underline{\Delta u_2} + \ldots \tag{D-17}$$

Displacements, velocities and accelerations are then obtained from Eq. (D-7).

(b) Average-Stiffness Predictor-Corrector Scheme

(1) After the first guess of the incremental displacements $\underline{\Delta u_0}$ and incremental forces $\underline{\Delta F_0}$ are obtained, the new forces are estimated as

$$\underline{F'} = \underline{F_t} + \underline{\Delta F_0} \tag{D-18}$$

where $\underline{F_t}$ is the force vector at time t, i.e. at the beginning of the time step.

(2) The tangent stiffness matrix $\underline{K_t'}$ associated with the forces $\underline{F'}$ (without pull-back of element forces onto yield surfaces) is evaluated according to Eqs. (3.3) to (3.6) or Eq. (3.8). Then an average tangent stiffness matrix, $\underline{K_{ta}}$, is formed by averaging

the tangent stiffness matrices at the beginning of the time step and from the first guess:

$$\underline{K}_{ta} = \frac{1}{2}(\underline{K}_{t0} + \underline{K}_t') \tag{D-19}$$

where $\underline{K}_{t0}$ is the tangent stiffness of the system at the beginning of the time step.

(3) The incremental displacements for this time step are then re-evaluated from Eq. (D-4), with $\underline{K}_{ta}$ as the tangent stiffness in Eq. (D-5). Denoting these updated incremental displacements as $\underline{\Delta u}_1$, the corresponding incremental forces $\underline{\Delta F}_1$ may be calculated as

$$\underline{\Delta F}_1 = \underline{K}_{ta}\,\underline{\Delta u}_1 \tag{D-20}$$

(4) The above procedure is repeated, each time with a new $\underline{K}_{ta}$ which is the average of $\underline{K}_{t0}$ and the tangent stiffness at the end of the last guess, until certain convergence criteria are satisfied:

$$\begin{gathered} \Big|\,||\underline{\Delta F}_{i+1}|| - ||\underline{\Delta F}_i||\,\Big| \leqslant \text{force tolerance} \\ \text{and} \\ \Big|\,||\underline{\Delta u}_{i+1}|| - ||\underline{\Delta u}_i||\,\Big| \leqslant \text{displacement tolerance} \end{gathered} \tag{D-21}$$

(5) When the convergence criteria of Eq. (D-21) are satisfied, the element forces $\underline{S}_i$ are evaluated. If, for an element that should be plastic, the element forces are not in the yield surface, they are pulled back. The element forces after such a pull-back are given by

$$\underline{S}_i' = \frac{1}{\sqrt{\phi_i}}\,\underline{S}_i \tag{D-22}$$

where ϕ_i is calculated from Eq. (D-9) or (D-10) from $\underline{S}_i$, the forces before pull-back. The force vector on the system $\underline{F}$ is then re-evaluated by summing up the element forces.

(c) Average-Stiffness Predictor-Corrector Scheme No. 2

This scheme is completely identical to the preceding one, except that $\underline{K}_{ta}$, instead of being evaluated from Eq. (D-19), is evaluated as the tangent stiffness matrix associated with the forces given by

$$\underline{F}_a = \frac{1}{2}(\underline{F}' + \underline{F}_t) \qquad \text{(D-23)}$$

The first scheme, the Newton-Raphson procedure, is well established in the literature (Ref. 23). But through numerical experiments for this problem, the last two procedures (both equivalents of a second order Runge-Kutta predictor-corrector scheme) have been found to be more accurate (than the Newton-Raphson scheme with n=4) as well as simpler and time-efficient in computation. Little differences were found between the numerical results from the last two schemes, although the last scheme appears to be slightly, almost imperceptibly, better. However, for the single-element model where c is not zero in Eq. (3.7) and there are discontinuities in the slope of the yield surface, the last two schemes may sometimes fail to converge. In such cases, the Newton-Raphson scheme was resorted to. Otherwise, almost all the numerical results were generated using the last predictor-corrector scheme.

D.2.2 Elastic-to-Plastic State

If the system is elastic at the beginning of a time step and during the time step one or more elements pass from an elastic to a plastic state, the computations are restarted for that time increment and the procedure of determining the incremental displacements $\underline{\Delta u}$ and the corresponding incremental forces is carried out in two steps:

(a) An elastic displacement increment, $\underline{\Delta u}_e$, is obtained as a fraction of the displacement increment $\underline{\Delta u}_0$ that was originally calculated:

$$\underline{\Delta u}_e = a_e \, \underline{\Delta u}_0 \qquad \text{(D-24)}$$

where a_e is a scalar (less than 1) such that the system just reaches inelasticity.

(b) The inelastic displacement increment, $\underline{\Delta u}_p$, corresponding to an effective load $(1-a_e)\,\underline{\Delta P}$ on the right side of Eq. (D-4) is then calculated as described in D.2.1 for transition from one plastic state to another.

The total incremental displacement $\Delta\underline{u}$ for the time step is then the sum of $\Delta\underline{u}_e$ and $\Delta\underline{u}_p$. And the displacements, velocities and accelerations may be computed from Eq. (D-7).

D.2.3 Plastic-to-Elastic State

Let the forces on element i be given by $\underline{S}_i$ and its displacements by $\underline{v}_i$. The element is considered to have unloaded from a plastic state if the plastic work increment ΔW_i^p is negative for that time step. The plastic work increment is given by

$$\Delta W_i^p = \underline{S}_i^T \, \Delta\underline{v}_i^p \tag{D-25}$$

where $\Delta\underline{v}_i^p$, the plastic displacement increment of element i, is given in turn by

$$\Delta\underline{v}_i^p = \Delta\underline{v}_i - \underline{k}_{ie}^{-1} \, \Delta\underline{S}_i \tag{D-26}$$

in which $\Delta\underline{v}_i$ is the total displacement increment of element i in that time step, and $\underline{k}_{ie}$ is the elastic stiffness matrix of the element.

When an element is found to have unloaded from plasticity, its stiffness within that time step is assumed to be the same as its elastic stiffness.

E. YIELD SURFACES FOR EIGHT-ELEMENT SYSTEM

Consider the system in Fig. 3.11 which consists of a square deck supported on eight identical columns located on its plan perimeter. The system is symmetrical with respect to both the x and y axes, and the dimensions of the square deck are 2a by 2a. Each column is assumed (as in Appendix III-C) to have equal translational stiffness and plastic yield displacement in any horizontal direction.

E.1 Initial Yield Surface

Let the system be subjected to a shear V_x and a torque T_R. Yielding is initiated in the system when one of the corner columns yields. This condition, also the expression for the yield surface, is given by

$$\left(\frac{V_x}{V_{xp}}\right)^2 + \frac{2}{3}(1+\sqrt{2})\left(\frac{V_x}{V_{xp}}\right)\left(\frac{T_R}{T_{Rp}}\right) + \frac{2}{9}(3+2\sqrt{2})\left(\frac{T_R}{T_{Rp}}\right)^2 = 1 \qquad \text{(E-1)}$$

where the yield torque T_{Rp} is related to the yield shear by

$$\frac{T_{Rp}}{V_{xp}r} = \sqrt{\frac{3}{2}}\ \frac{(1+\sqrt{2})}{2} \qquad \text{(E-2)}$$

E.2 Limit Yield Surface

It is found that the eight-element system reaches limit yield under two different conditions: (i) when all its elements have become plastic and (ii) when the system is no longer stable, although one or more members is still elastic.

(a) Limit yield with full plastification of all eight elements is reached when the least stressed element finally yields. This condition is given by the following parametric equations:

$$\frac{V_x}{V_{xp}} = \frac{1}{4}\left[\frac{s_x - s_t}{f_1} + \frac{s_x + s_t}{f_2} + \frac{s_x}{f_3}\right] + \frac{1}{8}\left[\frac{s_x + s_t}{f_4} + \frac{s_x - s_t}{f_5}\right]$$

$$\frac{T_R}{T_{Rp}} = \frac{1}{2(1+\sqrt{2})}\left[\frac{2s_t - s_x}{f_1} + \frac{2s_t + s_x}{f_2} + \frac{s_t}{f_3}\right] + \frac{1}{4(1+\sqrt{2})}\left[\frac{s_x + s_t}{f_4} - \frac{s_x - s_t}{f_5}\right] \qquad \text{(E-3)}$$

where
$$\begin{aligned}
f_1^2 &= (s_x - s_t)^2 + s_t^2 \\
f_2^2 &= (s_x + s_t)^2 + s_t^2 \\
f_3^2 &= s_x^2 + s_t^2 \\
f_4^2 &= (s_x + s_t)^2 \\
f_5^2 &= (s_x - s_t)^2
\end{aligned} \tag{E-4}$$

and it is specified that

$$s_x - s_t = \pm 1 \tag{E-5}$$

where s_x and s_t must have the same numerical sign.

(b) The bounds on the forces imposed by considerations of stability are given by

$$\frac{T_R}{T_{Rp}} + \frac{2}{1 + \sqrt{2}} \frac{V_x}{V_{xp}} = \pm R$$

and (E-6)

$$\frac{T_R}{T_{Rp}} - \frac{2}{1 + \sqrt{2}} \frac{V_x}{V_{xp}} = \pm R$$

where
$$R = \frac{1}{2(1 + \sqrt{2})} (2 + \sqrt{2} + \sqrt{5})$$

The limit yield surface of the system is given in part by Eq. (E-3) and in part by Eq. (E-6). When there is overlap between the two sets of equations, the limit yield is given by the lower bound.

F. YIELD TORQUES FOR MULTI-ELEMENT SYSTEMS

The yield torques in a multi-element system should be expected to increase with the yield strength in shear of the system. It should also increase with the ratio of torsional to translational stiffnesses of the structure. Such a relationship may be expressed dimensionlessly by

$$\frac{T_{Rp}}{V_{xp} r} = q \frac{K_{\theta R}}{K_x r^2} \tag{F-1}$$

where

$$K_{\theta R} = K_\theta - e^2 K_x \tag{F-2}$$

is the torsional stiffness of the structure with respect to the center of resistance. (Substitution of Eq. (2.5) into Eq. (F-1) gives Eq. (3.9). The coefficient q depends on the type and number of the resisting elements in the structure, and whether T_{Rp} in Eq. (F-1) is used to represent the torque at initial yield or limit yield. The range of values over which the coefficient q varies, the upper and lower bounds in particular, may be determined by examining the initial and limit yield torque for a number of basic representative structural systems.

F.1 Initial Yield Torque

Consider the rectangular plan in Fig. F-1, a system with elements located at the corners of the plan. Assume that all the elements have the same yield displacement in shear, u_p. This yield displacement is then given by

$$u_p = \frac{V_{xp}}{K_x} \tag{F-3}$$

Then, regardless of the number of elements within the perimeter of the plan, the initial torque is defined by the value at which the corner elements begin to yield. With the plan being symmetrical, yielding in the corner columns occurs when

$$\sqrt{a^2 + b^2}\, u_\theta = u_p \tag{F-4}$$

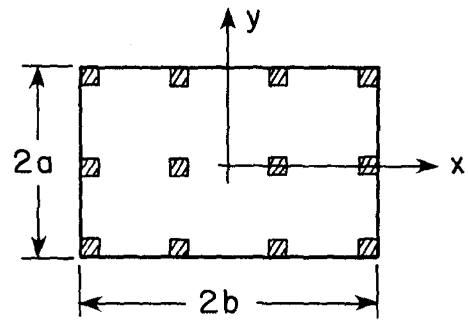

FIG. F-1 SYMMETRICAL RECTANGULAR PLAN

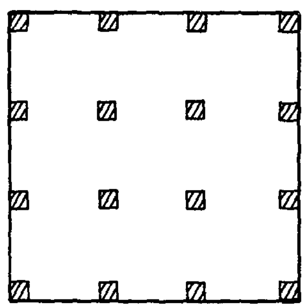

(a) UNIFORMLY DISTRIBUTED COLUMNS

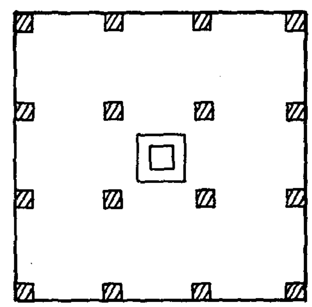

(b) COLUMNS WITH A SHEAR CORE

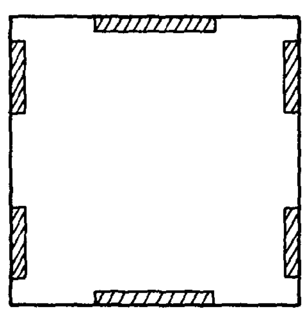

(c) PERIPHERAL SHEAR WALLS

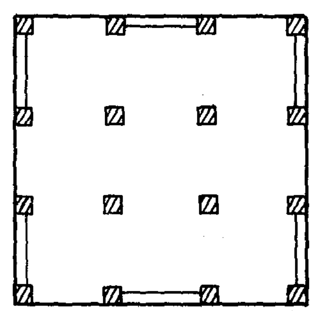

(d) COLUMNS WITH PERIPHERAL SHEAR WALLS

FIG. F-2 SYSTEMS WITH DIFFERENT RESISTING ELEMENTS

And since the radius of gyration r is given by

$$r^2 = \frac{1}{3}(a^2 + b^2) \tag{F-5}$$

Eq. (F-4), after substitution of Eq. (F-3), gives

$$u_\theta = \frac{1}{\sqrt{3}} \frac{V_{xp}}{K_x r} \tag{F-6}$$

Now, the initial yield torque T_{Ri} is given by

$$T_{Ri} = K_\theta u_\theta \tag{F-7}$$

Substitution of Eq. (F-6) into Eq. (F-7) and recalling that for a symmetric system K_θ is identical to $K_{\theta R}$ gives

$$\frac{T_{Ri}}{V_{xp} r} = \frac{1}{\sqrt{3}} \frac{K_{\theta R}}{K_x r^2} \tag{F-8}$$

If no elements were located at the corners, the coefficient in Eq. (F-8) will always be greater than $1/\sqrt{3}$. And since the torque in Eq. (F-8) is the initial yield torque, $1/\sqrt{3}$ may be considered the lower bound of the coefficient q (Eq. F-1).

F.2 Limit Yield Torque

When T_{Rp} in Eq. (F-1) represents the limit yield torque of a system, the coefficient q varies with building plan as well as the number and types of resisting elements. Square plans and then rectangular plans are considered below. And three types of resisting elements are considered: (1) columns, (2) shear cores, and (3) shear walls (which are assumed to present resistance only along their longitudinal directions).

(a) Square Plans

Consider first structural systems where the resisting elements consist only of columns uniformly distributed over the building plan (Fig. F-2a). For such systems, the value of the coefficient q increases with the number of columns in the system, as illustrated in Table F-1, but levels off rapidly. Since most buildings have less than 100 columns, a value of 0.85 may be considered a fair upper bound for q from Table F-1.

Next consider the addition of a shear core to the system, which is located near the center of the building (Fig. F-2b). The addition of such a shear core, while increasing the translational stiffness K_x by a certain factor, will also increase the yield shear by approximately the same factor. By being located near the center of the building, the addition of the shear core contributes relatively little to the torsional stiffness of the structure $K_{\theta R}$. The result of all these is that the coefficient q in Eq. (F-1) is not affected much by the addition of such a shear core.

Next consider systems where the resisting elements consist only of shear walls located on the perimeter of the building plan (Fig. F-2c). For the square plan, the limit yield torque is given by $q = \sqrt{2/3} = 0.817$ (Eq. F-1), regardless of the relative stiffnesses of the longitudinal walls to that of the transverse walls. Now, if the system consists of both peripheral shear walls and uniformly distributed columns (Fig. F-2d), the limit yield torque is defined by a value of q between 0.817 and the value of q if there were only the columns. For example, if there were 100 columns beside the shear walls, the limit yield torque would be defined by a value between 0.817 and 0.849; and the exact value will depend on the strengths of the shear walls relative to those of the columns. So a value of 0.85 may also be considered a practical upper bound for q for such systems. Addition of a shear core will again change the value of q very little.

(b) Rectangular Plans

For a rectangular plan, the radius of gyration r is always larger than that for a square plan with the same area. Hence, the value of q defining the limit yield torque for a rectangular plan is usually slightly smaller than that for a square plan with equal surface area. The difference, however, is generally not large. But if the elements in the rectangular plan are more crowded together than in the square plan, the value of q may be somewhat larger. In any case, a fairly practical upper bound for the coefficient with up to 100 elements may be considered to be given by 0.86.

TABLE F-1. Values of Coefficient q for Systems with Square Plans and Uniformly Distributed Columns

No. of Columns	q
4	0.5774
9	0.6570
16	0.7337
25	0.7652
36	0.7954
49	0.8122
64	0.8285
81	0.8388
100	0.8489
400	0.8917

NOTE: Numbers in parenthesis are Accession Numbers assigned by the National Technical Information Service; these are followed by a price code. Copies of the reports may be ordered from the National Technical Information Service, 5285 Port Royal Road, Springfield, Virginia, 22161. Accession Numbers should be quoted on orders for reports (PB --- ---) and remittance must accompany each order. Reports without this information were not available at time of printing. Upon request, EERC will mail inquirers this information when it becomes available.

EERC 67-1 "Feasibility Study Large-Scale Earthquake Simulator Facility," by J. Penzien, J.G. Bouwkamp, R.W. Clough and D. Rea - 1967 (PB 187 905)A07

EERC 68-1 Unassigned

EERC 68-2 "Inelastic Behavior of Beam-to-Column Subassemblages Under Repeated Loading," by V.V. Bertero - 1968 (PB 184 888)A05

EERC 68-3 "A Graphical Method for Solving the Wave Reflection-Refraction Problem," by H.D. McNiven and Y. Mengi - 1968 (PB 187 943)A03

EERC 68-4 "Dynamic Properties of McKinley School Buildings," by D. Rea, J.G. Bouwkamp and R.W. Clough - 1968 (PB 187 902)A07

EERC 68-5 "Characteristics of Rock Motions During Earthquakes," by H.B. Seed, I.M. Idriss and F.W. Kiefer - 1968 (PB 188 338)A03

EERC 69-1 "Earthquake Engineering Research at Berkeley," - 1969 (PB 187 906)A11

EERC 69-2 "Nonlinear Seismic Response of Earth Structures," by M. Dibaj and J. Penzien - 1969 (PB 187 904)A08

EERC 69-3 "Probabilistic Study of the Behavior of Structures During Earthquakes," by R. Ruiz and J. Penzien - 1969 (PB 187 886)A06

EERC 69-4 "Numerical Solution of Boundary Value Problems in Structural Mechanics by Reduction to an Initial Value Formulation," by N. Distefano and J. Schujman - 1969 (PB 187 942)A02

EERC 69-5 "Dynamic Programming and the Solution of the Biharmonic Equation," by N. Distefano - 1969 (PB 187 941)A03

EERC 69-6 "Stochastic Analysis of Offshore Tower Structures," by A.K. Malhotra and J. Penzien - 1969 (PB 187 903)A09

EERC 69-7 "Rock Motion Accelerograms for High Magnitude Earthquakes," by H.B. Seed and I.M. Idriss - 1969 (PB 187 940)A02

EERC 69-8 "Structural Dynamics Testing Facilities at the University of California, Berkeley," by R.M. Stephen, J.G. Bouwkamp, R.W. Clough and J. Penzien - 1969 (PB 189 111)A04

EERC 69-9 "Seismic Response of Soil Deposits Underlain by Sloping Rock Boundaries," by H. Dezfulian and H.B. Seed 1969 (PB 189 114)A03

EERC 69-10 "Dynamic Stress Analysis of Axisymmetric Structures Under Arbitrary Loading," by S. Ghosh and E.L. Wilson 1969 (PB 189 026)A10

EERC 69-11 "Seismic Behavior of Multistory Frames Designed by Different Philosophies," by J.C. Anderson and V. V. Bertero - 1969 (PB 190 662)A10

EERC 69-12 "Stiffness Degradation of Reinforcing Concrete Members Subjected to Cyclic Flexural Moments," by V.V. Bertero, B. Bresler and H. Ming Liao - 1969 (PB 202 942)A07

EERC 69-13 "Response of Non-Uniform Soil Deposits to Travelling Seismic Waves," by H. Dezfulian and H.B. Seed - 1969 (PB 191 023)A03

EERC 69-14 "Damping Capacity of a Model Steel Structure," by D. Rea, R.W. Clough and J.G. Bouwkamp - 1969 (PB 190 663)A06

EERC 69-15 "Influence of Local Soil Conditions on Building Damage Potential during Earthquakes," by H.B. Seed and I.M. Idriss - 1969 (PB 191 036)A03

EERC 69-16 "The Behavior of Sands Under Seismic Loading Conditions," by M.L. Silver and H.B. Seed - 1969 (AD 714 982)A07

EERC 70-1 "Earthquake Response of Gravity Dams," by A.K. Chopra - 1970 (AD 709 640)A03

EERC 70-2 "Relationships between Soil Conditions and Building Damage in the Caracas Earthquake of July 29, 1967," by H.B. Seed, I.M. Idriss and H. Dezfulian - 1970 (PB 195 762)A05

EERC 70-3 "Cyclic Loading of Full Size Steel Connections," by E.P. Popov and R.M. Stephen - 1970 (PB 213 545)A04

EERC 70-4 "Seismic Analysis of the Charaima Building, Caraballeda, Venezuela," by Subcommittee of the SEAONC Research Committee: V.V. Bertero, P.F. Fratessa, S.A. Mahin, J.H. Sexton, A.C. Scordelis, E.L. Wilson, L.A. Wyllie, H.B. Seed and J. Penzien, Chairman - 1970 (PB 201 455)A06

EERC 70-5 "A Computer Program for Earthquake Analysis of Dams," by A.K. Chopra and P. Chakrabarti - 1970 (AD 723 994)A05

EERC 70-6 "The Propagation of Love Waves Across Non-Horizontally Layered Structures," by J. Lysmer and L.A. Drake 1970 (PB 197 896)A03

EERC 70-7 "Influence of Base Rock Characteristics on Ground Response," by J. Lysmer, H.B. Seed and P.B. Schnabel 1970 (PB 197 897)A03

EERC 70-8 "Applicability of Laboratory Test Procedures for Measuring Soil Liquefaction Characteristics under Cyclic Loading," by H.B. Seed and W.H. Peacock - 1970 (PB 198 016)A03

EERC 70-9 "A Simplified Procedure for Evaluating Soil Liquefaction Potential," by H.B. Seed and I.M. Idriss - 1970 (PB 198 009)A03

EERC 70-10 "Soil Moduli and Damping Factors for Dynamic Response Analysis," by H.B. Seed and I.M. Idriss - 1970 (PB 197 869)A03

EERC 71-1 "Koyna Earthquake of December 11, 1967 and the Performance of Koyna Dam," by A.K. Chopra and P. Chakrabarti 1971 (AD 731 496)A06

EERC 71-2 "Preliminary In-Situ Measurements of Anelastic Absorption in Soils Using a Prototype Earthquake Simulator," by R.D. Borcherdt and P.W. Rodgers - 1971 (PB 201 454)A03

EERC 71-3 "Static and Dynamic Analysis of Inelastic Frame Structures," by F.L. Porter and G.H. Powell - 1971 (PB 210 135)A06

EERC 71-4 "Research Needs in Limit Design of Reinforced Concrete Structures," by V.V. Bertero - 1971 (PB 202 943)A04

EERC 71-5 "Dynamic Behavior of a High-Rise Diagonally Braced Steel Building," by D. Rea, A.A. Shah and J.G. Bouwkamp 1971 (PB 203 584)A06

EERC 71-6 "Dynamic Stress Analysis of Porous Elastic Solids Saturated with Compressible Fluids," by J. Ghaboussi and E. L. Wilson - 1971 (PB 211 396)A06

EERC 71-7 "Inelastic Behavior of Steel Beam-to-Column Subassemblages," by H. Krawinkler, V.V. Bertero and E.P. Popov 1971 (PB 211 335)A14

EERC 71-8 "Modification of Seismograph Records for Effects of Local Soil Conditions," by P. Schnabel, H.B. Seed and J. Lysmer - 1971 (PB 214 450)A03

EERC 72-1 "Static and Earthquake Analysis of Three Dimensional Frame and Shear Wall Buildings," by E.L. Wilson and H.H. Dovey - 1972 (PB 212 904)A05

EERC 72-2 "Accelerations in Rock for Earthquakes in the Western United States," by P.B. Schnabel and H.B. Seed - 1972 (PB 213 100)A03

EERC 72-3 "Elastic-Plastic Earthquake Response of Soil-Building Systems," by T. Minami - 1972 (PB 214 868)A08

EERC 72-4 "Stochastic Inelastic Response of Offshore Towers to Strong Motion Earthquakes," by M.K. Kaul - 1972 (PB 215 713)A05

EERC 72-5 "Cyclic Behavior of Three Reinforced Concrete Flexural Members with High Shear," by E.P. Popov, V.V. Bertero and H. Krawinkler - 1972 (PB 214 555)A05

EERC 72-6 "Earthquake Response of Gravity Dams Including Reservoir Interaction Effects," by P. Chakrabarti and A.K. Chopra - 1972 (AD 762 330)A08

EERC 72-7 "Dynamic Properties of Pine Flat Dam," by D. Rea, C.Y. Liaw and A.K. Chopra - 1972 (AD 763 928)A05

EERC 72-8 "Three Dimensional Analysis of Building Systems," by E.L. Wilson and H.H. Dovey - 1972 (PB 222 438)A06

EERC 72-9 "Rate of Loading Effects on Uncracked and Repaired Reinforced Concrete Members," by S. Mahin, V.V. Bertero, D. Rea and M. Atalay - 1972 (PB 224 520)A08

EERC 72-10 "Computer Program for Static and Dynamic Analysis of Linear Structural Systems," by E.L. Wilson, K.-J. Bathe, J.E. Peterson and H.H.Dovey - 1972 (PB 220 437)A04

EERC 72-11 "Literature Survey - Seismic Effects on Highway Bridges," by T. Iwasaki, J. Penzien and R.W. Clough - 1972 (PB 215 613)A19

EERC 72-12 "SHAKE-A Computer Program for Earthquake Response Analysis of Horizontally Layered Sites," by P.B. Schnabel and J. Lysmer - 1972 (PB 220 207)A06

EERC 73-1 "Optimal Seismic Design of Multistory Frames," by V.V. Bertero and H. Kamil - 1973

EERC 73-2 "Analysis of the Slides in the San Fernando Dams During the Earthquake of February 9, 1971," by H.B. Seed, K.L. Lee, I.M. Idriss and F. Makdisi - 1973 (PB 223 402)A14

EERC 73-3 "Computer Aided Ultimate Load Design of Unbraced Multistory Steel Frames," by M.B. El-Hafez and G.H. Powell 1973 (PB 248 315)A09

EERC 73-4 "Experimental Investigation into the Seismic Behavior of Critical Regions of Reinforced Concrete Components as Influenced by Moment and Shear," by M. Celebi and J. Penzien - 1973 (PB 215 884)A09

EERC 73-5 "Hysteretic Behavior of Epoxy-Repaired Reinforced Concrete Beams," by M. Celebi and J. Penzien - 1973 (PB 239 568)A03

EERC 73-6 "General Purpose Computer Program for Inelastic Dynamic Response of Plane Structures," by A. Kanaan and G.H. Powell - 1973 (PB 221 260)A08

EERC 73-7 "A Computer Program for Earthquake Analysis of Gravity Dams Including Reservoir Interaction," by P. Chakrabarti and A.K. Chopra - 1973 (AD 766 271)A04

EERC 73-8 "Behavior of Reinforced Concrete Deep Beam-Column Subassemblages Under Cyclic Loads," by O. Küstü and J.G. Bouwkamp - 1973 (PB 246 117)A12

EERC 73-9 "Earthquake Analysis of Structure-Foundation Systems," by A.K. Vaish and A.K. Chopra - 1973 (AD 766 272)A07

EERC 73-10 "Deconvolution of Seismic Response for Linear Systems," by R.B. Reimer - 1973 (PB 227 179)A08

EERC 73-11 "SAP IV: A Structural Analysis Program for Static and Dynamic Response of Linear Systems," by K.-J. Bathe, E.L. Wilson and F.E. Peterson - 1973 (PB 221 967)A09

EERC 73-12 "Analytical Investigations of the Seismic Response of Long, Multiple Span Highway Bridges," by W.S. Tseng and J. Penzien - 1973 (PB 227 816)A10

EERC 73-13 "Earthquake Analysis of Multi-Story Buildings Including Foundation Interaction," by A.K. Chopra and J.A. Gutierrez - 1973 (PB 222 970)A03

EERC 73-14 "ADAP: A Computer Program for Static and Dynamic Analysis of Arch Dams," by R.W. Clough, J.M. Raphael and S. Mojtahedi - 1973 (PB 223 763)A09

EERC 73-15 "Cyclic Plastic Analysis of Structural Steel Joints," by R.B. Pinkney and R.W. Clough - 1973 (PB 226 843)A08

EERC 73-16 "QUAD-4: A Computer Program for Evaluating the Seismic Response of Soil Structures by Variable Damping Finite Element Procedures," by I.M. Idriss, J. Lysmer, R. Hwang and H.B. Seed - 1973 (PB 229 424)A05

EERC 73-17 "Dynamic Behavior of a Multi-Story Pyramid Shaped Building," by R.M. Stephen, J.P. Hollings and J.G. Bouwkamp - 1973 (PB 240 718)A06

EERC 73-18 "Effect of Different Types of Reinforcing on Seismic Behavior of Short Concrete Columns," by V.V. Bertero, J. Hollings, O. Küstü, R.M. Stephen and J.G. Bouwkamp - 1973

EERC 73-19 "Olive View Medical Center Materials Studies, Phase I," by B. Bresler and V.V. Bertero - 1973 (PB 235 986)A06

EERC 73-20 "Linear and Nonlinear Seismic Analysis Computer Programs for Long Multiple-Span Highway Bridges," by W.S. Tseng and J. Penzien - 1973

EERC 73-21 "Constitutive Models for Cyclic Plastic Deformation of Engineering Materials," by J.M. Kelly and P.P. Gillis 1973 (PB 226 024)A03

EERC 73-22 "DRAIN - 2D User's Guide," by G.H. Powell - 1973 (PB 227 016)A05

EERC 73-23 "Earthquake Engineering at Berkeley - 1973," (PB 226 033)A11

EERC 73-24 Unassigned

EERC 73-25 "Earthquake Response of Axisymmetric Tower Structures Surrounded by Water," by C.Y. Liaw and A.K. Chopra 1973 (AD 773 052)A09

EERC 73-26 "Investigation of the Failures of the Olive View Stairtowers During the San Fernando Earthquake and Their Implications on Seismic Design," by V.V. Bertero and R.G. Collins - 1973 (PB 235 106)A13

EERC 73-27 "Further Studies on Seismic Behavior of Steel Beam-Column Subassemblages," by V.V. Bertero, H. Krawinkler and E.P. Popov - 1973 (PB 234 172)A06

EERC 74-1 "Seismic Risk Analysis," by C.S. Oliveira - 1974 (PB 235 920)A06

EERC 74-2 "Settlement and Liquefaction of Sands Under Multi-Directional Shaking," by R. Pyke, C.K. Chan and H.B. Seed 1974

EERC 74-3 "Optimum Design of Earthquake Resistant Shear Buildings," by D. Ray, K.S. Pister and A.K. Chopra - 1974 (PB 231 172)A06

EERC 74-4 "LUSH - A Computer Program for Complex Response Analysis of Soil-Structure Systems," by J. Lysmer, T. Udaka, H.B. Seed and R. Hwang - 1974 (PB 236 796)A05

EERC 74-5 "Sensitivity Analysis for Hysteretic Dynamic Systems: Applications to Earthquake Engineering," by D. Ray 1974 (PB 233 213)A06

EERC 74-6 "Soil Structure Interaction Analyses for Evaluating Seismic Response," by H.B. Seed, J. Lysmer and R. Hwang 1974 (PB 236 519)A04

EERC 74-7 Unassigned

EERC 74-8 "Shaking Table Tests of a Steel Frame - A Progress Report," by R.W. Clough and D. Tang - 1974 (PB 240 869)A03

EERC 74-9 "Hysteretic Behavior of Reinforced Concrete Flexural Members with Special Web Reinforcement," by V.V. Bertero, E.P. Popov and T.Y. Wang - 1974 (PB 236 797)A07

EERC 74-10 "Applications of Reliability-Based, Global Cost Optimization to Design of Earthquake Resistant Structures," by E. Vitiello and K.S. Pister - 1974 (PB 237 231)A06

EERC 74-11 "Liquefaction of Gravelly Soils Under Cyclic Loading Conditions," by R.T. Wong, H.B. Seed and C.K. Chan 1974 (PB 242 042)A03

EERC 74-12 "Site-Dependent Spectra for Earthquake-Resistant Design," by H.B. Seed, C. Ugas and J. Lysmer - 1974 (PB 240 953)A03

EERC 74-13 "Earthquake Simulator Study of a Reinforced Concrete Frame," by P. Hidalgo and R.W. Clough - 1974 (PB 241 944)A13

EERC 74-14 "Nonlinear Earthquake Response of Concrete Gravity Dams," by N. Pal - 1974 (AD/A 006 583)A06

EERC 74-15 "Modeling and Identification in Nonlinear Structural Dynamics - I. One Degree of Freedom Models," by N. Distefano and A. Rath - 1974 (PB 241 548)A06

EERC 75-1 "Determination of Seismic Design Criteria for the Dumbarton Bridge Replacement Structure, Vol. I: Description, Theory and Analytical Modeling of Bridge and Parameters," by F. Baron and S.-H. Pang - 1975 (PB 259 407)A15

EERC 75-2 "Determination of Seismic Design Criteria for the Dumbarton Bridge Replacement Structure, Vol. II: Numerical Studies and Establishment of Seismic Design Criteria," by F. Baron and S.-H. Pang - 1975 (PB 259 408)A11 (For set of EERC 75-1 and 75-2 (PB 259 406))

EERC 75-3 "Seismic Risk Analysis for a Site and a Metropolitan Area," by C.S. Oliveira - 1975 (PB 248 134)A09

EERC 75-4 "Analytical Investigations of Seismic Response of Short, Single or Multiple-Span Highway Bridges," by M.-C. Chen and J. Penzien - 1975 (PB 241 454)A09

EERC 75-5 "An Evaluation of Some Methods for Predicting Seismic Behavior of Reinforced Concrete Buildings," by S.A. Mahin and V.V. Bertero - 1975 (PB 246 306)A16

EERC 75-6 "Earthquake Simulator Study of a Steel Frame Structure, Vol. I: Experimental Results," by R.W. Clough and D.T. Tang - 1975 (PB 243 981)A13

EERC 75-7 "Dynamic Properties of San Bernardino Intake Tower," by D. Rea, C.-Y. Liaw and A.K. Chopra - 1975 (AD/A008 406) A05

EERC 75-8 "Seismic Studies of the Articulation for the Dumbarton Bridge Replacement Structure, Vol. I: Description, Theory and Analytical Modeling of Bridge Components," by F. Baron and R.E. Hamati - 1975 (PB 251 539)A07

EERC 75-9 "Seismic Studies of the Articulation for the Dumbarton Bridge Replacement Structure, Vol. 2: Numerical Studies of Steel and Concrete Girder Alternates," by F. Baron and R.E. Hamati - 1975 (PB 251 540)A10

EERC 75-10 "Static and Dynamic Analysis of Nonlinear Structures," by D.P. Mondkar and G.H. Powell - 1975 (PB 242 434)A08

EERC 75-11 "Hysteretic Behavior of Steel Columns," by E.P. Popov, V.V. Bertero and S. Chandramouli - 1975 (PB 252 365)A11

EERC 75-12 "Earthquake Engineering Research Center Library Printed Catalog," - 1975 (PB 243 711)A26

EERC 75-13 "Three Dimensional Analysis of Building Systems (Extended Version)," by E.L. Wilson, J.P. Hollings and H.H. Dovey - 1975 (PB 243 989)A07

EERC 75-14 "Determination of Soil Liquefaction Characteristics by Large-Scale Laboratory Tests," by P. De Alba, C.K. Chan and H.B. Seed - 1975 (NUREG 0027)A08

EERC 75-15 "A Literature Survey - Compressive, Tensile, Bond and Shear Strength of Masonry," by R.L. Mayes and R.W. Clough - 1975 (PB 246 292)A10

EERC 75-16 "Hysteretic Behavior of Ductile Moment Resisting Reinforced Concrete Frame Components," by V.V. Bertero and E.P. Popov - 1975 (PB 246 388)A05

EERC 75-17 "Relationships Between Maximum Acceleration, Maximum Velocity, Distance from Source, Local Site Conditions for Moderately Strong Earthquakes," by H.B. Seed, R. Murarka, J. Lysmer and I.M. Idriss - 1975 (PB 248 172)A03

EERC 75-18 "The Effects of Method of Sample Preparation on the Cyclic Stress-Strain Behavior of Sands," by J. Mulilis, C.K. Chan and H.B. Seed - 1975 (Summarized in EERC 75-28)

EERC 75-19 "The Seismic Behavior of Critical Regions of Reinforced Concrete Components as Influenced by Moment, Shear and Axial Force," by M.B. Atalay and J. Penzien - 1975 (PB 258 842)A11

EERC 75-20 "Dynamic Properties of an Eleven Story Masonry Building," by R.M. Stephen, J.P. Hollings, J.G. Bouwkamp and D. Jurukovski - 1975 (PB 246 945)A04

EERC 75-21 "State-of-the-Art in Seismic Strength of Masonry - An Evaluation and Review," by R.L. Mayes and R.W. Clough 1975 (PB 249 040)A07

EERC 75-22 "Frequency Dependent Stiffness Matrices for Viscoelastic Half-Plane Foundations," by A.K. Chopra, P. Chakrabarti and G. Dasgupta - 1975 (PB 248 121)A07

EERC 75-23 "Hysteretic Behavior of Reinforced Concrete Framed Walls," by T.Y. Wong, V.V. Bertero and E.P. Popov - 1975

EERC 75-24 "Testing Facility for Subassemblages of Frame-Wall Structural Systems," by V.V. Bertero, E.P. Popov and T. Endo - 1975

EERC 75-25 "Influence of Seismic History on the Liquefaction Characteristics of Sands," by H.B. Seed, K. Mori and C.K. Chan - 1975 (Summarized in EERC 75-28)

EERC 75-26 "The Generation and Dissipation of Pore Water Pressures during Soil Liquefaction," by H.B. Seed, P.P. Martin and J. Lysmer - 1975 (PB 252 648)A03

EERC 75-27 "Identification of Research Needs for Improving Aseismic Design of Building Structures," by V.V. Bertero 1975 (PB 248 136)A05

EERC 75-28 "Evaluation of Soil Liquefaction Potential during Earthquakes," by H.B. Seed, I. Arango and C.K. Chan - 1975 (NUREG 0026)A13

EERC 75-29 "Representation of Irregular Stress Time Histories by Equivalent Uniform Stress Series in Liquefaction Analyses," by H.B. Seed, I.M. Idriss, F. Makdisi and N. Banerjee - 1975 (PB 252 635)A03

EERC 75-30 "FLUSH - A Computer Program for Approximate 3-D Analysis of Soil-Structure Interaction Problems," by J. Lysmer, T. Udaka, C.-F. Tsai and H.B. Seed - 1975 (PB 259 332)A07

EERC 75-31 "ALUSH - A Computer Program for Seismic Response Analysis of Axisymmetric Soil-Structure Systems," by E. Berger, J. Lysmer and H.B. Seed - 1975

EERC 75-32 "TRIP and TRAVEL - Computer Programs for Soil-Structure Interaction Analysis with Horizontally Travelling Waves," by T. Udaka, J. Lysmer and H.B. Seed - 1975

EERC 75-33 "Predicting the Performance of Structures in Regions of High Seismicity," by J. Penzien - 1975 (PB 248 130)A03

EERC 75-34 "Efficient Finite Element Analysis of Seismic Structure - Soil - Direction," by J. Lysmer, H.B. Seed, T. Udaka, R.N. Hwang and C.-F. Tsai - 1975 (PB 253 570)A03

EERC 75-35 "The Dynamic Behavior of a First Story Girder of a Three-Story Steel Frame Subjected to Earthquake Loading," by R.W. Clough and L.-Y. Li - 1975 (PB 248 841)A05

EERC 75-36 "Earthquake Simulator Study of a Steel Frame Structure, Volume II - Analytical Results," by D.T. Tang - 1975 (PB 252 926)A10

EERC 75-37 "ANSR-I General Purpose Computer Program for Analysis of Non-Linear Structural Response," by D.P. Mondkar and G.H. Powell - 1975 (PB 252 386)A08

EERC 75-38 "Nonlinear Response Spectra for Probabilistic Seismic Design and Damage Assessment of Reinforced Concrete Structures," by M. Murakami and J. Penzien - 1975 (PB 259 530)A05

EERC 75-39 "Study of a Method of Feasible Directions for Optimal Elastic Design of Frame Structures Subjected to Earthquake Loading," by N.D. Walker and K.S. Pister - 1975 (PB 257 781)A06

EERC 75-40 "An Alternative Representation of the Elastic-Viscoelastic Analogy," by G. Dasgupta and J.L. Sackman - 1975 (PB 252 173)A03

EERC 75-41 "Effect of Multi-Directional Shaking on Liquefaction of Sands," by H.B. Seed, R. Pyke and G.R. Martin - 1975 (PB 258 781)A03

EERC 76-1 "Strength and Ductility Evaluation of Existing Low-Rise Reinforced Concrete Buildings - Screening Method," by T. Okada and B. Bresler - 1976 (PB 257 906)A11

EERC 76-2 "Experimental and Analytical Studies on the Hysteretic Behavior of Reinforced Concrete Rectangular and T-Beams," by S.-Y.M. Ma, E.P. Popov and V.V. Bertero - 1976 (PB 260 843)A12

EERC 76-3 "Dynamic Behavior of a Multistory Triangular-Shaped Building," by J. Petrovski, R.M. Stephen, E. Gartenbaum and J.G. Bouwkamp - 1976

EERC 76-4 "Earthquake Induced Deformations of Earth Dams," by N. Serff and H.B. Seed - 1976

EERC 76-5 "Analysis and Design of Tube-Type Tall Building Structures," by H. de Clercq and G.H. Powell - 1976 (PB 252 220) A10

EERC 76-6 "Time and Frequency Domain Analysis of Three-Dimensional Ground Motions, San Fernando Earthquake," by T. Kubo and J. Penzien (PB 260 556)A11

EERC 76-7 "Expected Performance of Uniform Building Code Design Masonry Structures," by R.L. Mayes, Y. Omote, S.W. Chen and R.W. Clough - 1976

EERC 76-8 "Cyclic Shear Tests on Concrete Masonry Piers," Part I - Test Results," by R.L. Mayes, Y. Omote and R.W. Clough - 1976 (PB 264 424)A06

EERC 76-9 "A Substructure Method for Earthquake Analysis of Structure - Soil Interaction," by J.A. Gutierrez and A.K. Chopra - 1976 (PB 257 783)A08

EERC 76-10 "Stabilization of Potentially Liquefiable Sand Deposits using Gravel Drain Systems," by H.B. Seed and J.R. Booker - 1976 (PB 258 820)A04

EERC 76-11 "Influence of Design and Analysis Assumptions on Computed Inelastic Response of Moderately Tall Frames," by G.H. Powell and D.G. Row - 1976

EERC 76-12 "Sensitivity Analysis for Hysteretic Dynamic Systems: Theory and Applications," by D. Ray, K.S. Pister and E. Polak - 1976 (PB 262 859)A04

EERC 76-13 "Coupled Lateral Torsional Response of Buildings to Ground Shaking," by C.L. Kan and A.K. Chopra - 1976 (PB 257 907)A09

EERC 76-14 "Seismic Analyses of the Banco de America," by V.V. Bertero, S.A. Mahin and J.A. Hollings - 1976

EERC 76-15 "Reinforced Concrete Frame 2: Seismic Testing and Analytical Correlation," by R.W. Clough and J. Gidwani - 1976 (PB 261 323)A08

EERC 76-16 "Cyclic Shear Tests on Masonry Piers, Part II - Analysis of Test Results," by R.L. Mayes, Y. Omote and R.W. Clough - 1976

EERC 76-17 "Structural Steel Bracing Systems: Behavior Under Cyclic Loading," by E.P. Popov, K. Takanashi and C.W. Roeder - 1976 (PB 260 715)A05

EERC 76-18 "Experimental Model Studies on Seismic Response of High Curved Overcrossings," by D. Williams and W.G. Godden - 1976

EERC 76-19 "Effects of Non-Uniform Seismic Disturbances on the Dumbarton Bridge Replacement Structure," by F. Baron and R.E. Hamati - 1976

EERC 76-20 "Investigation of the Inelastic Characteristics of a Single Story Steel Structure Using System Identification and Shaking Table Experiments," by V.C. Matzen and H.D. McNiven - 1976 (PB 258 453)A07

EERC 76-21 "Capacity of Columns with Splice Imperfections," by E.P. Popov, R.M. Stephen and R. Philbrick - 1976 (PB 260 378)A04

EERC 76-22 "Response of the Olive View Hospital Main Building during the San Fernando Earthquake," by S. A. Mahin, R. Collins, A.K. Chopra and V.V. Bertero - 1976

EERC 76-23 "A Study on the Major Factors Influencing the Strength of Masonry Prisms," by N.M. Mostaghel, R.L. Mayes, R. W. Clough and S.W. Chen - 1976

EERC 76-24 "GADFLEA - A Computer Program for the Analysis of Pore Pressure Generation and Dissipation during Cyclic or Earthquake Loading," by J.R. Booker, M.S. Rahman and H.B. Seed - 1976 (PB 263 947)A04

EERC 76-25 "Rehabilitation of an Existing Building: A Case Study," by B. Bresler and J. Axley - 1976

EERC 76-26 "Correlative Investigations on Theoretical and Experimental Dynamic Behavior of a Model Bridge Structure," by K. Kawashima and J. Penzien - 1976 (PB 263 388)A11

EERC 76-27 "Earthquake Response of Coupled Shear Wall Buildings," by T. Srichatrapimuk - 1976 (PB 265 157)A07

EERC 76-28 "Tensile Capacity of Partial Penetration Welds," by E.P. Popov and R.M. Stephen - 1976 (PB 262 899)A03

EERC 76-29 "Analysis and Design of Numerical Integration Methods in Structural Dynamics," by H.M. Hilber - 1976 (PB 264 410)A06

EERC 76-30 "Contribution of a Floor System to the Dynamic Characteristics of Reinforced Concrete Buildings," by L.J. Edgar and V.V. Bertero - 1976

EERC 76-31 "The Effects of Seismic Disturbances on the Golden Gate Bridge," by F. Baron, M. Arikan and R.E. Hamati - 1976

EERC 76-32 "Infilled Frames in Earthquake Resistant Construction," by R.E. Klingner and V.V. Bertero - 1976 (PB 265 892)A13

UCB/EERC-77/01 "PLUSH - A Computer Program for Probabilistic Finite Element Analysis of Seismic Soil-Structure Interaction," by M.P. Romo Organista, J. Lysmer and H.B. Seed - 1977

UCB/EERC-77/02 "Soil-Structure Interaction Effects at the Humboldt Bay Power Plant in the Ferndale Earthquake of June 7, 1975," by J.E. Valera, H.B. Seed, C.F. Tsai and J. Lysmer - 1977 (PB 265 795)A04

UCB/EERC-77/03 "Influence of Sample Disturbance on Sand Response to Cyclic Loading," by K. Mori, H.B. Seed and C.K. Chan - 1977 (PB 267 352)A04

UCB/EERC-77/04 "Seismological Studies of Strong Motion Records," by J. Shoja-Taheri - 1977 (PB 269 655)A10

UCB/EERC-77/05 "Testing Facility for Coupled-Shear Walls," by L. Li-Hyung, V.V. Bertero and E.P. Popov - 1977

UCB/EERC-77/06 "Developing Methodologies for Evaluating the Earthquake Safety of Existing Buildings," by No. 1 - B. Bresler; No. 2 - B. Bresler, T. Okada and D. Zisling; No. 3 - T. Okada and B. Bresler; No. 4 - V.V. Bertero and B. Bresler - 1977 (PB 267 354)A08

UCB/EERC-77/07 "A Literature Survey - Transverse Strength of Masonry Walls," by Y. Omote, R.L. Mayes, S.W. Chen and R.W. Clough - 1977 (PB 277 933)A07

UCB/EERC-77/08 "DRAIN-TABS: A Computer Program for Inelastic Earthquake Response of Three Dimensional Buildings," by R. Guendelman-Israel and G.H. Powell - 1977 (PB 270 693)A07

UCB/EERC-77/09 "SUBWALL: A Special Purpose Finite Element Computer Program for Practical Elastic Analysis and Design of Structural Walls with Substructure Option," by D.Q. Le, H. Peterson and E.P. Popov - 1977 (PB 270 567)A05

UCB/EERC-77/10 "Experimental Evaluation of Seismic Design Methods for Broad Cylindrical Tanks," by D.P. Clough (PB 272 280)A13

UCB/EERC-77/11 "Earthquake Engineering Research at Berkeley - 1976," - 1977 (PB 273 507)A09

UCB/EERC-77/12 "Automated Design of Earthquake Resistant Multistory Steel Building Frames," by N.D. Walker, Jr. - 1977 (PB 276 526)A09

UCB/EERC-77/13 "Concrete Confined by Rectangular Hoops Subjected to Axial Loads," by J. Vallenas, V.V. Bertero and E.P. Popov - 1977 (PB 275 165)A06

UCB/EERC-77/14 "Seismic Strain Induced in the Ground During Earthquakes," by Y. Sugimura - 1977 (PB 284 201)A04

UCB/EERC-77/15 "Bond Deterioration under Generalized Loading," by V.V. Bertero, E.P. Popov and S. Viwathanatepa - 1977

UCB/EERC-77/16 "Computer Aided Optimum Design of Ductile Reinforced Concrete Moment Resisting Frames," by S.W. Zagajeski and V.V. Bertero - 1977 (PB 280 137)A07

UCB/EERC-77/17 "Earthquake Simulation Testing of a Stepping Frame with Energy-Absorbing Devices," by J.M. Kelly and D.F. Tsztoo - 1977 (PB 273 506)A04

UCB/EERC-77/18 "Inelastic Behavior of Eccentrically Braced Steel Frames under Cyclic Loadings," by C.W. Roeder and E.P. Popov - 1977 (PB 275 526)A15

UCB/EERC-77/19 "A Symplified Procedure for Estimating Earthquake-Induced Deformations in Dams and Embankments," by F.I. Makdisi and H.B. Seed - 1977 (PB 276 820) A04

UCB/EERC-77/20 "The Performance of Earth Dams during Earthquakes," by H.B. Seed, F.I. Makdisi and P. de Alba - 1977 (PB 276 821)A04

UCB/EERC-77/21 "Dynamic Plastic Analysis Using Stress Resultant Finite Element Formulation," by P. Lukkunapvasit and J.M. Kelly - 1977 (PB 275 453)A04

UCB/EERC-77/22 "Preliminary Experimental Study of Seismic Uplift of a Steel Frame," by R.W. Clough and A.A. Huckelbridge 1977 (PB 278 769)A08

UCB/EERC-77/23 "Earthquake Simulator Tests of a Nine-Story Steel Frame with Columns Allowed to Uplift," by A.A. Huckelbridge - 1977 (PB 277 944)A09

UCB/EERC-77/24 "Nonlinear Soil-Structure Interaction of Skew Highway Bridges," by M.-C. Chen and J. Penzien - 1977 (PB 276 176)A07

UCB/EERC-77/25 "Seismic Analysis of an Offshore Structure Supported on Pile Foundations," by D.D.-N. Liou and J. Penzien 1977 (PB 283 180)A06

UCB/EERC-77/26 "Dynamic Stiffness Matrices for Homogeneous Viscoelastic Half-Planes," by G. Dasgupta and A.K. Chopra - 1977 (PB 279 654)A06

UCB/EERC-77/27 "A Practical Soft Story Earthquake Isolation System," by J.M. Kelly and J.M. Eidinger - 1977 (PB 276 814)A07

UCB/EERC-77/28 "Seismic Safety of Existing Buildings and Incentives for Hazard Mitigation in San Francisco: An Exploratory Study," by A.J. Meltsner - 1977 (PB 281 970)A05

UCB/EERC-77/29 "Dynamic Analysis of Electrohydraulic Shaking Tables," by D. Rea, S. Abedi-Hayati and Y. Takahashi 1977 (PB 282 569)A04

UCB/EERC-77/30 "An Approach for Improving Seismic - Resistant Behavior of Reinforced Concrete Interior Joints," by B. Galunic, V.V. Bertero and E.P. Popov - 1977

UCB/EERC-78/01 "The Development of Energy-Absorbing Devices for Aseismic Base Isolation Systems," by J.M. Kelly and D.F. Tsztoo 1978 (PB 284 978)A04

UCB/EERC-78/02 "Effect of Tensile Prestrain on the Cyclic Response of Structural Steel Connections," by J.G. Bouwkamp and A. Mukhopadhyay - 1978

UCB/EERC-78/03 "Experimental Results of an Earthquake Isolation System using Natural Rubber Bearings," by J.M. Eidinger and J.M. Kelly - 1978

UCB/EERC-78/04 "Seismic Behavior of Tall Liquid Storage Tanks," by A. Niwa 1978

UCB/EERC-78/05 "Hysteretic Behavior of Reinforced Concrete Columns Subjected to High Axial and Cyclic Shear Forces," by S.W. Zagajeski, V.V. Bertero and J.G. Bouwkamp - 1978

UCB/EERC-78/06 "Inelastic Beam-Column Elements for the ANSR-I Program," by A. Riahi, D.G. Row and G.H. Powell - 1978

UCB/EERC-78/07 "Studies of Structural Response to Earthquake Ground Motion," by O.A. Lopez and A.K. Chopra - 1978

UCB/EERC-78/08 "A Laboratory Study of the Fluid-Structure Interaction of Submerged Tanks and Caissons in Earthquakes," by R.C. Byrd - 1978 (PB 284 957)A08

UCB/EERC-78/09 "Models for Evaluating Damageability of Structures," by I. Sakamoto and B. Bresler - 1978

UCB/EERC-78/10 "Seismic Performance of Secondary Structural Elements," by I. Sakamoto - 1978

UCB/EERC-78/11 Case Study--Seismic Safety Evaluation of a Reinforced Concrete School Building," by J. Axley and B. Bresler 1978

UCB/EERC-78/12 "Potential Damageability in Existing Buildings," by T. Blejwas and B. Bresler - 1978

UCB/EERC-78/13 "Dynamic Behavior of a Pedestal Base Multistory Building," by R. M. Stephen, E. L. Wilson, J. G. Bouwkamp and M. Button - 1978

UCB/EERC-78/14 "Seismic Response of Bridges - Case Studies," by R.A. Imbsen, V. Nutt and J. Penzien - 1978

UCB/EERC-78/15 "A Substructure Technique for Nonlinear Static and Dynamic Analysis," by D.G. Row and G.H. Powell - 1978

UCB/EERC-78/16 "Seismic Performance of Nonstructural and Secondary Structural Elements," by Isao Sakamoto - 1978

UCB/EERC-78/17 "Model for Evaluating Damageability of Structures," by Isao Sakamoto and B. Bresler - 1978

UCB/EERC-78/18 "Response of K-Braced Steel Frame Models to Lateral Loads," by J.G. Bouwkamp, R.M. Stephen and E.P. Popov - 1978

UCB/EERC-78/19 "Rational Design Methods for Light Equipment in Structures Subjected to Ground Motion," by Jerome L. Sackman and James M. Kelly - 1978

UCB/EERC-78/20 "Testing of a Wind Restraint for Aseismic Base Isolation," by James M. Kelly and Daniel E. Chitty - 1978

UCB/EERC-78/21 "APOLLO A Computer Program for the Analysis of Pore Pressure Generation and Dissipation in Horizontal Sand Layers During Cyclic or Earthquake Loading," by Philippe P. Martin and H. Bolton Seed - 1978

UCB/EERC-78/22 "Optimal Design of an Earthquake Isolation System," by M.A. Bhatti, K.S. Pister and E. Polak - 1978

UCB/EERC-78/23 "MASH A Computer Program for the Non-Linear Analysis of Vertically Propagating Shear Waves in Horizontally Layered Deposits," by Philippe P. Martin and H. Bolton Seed - 1978

UCB/EERC-78/24 "Investigation of the Elastic Characteristics of a Three Story Steel Frame Using System Identification," by Izak Kaya and Hugh D. McNiven - 1978

UCB/EERC-78/25 "Investigation of the Nonlinear Characteristics of a Three-Story Steel Frame Using System Identification," by I. Kaya and H.D. McNiven - 1978

UCB/EERC-78/26 "Studies of Strong Ground Motion in Taiwan," by Y.M. Hsiung, B.A. Bolt and J. Penzien - 1978

UCB/EERC-78/27 "Cyclic Loading Tests of Masonry Single Piers Volume 1 - Height to Width Ratio of 2," by P.A. Hidalgo, R.L. Mayes, H.D. McNiven & R.W. Clough - 1978

UCB/EERC-78/28 "Cyclic Loading Tests of Masonry Single Piers Volume 2 - Height to Width Radio of 1," by S.-W.J.Chen, P.A. Hidalgo, R.L. Mayes, R.W. Clough & H.D. McNiven - 1978

UCB/EERC-78/29 "Analytical Procedures in Soil Dynamics," by J. Lysmer - 1978

UCB/EERC-79/01 "Hysteretic Behavior of Lightweight Reinforced Concrete Beam-Column Subassemblages," by B. Forzani, E.P. Popov, and V.V. Bertero - 1979

UCB/EERC-79/02 "The Development of a Mathematical Model to Predict the Flexural Response of Reinforced Concrete Beams to Cyclic Loads, Using System Identification," by J.F. Stanton and H.D. McNiven - 1979